MULTIVARIABLE FEEDBACK CONTROL
Analysis and Design

Second Edition

Sigurd Skogestad
Norwegian University of Science and Technology

Ian Postlethwaite
University of Leicester

John Wiley & Sons, Ltd

Telephone (+44) 1243 779777

Email (for orders and customer service enquiries): cs-books@wiley.co.uk
Visit our Home Page on www.wiley.com

Other Wiley Editorial Offices

John Wiley & Sons Inc., 111 River Street, Hoboken, NJ 07030, USA

Jossey-Bass, 989 Market Street, San Francisco, CA 94103-1741, USA

Wiley-VCH Verlag GmbH, Boschstr. 12, D-69469 Weinheim, Germany

John Wiley & Sons Australia Ltd, 42 McDougall Street, Milton, Queensland 4064, Australia

John Wiley & Sons (Asia) Pte Ltd, 2 Clementi Loop #02-01, Jin Xing Distripark, Singapore 129809

John Wiley & Sons Canada Ltd, 22 Worcester Road, Etobicoke, Ontario, Canada M9W 1L1

Wiley also publishes its books in a variety of electronic formats. Some content that appears in print may not be available in electronic books.

British Library Cataloguing in Publication Data

A catalogue record for this book is available from the British Library

ISBN-13 978-0-470-01167-6 (HB) 978-0-470-01168-3 (PBK)
ISBN-10 0-470-01167-X (HB) 0-470-01168-8 (PBK)
Produced from camera-ready copy supplied by the authors
Printed and bound in Great Britain by Antony Rowe Ltd, Chippenham, Wiltshire
This book is printed on acid-free paper responsibly manufactured from sustainable forestry in which at least two trees are planted for each one used for paper production.

To my parents, Ingulf and Patricia
S.S.

To Elizabeth, Stella and Rosa
I.P.

CONTENTS

PREFACE

This is a book on practical feedback control and not on system theory in general. Feedback is used in control systems to change the dynamics of the system (usually to make the response stable and sufficiently fast), and to reduce the sensitivity of the system to signal uncertainty (disturbances) and model uncertainty. Important topics covered in the book, include

- classical frequency domain methods
- analysis of directions in multivariable systems using the singular value decomposition
- input–output controllability (inherent control limitations in the plant)
- model uncertainty and robustness
- performance requirements
- methods for controller design and model reduction
- control structure selection and decentralized control
- linear matrix inequalities, LMIs

The treatment is for linear systems. The theory is then much simpler and more well developed, and a large amount of practical experience tells us that in many cases linear controllers designed using linear methods provide satisfactory performance when applied to real nonlinear plants.

We have attempted to keep the mathematics at a reasonably simple level, and we emphasize results that enhance *insight* and *intuition*. The design methods currently available for linear systems are well developed, and with associated software it is relatively straightforward to design controllers for most multivariable plants. However, without insight and intuition it is difficult to judge a solution, and to know how to proceed (e.g. how to change weights) in order to improve a design.

The book is appropriate for use as a text for an introductory graduate course in multivariable control or for an advanced undergraduate course. We also think it will be useful for engineers who want to understand multivariable control, its limitations, and how it can be applied in industrial practice. The analysis techniques and the material on control structure design should prove very useful in the new emerging area of systems biology. There are numerous worked examples, exercises and case studies which make frequent use of Matlab™ [1].

The prerequisites for reading this book are an introductory course in classical single-input single-output (SISO) control and some elementary knowledge of matrices and linear algebra. Parts of the book can be studied alone, and provide an appropriate background for a number of linear control courses at both undergraduate and graduate levels: classical loop-shaping control, an introduction to multivariable control, advanced multivariable control,

[1] Matlab is a registered trademark of The MathWorks, Inc.

robust control, controller design, control structure design and controllability analysis. It may be desirable to teach the material in a different order from that given in the book. For example, in his course at ETH Zurich, Professor Manfred Morari has chosen to start with SISO systems (Chapters 1, 2, 5 and 7) and then system theory (Chapter 4), before moving on to MIMO systems (Chapters 3, 6, 8 and 9).

The book is partly based on a graduate multivariable control course given by the first author in the Cybernetics Department at the Norwegian University of Science and Technology in Trondheim. The course, attended by students from Electrical, Chemical and Mechanical Engineering, has usually consisted of 3 lectures a week for 12 weeks. In addition to regular assignments, the students have been required to complete a 50-hour design project using Matlab. In Appendix B, a project outline is given together with a sample exam.

Examples and Internet

All of the numerical examples have been solved using Matlab. Some sample files are included in the text to illustrate the steps involved. All these files use either the new Robust Control toolbox or the Control toolbox, but the problems could have been solved easily using other software packages.

The following are available over the Internet:

- Matlab files for examples and figures
- Solutions to selected exercises (those marked with a $*$)[2]
- Linear state-space models for plants used in the case studies
- Corrections, comments, extra exercises and exam sets
- Lecture notes for courses based on the book

This information can be accessed from the authors' home pages, which are easily found using a search engine like Google. The current addresses are:

- `http://www.nt.ntnu.no/users/skoge`
- `http://www.le.ac.uk/engineering/staff/Postlethwaite`

Comments and questions

Please send questions, information on any errors and any comments you may have to the authors. Their email addresses are:

- `skoge@chemeng.ntnu.no`
- `ixp@le.ac.uk`

Acknowledgements

The contents of the book are strongly influenced by the ideas and courses of Professors John Doyle and Manfred Morari from the first author's time as a graduate student at Caltech during the period 1983–1986, and by the formative years, 1975–1981, the second author spent at Cambridge University with Professor Alistair MacFarlane. We thank the organizers of the

[2] Solutions to the remaining exercises are available to course lecturers by contacting the authors.

1993 European Control Conference for inviting us to present a short course on applied $\mathcal{H}_\infty$ control, which was the starting point for our collaboration. The final manuscript for the first edition began to take shape in 1994–1995 during a stay the authors had at the University of California at Berkeley – thanks to Andy Packard, Kameshwar Poolla, Masayoshi Tomizuka and others at the BCCI-lab, and to the stimulating coffee at *Brewed Awakening*.

We are grateful for the numerous technical and editorial contributions of Yi Cao, Kjetil Havre, Ghassan Murad and Ying Zhao. The computations for Example 4.5 were performed by Roy S. Smith who shared an office with the authors at Berkeley. Helpful comments, contributions and corrections were provided by Richard Braatz, Jie Chen, Atle C. Christiansen, Wankyun Chung, Bjørn Glemmestad, John Morten Godhavn, Finn Are Michelsen and Per Johan Nicklasson. A number of people have assisted in editing and typing various versions of the manuscript, including Zi-Qin Wang, Yongjiang Yu, Greg Becker, Fen Wu, Regina Raag and Anneli Laur. We also acknowledge the contributions from our graduate students, notably Neale Foster, Morten Hovd, Elling W. Jacobsen, Petter Lundström, John Morud, Raza Samar and Erik A. Wolff.

For the *second edition*, we are indebted to Vinay Kariwala for many technical contributions and editorial changes. Other researchers at Trondheim have also been helpful and we are especially grateful to Vidar Alstad and Espen Storkaas. From Leicester, Matthew Turner and Guido Herrmann were extremely helpful with the preparation of the new chapter on LMIs. Finally, thanks to colleagues and former colleagues at Trondheim and Caltech from the first author, and at Leicester, Oxford and Cambridge from the second author.

The aero-engine model (Chapters 11 and 13) and the helicopter model (Chapter 13) are provided with the kind permission of Rolls-Royce Military Aero Engines Ltd and the UK Ministry of Defence, DRA (now QinetiQ) Bedford, respectively.

We have made use of material from several books. In particular, we recommend Zhou et al. (1996) as an excellent reference on system theory and $\mathcal{H}_\infty$ control and *The Control Handbook* (Levine, 1996) as a good general reference. Of the others we would like to acknowledge, and recommend for further reading, the following: Rosenbrock (1970), Rosenbrock (1974), Kwakernaak and Sivan (1972), Kailath (1980), Chen (1984), Francis (1987), Anderson and Moore (1989), Maciejowski (1989), Morari and Zafiriou (1989), Boyd and Barratt (1991), Doyle et al. (1992), Boyd et al. (1994), Green and Limebeer (1995), and the Matlab toolbox manuals of Grace et al. (1992), Balas et al. (1993), Chiang and Safonov (1992) and Balas et al. (2005).

Second edition

In this second edition, we have corrected a number of minor mistakes and made numerous changes and additions throughout the text, partly arising from the many questions and comments we have received from interested readers and partly to reflect developments in the field. The main additions and changes are:

Chapter 2: Material has been included on unstable plants, the feedback amplifier, the lower gain margin, simple IMC tuning rules for PID control, and the half rule for estimating the effective delay.

Chapter 3: Some material on the relative gain array has been moved in from Chapter 10.

Chapter 4: Changes have been made to the tests of state controllability and observability (of course, they are equivalent to the old ones).

Chapters 5 and 6: New results have been included on fundamental performance limitations introduced by RHP-poles and RHP-zeros.

Chapter 6: The section on limitations imposed by uncertainty has been rewritten

Chapter 7: The examples of parametric uncertainty have been introduced earlier and shortened.

Chapter 9: A clear strategy is given for incorporating integral action into LQG control.

Chapter 10: The chapter has been reorganized. New material has been included on the selection of controlled variables and self-optimizing control. The section on decentralized control has been rewritten and several examples have been added.

Chapter 12: A complete new chapter on LMIs.

Appendix: Minor changes to positive definite matrices and the all-pass factorization.

In reality, the book has been expanded by more than 100 pages, but this is not reflected in the number of pages in the second edition because the page size has also been increased.

All the Matlab programs have been updated for compatibility with the new Robust Control toolbox.

Sigurd Skogestad
Ian Postlethwaite
August 2005

BORGHEIM, an engineer:

> *Herregud, en kan da ikke gjøre noe bedre enn leke i denne velsignede verden. Jeg synes hele livet er som en lek, jeg!*
>
> Good heavens, one can't do anything better than play in this blessed world. The whole of life seems like playing to me!

Act one, LITTLE EYOLF, Henrik Ibsen.

1

INTRODUCTION

In this chapter, we begin with a brief outline of the design process for control systems. We then discuss linear models and transfer functions which are the basic building blocks for the analysis and design techniques presented in this book. The scaling of variables is critical in applications and so we provide a simple procedure for this. An example is given to show how to derive a linear model in terms of deviation variables for a practical application. Finally, we summarize the most important notation used in the book.

1.1 The process of control system design

Control is the adjustment of the available degrees of freedom (manipulated variables) to assist in achieving acceptable operation of a system (process, plant). The process of designing (automatic) control systems usually makes many demands on the engineer or engineering team. These demands often emerge in a step-by-step design procedure as follows:

1. Study the system (process, plant) to be controlled and obtain initial information about the control objectives.
2. Model the system and simplify the model, if necessary.
3. Scale the variables and analyze the resulting model; determine its properties.
4. Decide which variables are to be controlled (controlled outputs).
5. Decide on the measurements and manipulated variables: what sensors and actuators will be used and where will they be placed?
6. Select the control configuration.
7. Decide on the type of controller to be used.
8. Decide on performance specifications, based on the overall control objectives.
9. Design a controller.
10. Analyze the resulting controlled system to see if the specifications are satisfied; and if they are not satisfied modify the specifications or the type of controller.
11. Simulate the resulting controlled system, on either a computer or a pilot plant.
12. Repeat from step 2, if necessary.
13. Choose hardware and software and implement the controller.
14. Test and validate the control system, and tune the controller on-line, if necessary.

Control courses and textbooks usually focus on steps 9 and 10 in the above procedure; that is, on methods for controller design and control system analysis. Interestingly, many real control systems are designed without any consideration of these two steps. For example, even for complex systems with many inputs and outputs, it may be possible to design workable

control systems, often based on a hierarchy of cascaded control loops, using only on-line tuning (involving steps 1, 4, 5, 6, 7, 13 and 14). However, even in such cases a suitable control structure may not be known at the outset, and there is a need for systematic tools and insights to assist the designer with steps 4, 5 and 6. A special feature of this book is the provision of tools for *input–output controllability analysis* (step 3) and for *control structure design* (steps 4, 5, 6 and 7).

Input–output controllability is the ability to achieve acceptable control performance. It is affected by the locations of the sensors and actuators, but otherwise it cannot be changed by the control engineer. Simply stated, "even the best control system cannot make a Ferrari out of a Volkswagen". Therefore, the process of control system design should in some cases also include a step 0, involving the design of the process equipment itself. The idea of looking at process equipment design and control system design as an integrated whole is not new, as is clear from the following quote taken from a paper by Ziegler and Nichols (1943):

> In the application of automatic controllers, it is important to realize that controller and process form a unit; credit or discredit for results obtained are attributable to one as much as the other. A poor controller is often able to perform acceptably on a process which is easily controlled. The finest controller made, when applied to a miserably designed process, may not deliver the desired performance. True, on badly designed processes, advanced controllers are able to eke out better results than older models, but on these processes, there is a definite end point which can be approached by instrumentation and it falls short of perfection.

Ziegler and Nichols then proceed to observe that there is a factor in equipment design that is neglected, and state that

> the missing characteristic can be called the "controllability", the ability of the process to achieve and maintain the desired equilibrium value.

To derive simple tools with which to quantify the inherent input–output controllability of a plant is the goal of Chapters 5 and 6.

1.2 The control problem

The objective of a control system is to make the output y behave in a desired way by manipulating the plant input u. The *regulator problem* is to manipulate u to counteract the effect of a disturbance d. The *servo problem* is to manipulate u to keep the output close to a given reference input r. Thus, in both cases we want the *control error* $e = y - r$ to be small. The algorithm for adjusting u based on the available information is the controller K. To arrive at a good design for K we need *a priori* information about the expected disturbances and reference inputs, and of the plant model (G) and disturbance model (G_d). In this book, we make use of linear models of the form

$$y = Gu + G_d d \tag{1.1}$$

A major source of difficulty is that the models (G, G_d) may be inaccurate or may change with time. In particular, inaccuracy in G may cause problems because the plant will be part

of a feedback loop. To deal with such a problem we will make use of the concept of model uncertainty. For example, instead of a single model G we may study the behaviour of a class of models, $G_p = G + E$, where the model "uncertainty" or "perturbation" E is bounded, but otherwise unknown. In most cases weighting functions, $w(s)$, are used to express $E = w\Delta$ in terms of normalized perturbations, Δ, where the magnitude (norm) of Δ is less than or equal to 1. The following terms are useful:

Nominal stability (NS). The system is stable with no model uncertainty.

Nominal performance (NP). The system satisfies the performance specifications with no model uncertainty.

Robust stability (RS). The system is stable for all perturbed plants about the nominal model up to the worst-case model uncertainty.

Robust performance (RP). The system satisfies the performance specifications for all perturbed plants about the nominal model up to the worst-case model uncertainty.

1.3 Transfer functions

The book makes extensive use of transfer functions, $G(s)$, and of the frequency domain, which are very useful in applications for the following reasons:

- Invaluable insights are obtained from simple frequency-dependent plots.
- Important concepts for feedback such as bandwidth and peaks of closed-loop transfer functions may be defined.
- $G(j\omega)$ gives the response to a sinusoidal input of frequency ω.
- A series interconnection of systems corresponds in the frequency domain to the multiplication of the individual system transfer functions, whereas in the time domain, the evaluation of complicated convolution integrals is required.
- Poles and zeros appear explicitly in factorized scalar transfer functions.
- Uncertainty is more easily handled in the frequency domain. This is related to the fact that two systems can be described as close (i.e. have similar behaviour) if their frequency responses are similar. On the other hand, a small change in a parameter in a state-space description can result in an entirely different system response.

We consider linear, time-invariant systems whose input–output responses are governed by linear ordinary differential equations with constant coefficients. An example of such a system is

$$\begin{aligned} \dot{x}_1(t) &= -a_1 x_1(t) + x_2(t) + \beta_1 u(t) \\ \dot{x}_2(t) &= -a_0 x_1(t) + \beta_0 u(t) \\ y(t) &= x_1(t) \end{aligned} \tag{1.2}$$

where $\dot{x}(t) \equiv dx/dt$. Here $u(t)$ represents the input signal, $x_1(t)$ and $x_2(t)$ the states, and $y(t)$ the output signal. The system is time-invariant since the coefficients a_1, a_0, β_1 and β_0 are independent of time. If we apply the Laplace transform to (1.2) we obtain

$$\begin{aligned} s\bar{x}_1(s) - x_1(t=0) &= -a_1 \bar{x}_1(s) + \bar{x}_2(s) + \beta_1 \bar{u}(s) \\ s\bar{x}_2(s) - x_2(t=0) &= -a_0 \bar{x}_1(s) + \beta_0 \bar{u}(s) \\ \bar{y}(s) &= \bar{x}_1(s) \end{aligned} \tag{1.3}$$

where $\bar{y}(s)$ denotes the Laplace transform of $y(t)$, and so on. To simplify our presentation we will make the usual abuse of notation and replace $\bar{y}(s)$ by $y(s)$, etc. In addition, we will omit the independent variables s and t when the meaning is clear.

If $u(t), x_1(t), x_2(t)$ and $y(t)$ represent deviation variables away from a nominal operating point or trajectory, then we can assume $x_1(t=0) = x_2(t=0) = 0$. The elimination of $\bar{x}_1(s)$ and $\bar{x}_2(s)$ from (1.3) then yields the transfer function

$$\frac{y(s)}{u(s)} = G(s) = \frac{\beta_1 s + \beta_0}{s^2 + a_1 s + a_0} \tag{1.4}$$

Importantly, for linear systems, the transfer function is independent of the input signal (forcing function). Notice that the transfer function in (1.4) may also represent the following system:

$$\ddot{y}(t) + a_1 \dot{y}(t) + a_0 y(t) = \beta_1 \dot{u}(t) + \beta_0 u(t) \tag{1.5}$$

with input $u(t)$ and output $y(t)$.

Transfer functions, such as $G(s)$ in (1.4), will be used throughout the book to model systems and their components. More generally, we consider rational transfer functions of the form

$$G(s) = \frac{\beta_{n_z} s^{n_z} + \cdots + \beta_1 s + \beta_0}{s^n + a_{n-1} s^{n-1} + \cdots + a_1 s + a_0} \tag{1.6}$$

For multivariable systems, $G(s)$ is a matrix of transfer functions. In (1.6) n is the order of the denominator (or pole polynomial) and is also called the *order of the system*, and n_z is the order of the numerator (or zero polynomial). Then $n - n_z$ is referred to as the pole excess or *relative order*.

Definition 1.1

- *A system* $G(s)$ *is* **strictly proper** *if* $G(j\omega) \to 0$ *as* $\omega \to \infty$.
- *A system* $G(s)$ *is* **semi-proper** *or* **bi-proper** *if* $G(j\omega) \to D \neq 0$ *as* $\omega \to \infty$.
- *A system* $G(s)$ *which is strictly proper or semi-proper is* **proper**.
- *A system* $G(s)$ *is* **improper** *if* $G(j\omega) \to \infty$ *as* $\omega \to \infty$.

For a proper system, with $n \geq n_z$, we may realize (1.6) by a state-space description, $\dot{x} = Ax + Bu,\ y = Cx + Du$, similar to (1.2). The transfer function may then be written as

$$G(s) = C(sI - A)^{-1}B + D \tag{1.7}$$

Remark. All practical systems have zero gain at a sufficiently high frequency, and are therefore strictly proper. It is often convenient, however, to model high-frequency effects by a non-zero D-term, and hence semi-proper models are frequently used. Furthermore, certain derived transfer functions, such as $S = (I + GK)^{-1}$, are semi-proper.

Usually we let $G(s)$ represent the effect of the inputs u on the outputs y, whereas $G_d(s)$ represents the effect on y of the disturbances d ("process noise"). We then have the following linear process model in terms of deviation variables

$$y(s) = G(s)u(s) + G_d(s)d(s) \tag{1.8}$$

We have here made use of the superposition principle for linear systems, which implies that a change in a dependent variable (here y) can simply be found by adding together the separate

effects resulting from changes in the independent variables (here u and d) considered one at a time.

All the signals $u(s)$, $d(s)$ and $y(s)$ are deviation variables. This is sometimes shown explicitly, for example, by use of the notation $\delta u(s)$, but since we always use deviation variables when we consider Laplace transforms, the δ is normally omitted.

1.4 Scaling

Scaling is very important in practical applications as it makes model analysis and controller design (weight selection) much simpler. It requires the engineer to make a judgement at the start of the design process about the required performance of the system. To do this, decisions are made on the expected magnitudes of disturbances and reference changes, on the allowed magnitude of each input signal, and on the allowed deviation of each output.

Let the unscaled (or originally scaled) linear model of the process in deviation variables be

$$\widehat{y} = \widehat{G}\widehat{u} + \widehat{G}_d\widehat{d}; \quad \widehat{e} = \widehat{y} - \widehat{r} \tag{1.9}$$

where a hat ($\widehat{\ }$) is used to show that the variables are in their unscaled units. A useful approach for scaling is to make the variables less than 1 in magnitude. This is done by *dividing each variable by its maximum expected or allowed change.* For disturbances and manipulated inputs, we use the scaled variables

$$d = \widehat{d}/\widehat{d}_{\max}, \quad u = \widehat{u}/\widehat{u}_{\max} \tag{1.10}$$

where:

- $\widehat{d}_{\max}$ – largest expected change in disturbance
- $\widehat{u}_{\max}$ – largest allowed input change

The maximum deviation from a nominal value should be chosen by thinking of the maximum value one can expect, or allow, as a function of time.

The variables $\widehat{y}$, $\widehat{e}$ and $\widehat{r}$ are in the same units, so the same scaling factor should be applied to each. Two alternatives are possible:

- $\widehat{e}_{\max}$ – largest allowed control error
- $\widehat{r}_{\max}$ – largest expected change in reference value

Since a major objective of control is to minimize the control error $\widehat{e}$, we here usually choose to scale with respect to the maximum control error:

$$y = \widehat{y}/\widehat{e}_{\max}, \quad r = \widehat{r}/\widehat{e}_{\max}, \quad e = \widehat{e}/\widehat{e}_{\max} \tag{1.11}$$

To formalize the scaling procedure, we introduce the scaling factors

$$D_e = \widehat{e}_{\max},\ D_u = \widehat{u}_{\max},\ D_d = \widehat{d}_{\max},\ D_r = \widehat{r}_{\max} \tag{1.12}$$

For multi-input multi-output (MIMO) systems, each variable in the vectors $\widehat{d}$, $\widehat{r}$, $\widehat{u}$ and $\widehat{e}$ may have a different maximum value, in which case D_e, D_u, D_d and D_r become diagonal scaling

matrices. This ensures, for example, that all errors (outputs) are of about equal importance in terms of their magnitude.

The corresponding scaled variables to use for control purposes are then

$$d = D_d^{-1}\widehat{d},\ u = D_u^{-1}\widehat{u},\ y = D_e^{-1}\widehat{y},\ e = D_e^{-1}\widehat{e},\ r = D_e^{-1}\widehat{r} \tag{1.13}$$

On substituting (1.13) into (1.9) we get

$$D_e y = \widehat{G} D_u u + \widehat{G}_d D_d d; \quad D_e e = D_e y - D_e r$$

and introduction of the scaled transfer functions

$$\boxed{G = D_e^{-1}\widehat{G} D_u, \quad G_d = D_e^{-1}\widehat{G}_d D_d} \tag{1.14}$$

yields the following model in terms of scaled variables:

$$y = Gu + G_d d; \quad e = y - r \tag{1.15}$$

Here u and d should be less than 1 in magnitude, and it is useful in some cases to introduce a scaled reference $\widetilde{r}$, which is less than 1 in magnitude. This is done by dividing the reference by the maximum expected reference change

$$\widetilde{r} = \widehat{r}/\widehat{r}_{\max} = D_r^{-1}\widehat{r} \tag{1.16}$$

We then have that

$$r = R\widetilde{r} \quad \text{where} \quad R \triangleq D_e^{-1} D_r = \widehat{r}_{\max}/\widehat{e}_{\max} \tag{1.17}$$

Here R is the largest expected change in reference relative to the allowed control error (typically, $R \geq 1$). The block diagram for the system in terms of scaled variables may then be written as shown in Figure 1.1, for which the following control objective is relevant:

- In terms of scaled variables we have that $|d(t)| \leq 1$ and $|\widetilde{r}(t)| \leq 1$, and our control objective is to manipulate u with $|u(t)| \leq 1$ such that $|e(t)| = |y(t) - r(t)| \leq 1$ (at least most of the time).

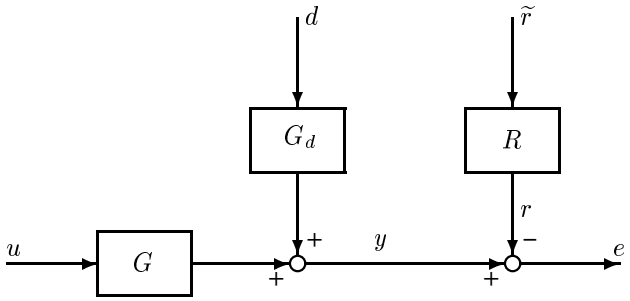

Figure 1.1: Model in terms of scaled variables

Remark 1 A number of the interpretations used in the book depend critically on a correct scaling. In particular, this applies to the input–output controllability analysis presented in Chapters 5 and 6. Furthermore, for a MIMO system one cannot correctly make use of the sensitivity function $S = (I + GK)^{-1}$ unless the output errors are of comparable magnitude.

Remark 2 With the above scalings, the worst-case behaviour of a system is analyzed by considering disturbances d of magnitude 1, and references $\widetilde{r}$ of magnitude 1.

Remark 3 The control error is

$$e = y - r = Gu + G_d d - R\widetilde{r} \tag{1.18}$$

and we see that a normalized reference change $\widetilde{r}$ may be viewed as a special case of a disturbance with $G_d = -R$, where R is usually a constant diagonal matrix. We will sometimes use this observation to unify our treatment of disturbances and references.

Remark 4 The scaling of the outputs in (1.11) in terms of the control error is used when analyzing a given plant. However, if the issue is to *select* which outputs to control, see Section 10.3, then one may choose to scale the outputs with respect to their expected variation (which is usually similar to $\widehat{r}_{\max}$).

Remark 5 If the expected or allowed variation of a variable about its nominal value is not symmetric, then to allow for the worst case, we should use the largest variation for the scaling $\widehat{d}_{\max}$ and the smallest variations for the scalings $\widehat{u}_{\max}$ and $\widehat{e}_{\max}$.

Specifically, let $\widetilde{\ }$ denote the original physical variable (before introducing any deviation or scaling), and let * denote the nominal value. Furthermore, assume that in terms of the physical variables we have that

$$\begin{aligned} \widetilde{d}_{\min} \le \widetilde{d} \le \widetilde{d}_{\max} \\ \widetilde{u}_{\min} \le \widetilde{u} \le \widetilde{u}_{\max} \\ -|\widetilde{e}_-| \le \widetilde{e} \le \widetilde{e}_+ \end{aligned}$$

where $\widetilde{e} = \widetilde{y} - \widetilde{r}$. Then we have the following scalings (or "ranges" or "spans"):

$$\widehat{d}_{\max} = \max\left(|\widetilde{d}_{\max} - \widetilde{d}^*|, |\widetilde{d}_{\min} - \widetilde{d}^*|\right) \tag{1.19}$$

$$\widehat{u}_{\max} = \min\left(|\widetilde{u}_{\max} - \widetilde{u}^*|, |\widetilde{u}_{\min} - \widetilde{u}^*|\right) \tag{1.20}$$

$$\widehat{e}_{\max} = \min\left(|\widetilde{e}_-|, |\widetilde{e}_+|\right) \tag{1.21}$$

For example, if for the unscaled physical input we have $0 \le \widetilde{u} \le 10$ with nominal value $\widetilde{u}^* = 4$, then the input scaling is $\widehat{u}_{\max} = \min\left(|10-4|, |0-4|\right) = \min(6, 4) = 4$.

Note that to get the worst case, we take the "max" for disturbances and "min" for inputs and outputs. For example, if the disturbance is $-5 \le \widetilde{d} \le 10$ with zero nominal value ($\widetilde{d}^* = 0$), then $\widehat{d}_{\max} = 10$, whereas if the manipulated input is $-5 \le \widetilde{u} \le 10$ with zero nominal value ($\widetilde{u}^* = 0$), then $\widehat{u}_{\max} = 5$. This approach may be conservative when the variations for *several* variables are not symmetric. The resulting scaled variables are

$$d = (\widetilde{d} - \widetilde{d}^*)/\widehat{d}_{\max} \tag{1.22}$$

$$u = (\widetilde{u} - \widetilde{u}^*)/\widehat{u}_{\max} \tag{1.23}$$

$$y = (\widetilde{y} - \widetilde{y}^*)/\widehat{e}_{\max} \tag{1.24}$$

A further discussion on scaling and performance is given in Chapter 5 on page 165.

1.5 Deriving linear models

Linear models may be obtained from physical "first-principle" models, from analyzing input–output data, or from a combination of these two approaches. Although modelling and system identification are not covered in this book, it is always important for a control engineer to have a good understanding of a model's origin. The following steps are usually taken when deriving a linear model for controller design based on a first-principle approach:

1. Formulate a nonlinear state-space model based on physical knowledge.
2. Determine the steady-state operating point (or trajectory) about which to linearize.
3. Introduce deviation variables and linearize the model. There are essentially three parts to this step:
   (a) Linearize the equations using a Taylor expansion where second- and higher-order terms are omitted.
   (b) Introduce the deviation variables, e.g. $\delta x(t)$ defined by
   $$\delta x(t) = x(t) - x^*$$
   where the superscript * denotes the steady-state operating point or trajectory along which we are linearizing.
   (c) Subtract the steady-state (or trajectory) to eliminate the terms involving only steady-state quantities.

   These parts are usually accomplished together. For example, for a nonlinear state-space model of the form
   $$\frac{dx}{dt} = f(x,u) \tag{1.25}$$
   the linearized model in deviation variables $(\delta x, \delta u)$ is
   $$\frac{d\delta x(t)}{dt} = \underbrace{\left(\frac{\partial f}{\partial x}\right)^*}_{A} \delta x(t) + \underbrace{\left(\frac{\partial f}{\partial u}\right)^*}_{B} \delta u(t) \tag{1.26}$$
   Here x and u may be vectors, in which case the Jacobians A and B are matrices.
4. Scale the variables to obtain scaled models which are more suitable for control purposes.

In most cases steps 2 and 3 are performed numerically based on the model obtained in step 1. Also, since (1.26) is in terms of deviation variables, its Laplace transform becomes $s\delta x(s) = A\delta x(s) + B\delta u(s)$, or
$$\delta x(s) = (sI - A)^{-1} B \delta u(s) \tag{1.27}$$

Example 1.1 Physical model of a room heating process. *The above steps for deriving a linear model will be illustrated on the simple example depicted in Figure 1.2, where the control problem is to adjust the heat input Q to maintain constant room temperature T (within ± 1 K). The outdoor temperature T_o is the main disturbance. Units are shown in square brackets.*

1. Physical model. *An energy balance for the room requires that the change in energy in the room must equal the net inflow of energy to the room (per unit of time). This yields the following state-space model:*
$$\frac{d}{dt}(C_V T) = Q + \alpha(T_o - T) \tag{1.28}$$
where T [K] is the room temperature, C_V [J/K] is the heat capacity of the room, Q [W] is the heat input (from some heat source), and the term $\alpha(T_o - T)$ [W] represents the net heat loss due to exchange of air and heat conduction through the walls.

2. Operating point. *Consider a case where the heat input Q^* is 2000 W and the difference between indoor and outdoor temperatures $T^* - T_o^*$ is 20 K. Then the steady-state energy balance yields $\alpha^* = 2000/20 = 100$ W/K. We assume the room heat capacity is constant, $C_V = 100$ kJ/K. (This value corresponds approximately to the heat capacity of air in a room of about 100 m^3; thus we neglect heat accumulation in the walls.)*

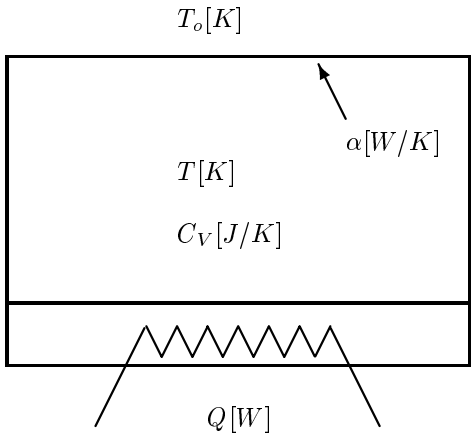

Figure 1.2: Room heating process

3. Linear model in deviation variables. *If we assume α is constant, the model in (1.28) is already linear. Then introducing deviation variables*

$$\delta T(t) = T(t) - T^*(t),\ \delta Q(t) = Q(t) - Q^*(t),\ \delta T_o(t) = T_o(t) - T_o^*(t)$$

yields

$$C_V \frac{d}{dt}\delta T(t) = \delta Q(t) + \alpha(\delta T_o(t) - \delta T(t)) \tag{1.29}$$

Remark. *If α depended on the state variable (T in this example), or on one of the independent variables of interest (Q or T_o in this example), then one would have to include an extra term $(T^* - T_o^*)\delta\alpha(t)$ on the right hand side of (1.29).*

On taking Laplace transforms in (1.29), assuming $\delta T(t) = 0$ at $t = 0$, and rearranging we get

$$\delta T(s) = \frac{1}{\tau s + 1}\left(\frac{1}{\alpha}\delta Q(s) + \delta T_o(s)\right);\quad \tau = \frac{C_V}{\alpha} \tag{1.30}$$

The time constant for this example is $\tau = 100 \cdot 10^3/100 = 1000\ s\ \approx 17$ min which is reasonable. It means that for a step increase in heat input it will take about 17 min for the temperature to reach 63% of its steady-state increase.

4. Linear model in scaled variables. *We introduce the following scaled variables:*

$$y(s) = \frac{\delta T(s)}{\delta T_{\max}};\quad u(s) = \frac{\delta Q(s)}{\delta Q_{\max}};\quad d(s) = \frac{\delta T_o(s)}{\delta T_{o,\max}} \tag{1.31}$$

In our case the acceptable variations in room temperature T are ± 1 K, i.e. $\delta T_{\max} = \delta e_{\max} = 1$ K. Furthermore, the heat input can vary between 0 W and 6000 W, and since its nominal value is 2000 W we have $\delta Q_{\max} = 2000$ W (see Remark 5 on page 7). Finally, the expected variations in outdoor temperature are ± 10 K, i.e. $\delta T_{o,\max} = 10$ K. The model in terms of scaled variables then becomes

$$\begin{aligned} G(s) &= \frac{1}{\tau s + 1}\frac{\delta Q_{\max}}{\delta T_{\max}}\frac{1}{\alpha} = \frac{20}{1000s + 1} \\ G_d(s) &= \frac{1}{\tau s + 1}\frac{\delta T_{o,\max}}{\delta T_{\max}} = \frac{10}{1000s + 1} \end{aligned} \tag{1.32}$$

Note that the static gain for the input is $k = 20$, whereas the static gain for the disturbance is $k_d = 10$. The fact that $|k_d| > 1$ means that we need some control (feedback or feedforward) to keep the output within its allowed bound ($|e| \leq 1$) when there is a disturbance of magnitude $|d| = 1$. The fact that $|k| > |k_d|$ means that we have enough "power" in the inputs to reject the disturbance at steady state; that is, we can, using an input of magnitude $|u| \leq 1$, have perfect disturbance rejection ($e = 0$) for the maximum disturbance ($|d| = 1$). We will return with a detailed discussion of this in Section 5.15.2 where we analyze the input–output controllability of the room heating process.

1.6 Notation

There is no standard notation to cover all of the topics covered in this book. We have tried to use the most familiar notation from the literature whenever possible, but an overriding concern has been to be consistent within the book, to ensure that the reader can follow the ideas and techniques through from one chapter to another.

The most important notation is summarized in Figure 1.3, which shows a one degree-of-freedom control configuration with negative feedback, a two degrees-of-freedom control configuration[1], and a general control configuration. The last configuration can be used to represent a wide class of controllers, including the one and two degrees-of-freedom configurations, as well as feedforward and estimation schemes and many others; and, as we will see, it can also be used to formulate optimization problems for controller design. The symbols used in Figure 1.3 are defined in Table 1.1. Apart from the use of v to represent the controller inputs for the general configuration, this notation is reasonably standard.

Lower-case letters are used for vectors and signals (e.g. u, y, n), and upper-case letters for matrices, transfer functions and systems (e.g. G, K). Matrix elements are usually denoted by lower-case letters, so g_{ij} is the ij'th element in the matrix G. However, sometimes we use upper-case letters G_{ij}, e.g. if G is partitioned so that G_{ij} is itself a matrix, or to avoid conflicts in notation. The Laplace variable s is often omitted for simplicity, so we often write G when we mean $G(s)$.

For state-space realizations we use the standard (A, B, C, D) notation. That is, a system G with a state-space realization (A, B, C, D) has a transfer function $G(s) = C(sI - A)^{-1}B + D$. We sometimes write

$$G(s) \stackrel{s}{=} \left[\begin{array}{c|c} A & B \\ \hline C & D \end{array}\right] \tag{1.33}$$

to mean that the transfer function $G(s)$ has a state-space realization given by the quadruple (A, B, C, D).

For closed-loop transfer functions we use S to denote sensitivity at the plant output, and $T = I - S$ to denote complementary sensitivity. With negative feedback, $S = (I + L)^{-1}$ and $T = L(I + L)^{-1}$, where L is the transfer function around the loop as seen from the output. In most cases $L = GK$, but if we also include measurement dynamics ($y_m = G_m y + n$) then $L = GKG_m$. The corresponding transfer functions as seen from the input of the plant are $L_I = KG$ (or $L_I = KG_mG$), $S_I = (I + L_I)^{-1}$ and $T_I = L_I(I + L_I)^{-1}$.

To represent uncertainty we use perturbations E (not normalized) or perturbations Δ (normalized such that their magnitude (norm) is less than or equal to 1). The nominal plant model is G, whereas the perturbed model with uncertainty is denoted G_p (usually for a set

[1] The one degree-of-freedom controller has only the control error $r - y_m$ as its input, whereas the two degrees-of-freedom controller has two inputs, namely r and y_m.

of possible perturbed plants) or G' (usually for a particular perturbed plant). For example, with additive uncertainty we may have $G_p = G + E_A = G + w_A\Delta_A$, where w_A is a weight representing the magnitude of the uncertainty.

By the right-half plane (RHP) we mean the closed right half of the complex plane, including the imaginary axis ($j\omega$-axis). The left-half plane (LHP) is the open left half of the complex plane, excluding the imaginary axis. A RHP-pole (unstable pole) is a pole located in the right-half plane, and thus includes poles on the imaginary axis. Similarly, a RHP-zero ("unstable" zero) is a zero located in the right-half plane.

We use A^T to denote the transpose of a matrix A, and A^H to represent its complex conjugate transpose.

Mathematical terminology

The symbol $\triangleq$ is used to denote *equal by definition*, $\overset{\text{def}}{\Leftrightarrow}$ is used to denote equivalent by definition, and $A \equiv B$ means that A is identically equal to B.

Let A and B be logic statements. Then the following expressions are equivalent:

A $\Leftarrow$ B
A if B, or: If B then A
A is necessary for B
B $\Rightarrow$ A, or: B implies A
B is sufficient for A
B only if A
not A $\Rightarrow$ not B

The remaining notation, special terminology and abbreviations will be defined in the text.

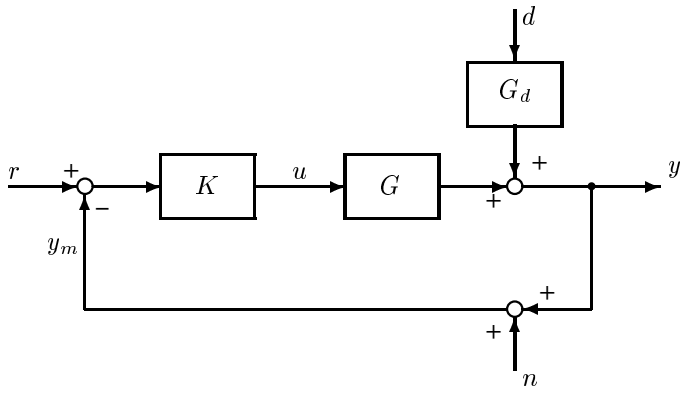

(a) One degree-of-freedom control configuration

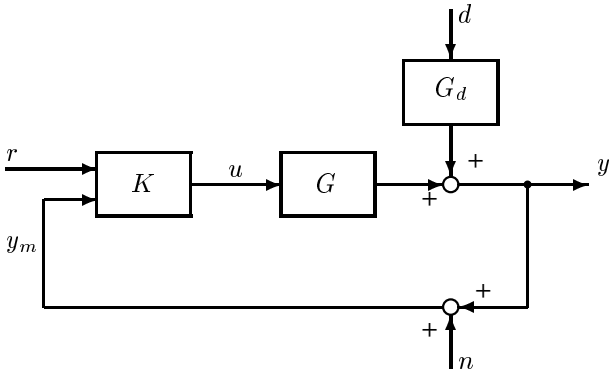

(b) Two degrees-of-freedom control configuration

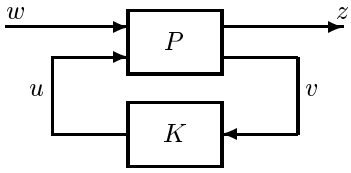

(c) General control configuration

Figure 1.3: Control configurations

Table 1.1: Nomenclature

K	controller, in whatever configuration. Sometimes the controller is broken down into its constituent parts. For example, in the two degrees-of-freedom controller in Figure 1.3(b), $K = \begin{bmatrix} K_r & K_y \end{bmatrix}$ where K_r is a prefilter and K_y is the feedback controller.
For the conventional control configurations (Figure 1.3(a) and (b)):	
G	plant model
G_d	disturbance model
r	reference inputs (commands, setpoints)
d	disturbances (process noise, DV)
n	measurement noise
y	plant outputs (controlled variables, CV)
y_m	measured y
u	plant inputs (manipulated variables, MV, control signals)
For the general control configuration (Figure 1.3(c)):	
P	generalized plant model. It will include G and G_d and the interconnection structure between the plant and the controller. In addition, if P is being used to formulate a design problem, then it will also include weighting functions.
w	exogenous inputs: commands, disturbances and noise
z	exogenous outputs; "error" signals to be minimized, e.g. $y - r$
v	controller inputs for the general configuration, e.g. commands, measured plant outputs, measured disturbances, etc. For the special case of a one degree-of-freedom controller with perfect measurements we have $v = r - y$.
u	control signals

2

CLASSICAL FEEDBACK CONTROL

In this chapter, we review the classical frequency response techniques for the analysis and design of single-loop (single-input single-output, SISO) feedback control systems. These loop-shaping techniques have been successfully used by industrial control engineers for decades, and have proved to be indispensable when it comes to providing insight into the benefits, limitations and problems of feedback control. During the 1980's the classical methods were extended to a more formal method based on shaping closed-loop transfer functions; for example, by considering the $\mathcal{H}_\infty$ norm of the weighted sensitivity function. We introduce this method at the end of the chapter.

The same underlying ideas and techniques will recur throughout the book as we present practical procedures for the analysis and design of multivariable (multi-input multi-output, MIMO) control systems.

2.1 Frequency response

On replacing s by $j\omega$ in a transfer function model $G(s)$ we get the so-called frequency response description. Frequency responses can be used to describe:

1. A system's response to sinusoids of varying frequency.
2. The frequency content of a deterministic signal via the Fourier transform.
3. The frequency distribution of a stochastic signal via the power spectral density function.

In this book, we use the first interpretation, namely that of frequency-by-frequency sinusoidal response. This interpretation has the advantage of being directly linked to the time domain, and at each frequency ω the complex number $G(j\omega)$ (or complex matrix for a MIMO system) has a clear physical interpretation. It gives the response to an input sinusoid of frequency ω. This will be explained in more detail below. For the other two interpretations we cannot assign a clear physical meaning to $G(j\omega)$ or $y(j\omega)$ at a particular frequency – it is the distribution relative to other frequencies which matters then.

One important advantage of a frequency response analysis of a system is that it provides insight into the benefits and trade-offs of feedback control. Although this insight may be obtained by viewing the frequency response in terms of its relationship between power spectral densities, as is evident from the excellent treatment by Kwakernaak and Sivan (1972), we believe that the frequency-by-frequency sinusoidal response interpretation is the most transparent and useful.

Frequency-by-frequency sinusoids

We now want to give a physical picture of frequency response in terms of a system's response to persistent sinusoids. It is important that the reader has this picture in mind when reading the rest of the book. For example, it is needed to understand the response of a multivariable system in terms of its singular value decomposition. A physical interpretation of the frequency response for a stable linear system $y = G(s)u$ is as follows. Apply a sinusoidal input signal with frequency ω [rad/s] and magnitude u_0, such that

$$u(t) = u_0 \sin(\omega t + \alpha)$$

This input signal is persistent; that is, it has been applied since $t = -\infty$. Then the output signal is also a persistent sinusoid of the same frequency, namely

$$y(t) = y_0 \sin(\omega t + \beta)$$

Here u_0 and y_0 represent magnitudes and are therefore both non-negative. Note that the output sinusoid has a different amplitude y_0 and is also shifted in phase from the input by

$$\phi \triangleq \beta - \alpha$$

Importantly, it can be shown that y_0/u_0 and ϕ can be obtained directly from the Laplace transform $G(s)$ after inserting the imaginary number $s = j\omega$ and evaluating the magnitude and phase of the resulting complex number $G(j\omega)$. We have

$$y_0/u_0 = |G(j\omega)|; \quad \phi = \angle G(j\omega) \text{ [rad]} \tag{2.1}$$

For example, let $G(j\omega) = a + jb$, with real part $a = \text{Re } G(j\omega)$ and imaginary part $b = \text{Im } G(j\omega)$, then

$$|G(j\omega)| = \sqrt{a^2 + b^2}; \quad \angle G(j\omega) = \arctan(b/a) \tag{2.2}$$

In words, (2.1) says that *after sending a sinusoidal signal through a system $G(s)$, the signal's magnitude is amplified by a factor $|G(j\omega)|$ and its phase is shifted by $\angle G(j\omega)$*. In Figure 2.1, this statement is illustrated for the following first-order delay system (time in seconds):

$$G(s) = \frac{ke^{-\theta s}}{\tau s + 1}; \quad k = 5, \theta = 2, \tau = 10 \tag{2.3}$$

At frequency $\omega = 0.2$ rad/s, we see that the output y lags behind the input by about a quarter of a period and that the amplitude of the output is approximately twice that of the input. More accurately, the amplification is

$$|G(j\omega)| = k/\sqrt{(\tau\omega)^2 + 1} = 5/\sqrt{(10\omega)^2 + 1} = 2.24$$

and the phase shift is

$$\phi = \angle G(j\omega) = -\arctan(\tau\omega) - \theta\omega = -\arctan(10\omega) - 2\omega = -1.51 \text{ rad} = -86.5^\circ$$

$G(j\omega)$ is called the *frequency response* of the system $G(s)$. It describes how the system responds to persistent sinusoidal inputs of frequency ω. The magnitude of the frequency

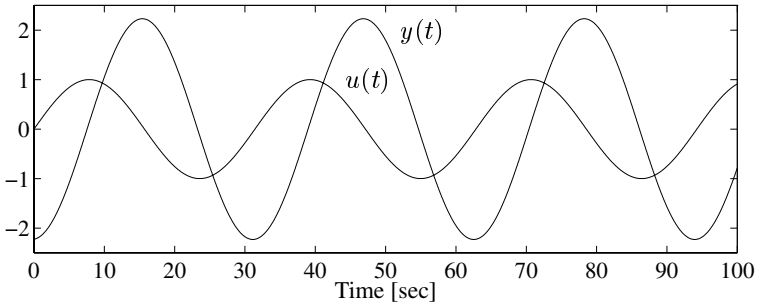

Figure 2.1: Sinusoidal response for system $G(s) = 5e^{-2s}/(10s+1)$ at frequency $\omega = 0.2$ rad/s

response, $|G(j\omega)|$, being equal to $|y_0(\omega)|/|u_0(\omega)|$, is also referred to as the *system gain*. Sometimes the gain is given in units of dB (decibel) defined as

$$A\ [\text{dB}] = 20 \log_{10} A \tag{2.4}$$

For example, $A = 2$ corresponds to $A = 6.02$ dB, and $A = \sqrt{2}$ corresponds to $A = 3.01$ dB, and $A = 1$ corresponds to $A = 0$ dB.

Both $|G(j\omega)|$ and $\angle G(j\omega)$ depend on the frequency ω. This dependency may be plotted explicitly in Bode plots (with ω as independent variable) or somewhat implicitly in a Nyquist plot (phase plane plot). In Bode plots we usually employ a log-scale for frequency and gain, and a linear scale for the phase.

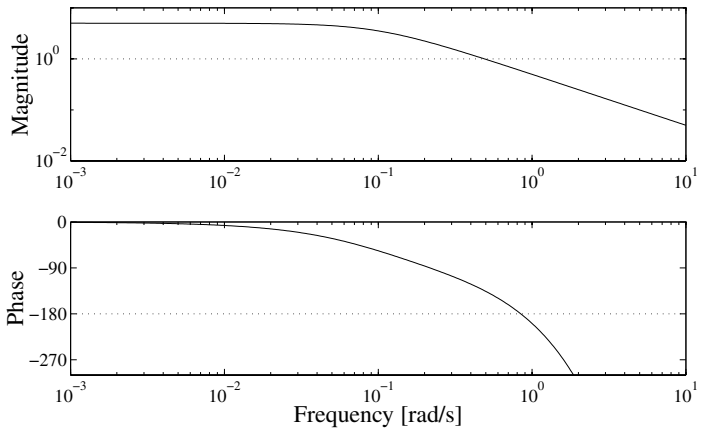

Figure 2.2: Frequency response (Bode plots) of $G(s) = 5e^{-2s}/(10s+1)$

In Figure 2.2, the Bode plots are shown for the system in (2.3). We note that in this case both the gain and phase fall monotonically with frequency. This is quite common for process control applications. The delay θ only shifts the sinusoid in time, and thus affects the phase but not the gain. The system gain $|G(j\omega)|$ is equal to k at low frequencies; this is the steady-state gain and is obtained by setting $s = 0$ (or $\omega = 0$). The gain remains relatively constant

up to the break frequency $1/\tau$ where it starts falling sharply. Physically, the system responds too slowly to let high-frequency ("fast") inputs have much effect on the outputs.

The frequency response is also useful for an *unstable plant* $G(s)$, which by itself has no steady-state response. Let $G(s)$ be stabilized by feedback control, and consider applying a sinusoidal forcing signal to the stabilized system. In this case all signals within the system are persistent sinusoids with the same frequency ω, and $G(j\omega)$ yields as before the sinusoidal response from the input to the output of $G(s)$.

Phasor notation. For any sinusoidal signal

$$u(t) = u_0 \sin(\omega t + \alpha)$$

we may introduce the phasor notation by defining the complex number

$$\boxed{u(\omega) \triangleq u_0 e^{j\alpha}} \tag{2.5}$$

We then have that

$$u_0 = |u(\omega)|; \quad \alpha = \angle u(\omega) \tag{2.6}$$

We use ω as an argument to show explicitly that this notation is used for sinusoidal signals, and also because u_0 and α generally depend on ω. Note that $u(\omega)$ is *not* equal to $u(s)$ evaluated at $s = \omega$ or $s = j\omega$, nor is it equal to $u(t)$ evaluated at $t = \omega$. From Euler's formula for complex numbers, we have that $e^{jz} = \cos z + j \sin z$. It then follows that $\sin(\omega t)$ is equal to the imaginary part of the complex function $e^{j\omega t}$, and we can write the time domain sinusoidal response in complex form as follows:

$$u(t) = u_0 \mathrm{Im}\ e^{j(\omega t+\alpha)} \text{ gives, as } t \to \infty: \quad y(t) = y_0 \mathrm{Im}\ e^{j(\omega t+\beta)} \tag{2.7}$$

where

$$y_0 = |G(j\omega)| u_0, \quad \beta = \angle G(j\omega) + \alpha \tag{2.8}$$

and $|G(j\omega)|$ and $\angle G(j\omega)$ are defined in (2.2). Since $G(j\omega) = |G(j\omega)|\ e^{j\angle G(j\omega)}$, the sinusoidal response in (2.7) and (2.8) can be compactly written in phasor notation as follows:

$$y(\omega) e^{j\omega t} = G(j\omega) u(\omega) e^{j\omega t} \tag{2.9}$$

or because the term $e^{j\omega t}$ appears on both sides

$$\boxed{y(\omega) = G(j\omega) u(\omega)} \tag{2.10}$$

At each frequency, $u(\omega)$, $y(\omega)$ and $G(j\omega)$ are complex numbers, and the usual rules for multiplying complex numbers apply. We will use this phasor notation throughout the book. Thus *whenever we use notation such as $u(\omega)$ (with ω and not $j\omega$ as an argument), the reader should interpret this as a (complex) sinusoidal signal, $u(\omega)e^{j\omega t}$*. The expression (2.10) also applies to MIMO systems where $u(\omega)$ and $y(\omega)$ are complex vectors representing the sinusoidal signals in the input and output channels, respectively, and $G(j\omega)$ is a complex matrix.

Minimum-phase systems. For stable systems which are minimum-phase (no time delays or right-half plane (RHP) zeros) there is a unique relationship between the gain and phase of the frequency response. This may be quantified by the Bode gain–phase relationship which

gives the phase of G (normalized[1] such that $G(0) > 0$) at a given frequency ω_0 as a function of $|G(j\omega)|$ over the entire frequency range:

$$\angle G(j\omega_0) = \frac{1}{\pi}\int_{-\infty}^{\infty} \underbrace{\frac{d\ln|G(j\omega)|}{d\ln\omega}}_{N(\omega)} \ln\left|\frac{\omega+\omega_0}{\omega-\omega_0}\right| \cdot \frac{d\omega}{\omega} \tag{2.11}$$

The name *minimum-phase* refers to the fact that such a system has the minimum possible phase lag for the given magnitude response $|G(j\omega)|$. The term $N(\omega)$ is the slope of the magnitude in log-variables at frequency ω. In particular, the local slope at frequency ω_0 is

$$N(\omega_0) = \left(\frac{d\ln|G(j\omega)|}{d\ln\omega}\right)_{\omega=\omega_0}$$

The term $\ln\left|\frac{\omega+\omega_0}{\omega-\omega_0}\right|$ in (2.11) is infinite at $\omega = \omega_0$, so it follows that $\angle G(j\omega_0)$ is primarily determined by the local slope $N(\omega_0)$. Also $\int_{-\infty}^{\infty} \ln\left|\frac{\omega+\omega_0}{\omega-\omega_0}\right| \cdot \frac{d\omega}{\omega} = \frac{\pi^2}{2}$ which justifies the commonly used approximation for stable minimum-phase systems

$$\angle G(j\omega_0) \approx \frac{\pi}{2} N(\omega_0)\ [\text{rad}] = 90^\circ \cdot N(\omega_0) \tag{2.12}$$

The approximation is exact for the system $G(s) = 1/s^n$ (where $N(\omega) = -n$), and it is good for stable minimum-phase systems except at frequencies close to those of resonant (complex) poles or zeros.

RHP-zeros and time delays contribute additional phase lag to a system when compared to that of a minimum-phase system with the same gain (hence the term *non-minimum-phase* system). For example, the system $G(s) = \frac{-s+a}{s+a}$ with a RHP-zero at $s = a$ has a constant gain of 1, but its phase is $-2\arctan(\omega/a)$ [rad] (and not 0 [rad] as it would be for the minimum-phase system $G(s) = 1$ of the same gain). Similarly, the time delay system $e^{-\theta s}$ has a constant gain of 1, but its phase is $-\omega\theta$ [rad].

Straight-line approximations (asymptotes). For the design methods used in this book it is useful to be able to sketch Bode plots quickly, and in particular the magnitude (gain) diagram. The reader is therefore advised to become familiar with asymptotic Bode plots (straight-line approximations). For example, for a transfer function

$$G(s) = k\frac{(s+z_1)(s+z_2)\cdots}{(s+p_1)(s+p_2)\cdots} \tag{2.13}$$

the asymptotic Bode plots of $G(j\omega)$ are obtained by using for each term $(s+a)$ the approximation $j\omega + a \approx a$ for $\omega < a$ and by $j\omega + a \approx j\omega$ for $\omega > a$. These approximations yield straight lines on a log–log plot which meet at the so-called *break point frequency* $\omega = a$. In (2.13) therefore, the frequencies $z_1, z_2, \ldots, p_1, p_2, \ldots$ are the break points where the asymptotes meet. For complex poles or zeros, the term $s^2 + 2\zeta s\omega_0 + \omega_0^2$ (where $|\zeta| < 1$) is approximated by ω_0^2 for $\omega < \omega_0$ and by $s^2 = (j\omega)^2 = -\omega^2$ for $\omega > \omega_0$. The magnitude of a transfer function is usually close to its asymptotic value, and the only case when there is

[1] The normalization of $G(s)$ is necessary to handle systems such as $\frac{1}{s+2}$ and $\frac{-1}{s+2}$, which have equal gain, are stable and minimum-phase, but their phases differ by 180°. Systems with integrators may be treated by replacing $\frac{1}{s}$ by $\frac{1}{s+\epsilon}$ where ϵ is a small positive number.

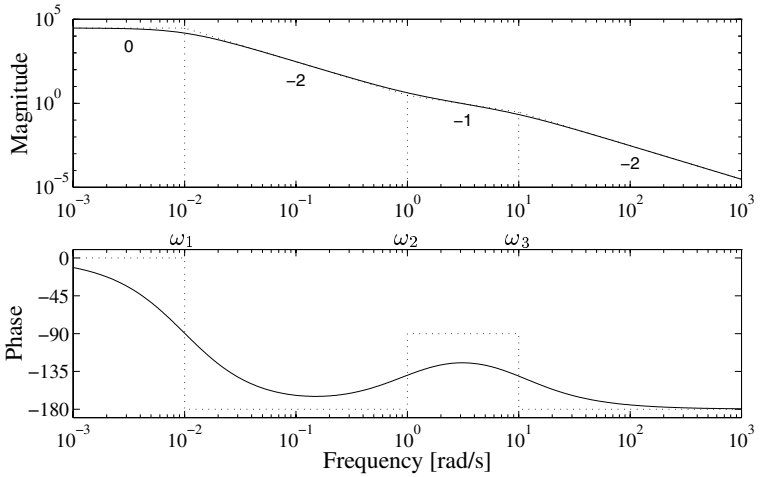

Figure 2.3: Bode plots of transfer function $L_1 = 30\frac{s+1}{(s+0.01)^2(s+10)}$. The asymptotes are given by dotted lines. The vertical dotted lines on the upper plot indicate the break frequencies ω_1, ω_2 and ω_3.

significant deviation is around the resonance frequency ω_0 for complex poles or zeros with a damping $|\zeta|$ of about 0.3 or less. In Figure 2.3, the Bode plots are shown for

$$L_1(s) = 30\frac{(s+1)}{(s+0.01)^2(s+10)} \tag{2.14}$$

The asymptotes (straight-line approximations) are shown by dotted lines. In this example the asymptotic slope of $|L_1|$ is 0 up to the first break frequency at $\omega_1 = 0.01$ rad/s where we have two poles and then the slope changes to $N = -2$. Then at $\omega_2 = 1$ rad/s there is a zero and the slope changes to $N = -1$. Finally, there is a break frequency corresponding to a pole at $\omega_3 = 10$ rad/s and so the slope is $N = -2$ at this and higher frequencies. We note that the magnitude follows the asymptotes closely, whereas the phase does not. The asymptotic phase jumps at the break frequency by -90^o (LHP-pole or RHP-zero) or $+90^o$ (LHP-zero or RHP-pole),

Remark. The phase approximation can be significantly improved if, for each term $j\omega + a$, we let the phase contribution be zero for $\omega \leq 0.1a$ and $\pi/2$ (90°) for $\omega \geq 10a$, and then connect these two lines by a third line from $(0, \omega = 0.1a)$ to $(\pi/2, \omega = 10a)$, which of course passes through the correct phase $\pi/4$ at $\omega = a$. For the terms $s^2 + 2\zeta s\omega_0 + \omega_0^2$, $\zeta < 1$, we can better approximate the phase by letting it be zero for $\omega \leq 0.1\omega_0$ and π for $\omega \geq 10\omega_0$, with a third line connecting $(0, \omega = 0.1\omega_0)$ to $(\pi, \omega = 10\omega_0)$, which passes through the correct phase $\pi/2$ at $\omega = \omega_0$.

2.2 Feedback control

2.2.1 One degree-of-freedom controller

In most of this chapter, we examine the simple one degree-of-freedom negative feedback structure shown in Figure 2.4. The input to the controller $K(s)$ is $r - y_m$ where $y_m = y + n$

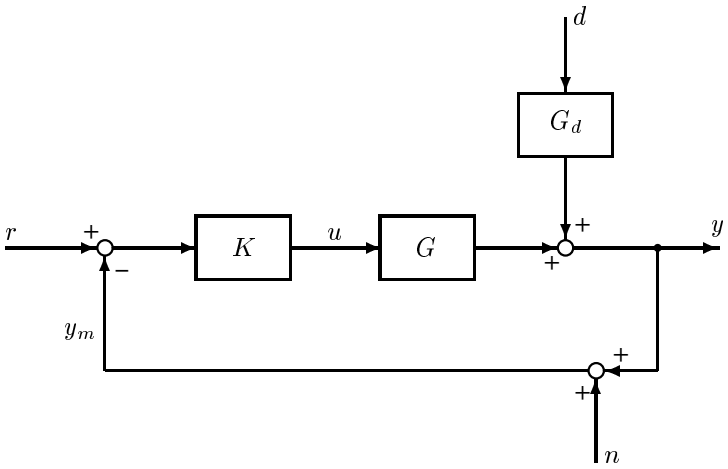

Figure 2.4: Block diagram of one degree-of-freedom feedback control system

is the measured output and n is the measurement noise. Thus, the input to the plant is

$$u = K(s)(r - y - n) \tag{2.15}$$

The objective of control is to manipulate u (design K) such that the control error e remains small in spite of disturbances d. The control error e is defined as

$$e = y - r \tag{2.16}$$

where r denotes the reference value (setpoint) for the output.

Remark. In the literature, the control error is frequently defined as $r - y_m$ which is often the controller input. However, this is not a good definition of an error variable. First, the error is normally defined as the actual value (here y) minus the desired value (here r). Second, the error should involve the actual value (y) and not the measured value (y_m). We therefore use the definition in (2.16).

2.2.2 Closed-loop transfer functions

The plant model is written as

$$y = G(s)u + G_d(s)d \tag{2.17}$$

and for a one degree-of-freedom controller the substitution of (2.15) into (2.17) yields

$$y = GK(r - y - n) + G_d d$$

or

$$(I + GK)y = GKr + G_d d - GKn \tag{2.18}$$

and hence the closed-loop response is

$$y = \underbrace{(I + GK)^{-1}GK}_{T} r + \underbrace{(I + GK)^{-1}}_{S} G_d d - \underbrace{(I + GK)^{-1}GK}_{T} n \tag{2.19}$$

The control error is

$$e = y - r = -Sr + SG_d d - Tn \tag{2.20}$$

where we have used the fact that $T - I = -S$. The corresponding plant input signal is

$$u = KSr - KSG_d d - KSn \tag{2.21}$$

The following notation and terminology are used:

$$\begin{aligned} L &= GK && \text{loop transfer function} \\ S &= (I + GK)^{-1} = (I + L)^{-1} && \text{sensitivity function} \\ T &= (I + GK)^{-1}GK = (I + L)^{-1}L && \text{complementary sensitivity function} \end{aligned}$$

We see that S is the closed-loop transfer function from the output disturbances to the outputs, while T is the closed-loop transfer function from the reference signals to the outputs. The term complementary sensitivity for T follows from the identity

$$S + T = I \tag{2.22}$$

To derive (2.22), we write $S+T = (I+L)^{-1}+(I+L)^{-1}L$ and factor out the term $(I+L)^{-1}$. The term sensitivity function is natural because S gives the sensitivity reduction afforded by feedback. To see this, consider the "open-loop" case, i.e. with no control ($K = 0$). Then the error is

$$e = y - r = -r + G_d d + 0 \cdot n \tag{2.23}$$

and a comparison with (2.20) shows that, with the exception of noise, the response with feedback is obtained by premultiplying the right hand side by S.

Remark 1 Actually, the above explanation is not the original reason for the name "sensitivity". Bode first called S sensitivity because it gives the relative sensitivity of the closed-loop transfer function T to the relative plant model error. In particular, at a given frequency ω we have for a SISO plant, by straightforward differentiation of T, that

$$\frac{dT/T}{dG/G} = S \tag{2.24}$$

Remark 2 Equations (2.15)–(2.23) are written in matrix form because they also apply to MIMO systems. Of course, for SISO systems we may write $S + T = 1$, $S = \frac{1}{1+L}$, $T = \frac{L}{1+L}$ and so on.

Remark 3 In general, closed-loop transfer functions for SISO systems with *negative* feedback may be obtained from the rule

$$\text{OUTPUT} = \frac{\text{"direct"}}{1 + \text{"loop"}} \cdot \text{INPUT} \tag{2.25}$$

where "direct" represents the transfer function for the direct effect of the input on the output (with the feedback path open) and "loop" is the transfer function around the loop (denoted $L(s)$). In the above case $L = GK$. If there is also a measurement device, $G_m(s)$, in the loop, then $L(s) = GKG_m$. The rule in (2.25) is easily derived by generalizing (2.18). In Section 3.2, we present a more general form of this rule which also applies to multivariable systems.

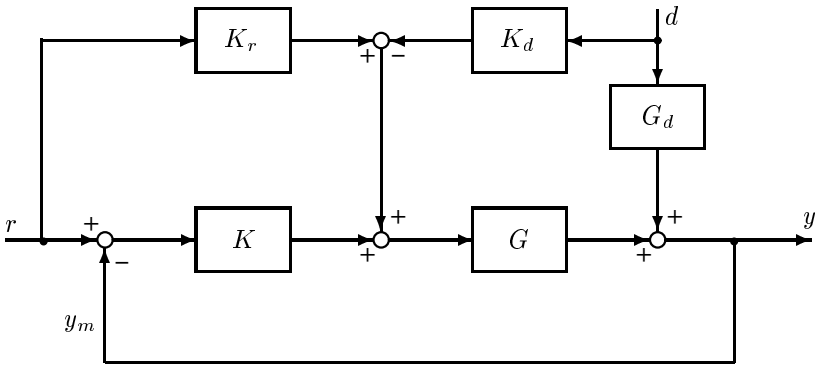

Figure 2.5: Two degrees-of-freedom feedback and feedforward control. Perfect measurements of y and d assumed.

2.2.3 Two degrees-of-freedom and feedforward control

The control structure in Figure 2.4 is called one degree-of-freedom because the controller K acts on a single signal, namely the difference $r - y_m$. In the two degrees-of-freedom structure of Figure 2.5, we treat the two signals y_m and r independently by introducing a "feedforward" controller K_r on the reference[2]. In Figure 2.5 we have also introduced a feedforward controller K_d for the measured disturbance d. The plant input in Figure 2.5 is the sum of the contributions from the feedback controller and the two feedforward controllers,

$$u = \underbrace{K(r-y)}_{\text{feedback}} + \underbrace{K_r r - K_d d}_{\text{feedforward}} \tag{2.26}$$

where for simplicity we have assumed perfect measurements of y and d. After substituting (2.26) into (2.17) and solving with respect to y,

$$y = (I + GK)^{-1} \left[G(K + K_r)r + (G_d - GK_d)d \right] \tag{2.27}$$

Using $SGK - I = T - I = -S$, the resulting control error is

$$e = y - r = S\left(-S_r r + S_d G_d d\right) \tag{2.28}$$

where the three "sensitivity" functions, giving the effect of control, are defined by

$$S = (I + GK)^{-1}, \quad S_r = I - GK_r, \quad S_d = I - GK_d G_d^{-1} \tag{2.29}$$

S is the classical feedback sensitivity function, whereas S_r and S_d are the "feedforward sensitivity functions" for reference and disturbance, respectively. Without feedback control ($K = 0$) we have $S = I$, and correspondingly without feedforward control ($K_d = 0$ and $K_r = 0$) we have $S_d = I$ and $S_r = I$. We want the sensitivities to be small to get a small error e. More precisely,

[2] There are many other ways of introducing two degrees-of-freedom control, see e.g. Figure 2.25 (page 52) for a "prefilter" structure. The form in Figure 2.5 is preferred here because it unifies the treatment of references and disturbances.

- For reference tracking we want the product SS_r to be small.
- For disturbance rejection we want the product SS_d to be small.

From this we get the important insight that that the primary objective of feedforward control is to improve performance (when required) at frequencies where feedback is not effective (i.e. where $|S| \geq 1$).

2.2.4 Why feedback?

"Perfect" control can be obtained, even without feedback ($K = 0$), by using the feedforward controllers

$$K_r(s) = G^{-1}(s); \quad K_d(s) = G^{-1}(s)G_d(s) \tag{2.30}$$

To confirm this, let $u = K_r r - K_d d$ and we get

$$y = G(G^{-1}r - G^{-1}G_d d) + G_d d = r$$

These controllers also give $S_r = 0$ and $S_d = 0$ in (2.28). However, note that in (2.30) we must assume that it is possible to realize physically the plant inverse G^{-1} and that both the plant G and the resulting controller containing the term G^{-1} are stable. These are serious considerations, but of more general concern is the loss of performance that inevitably arises because (1) the disturbances are never known (measured) exactly, and (2) G is never an exact model. *The fundamental reasons for using feedback control are therefore the presence of*

1. Signal uncertainty – unknown disturbance (d)
2. Model uncertainty (Δ)
3. An unstable plant

The third reason follows because unstable plants can only be stabilized by feedback (see Remark 2 on internal stability, page 145). In addition, for a nonlinear plant, feedback control provides a linearizing effect on the system's behaviour. This is discussed in the next section.

2.2.5 High-gain feedback

The benefits of feedback control require the use of "high" gains. As seen from (2.30), the perfect feedforward controller uses an *explicit* model of the plant inverse as part of the controller. With feedback, on the other hand, the use of high gains in GK *implicitly* generates an inverse. To see this, note that with $L = GK$ large, we get $S = (1 + GK)^{-1} \approx 0$ and $T = I - S \approx I$. From (2.21) the input signal generated by feedback is $u = KS(r - G_d d - n)$, and from the identity $KS = G^{-1}T$ it follows that with high-gain feedback the input signal is $u \approx G^{-1}(r - G_d d - n)$ and we get $y \approx r - n$. Thus, high-gain feedback generates the inverse without the need for an explicit model, and this also explains why feedback control is much less sensitive to uncertainty than feedforward control.

This is one of the beauties of feedback control; the problem is that high-gain feedback may induce instability. The solution is to use high feedback gains only over a limited frequency range (typically, at low frequencies), and to ensure that the gains "roll off" at higher frequencies where stability is a problem. The design is most critical around the "bandwidth" frequency where the loop gain $|L|$ drops below 1. The design of feedback controllers therefore

depends primarily on a good model description G around the "bandwidth" frequency. Closed-loop stability is discussed briefly in the next section, and is a recurring issue throughout the book.

As mentioned earlier, an additional benefit of feedback control is its ability to "linearize" a system's behaviour. Actually, there are two different *linearizing effects*:

1. *A "local" linearizing effect in terms of the validity model*: By use of feedback we can control the output y about an operating point and prevent the system from drifting too far away from its desired state. In this way, the system remains in the "linear region" where the linear models $G(s)$ and $G_d(s)$ are valid. This local linearizing effect justifies the use of linear models in feedback controller design and analysis, as presented in this book and as used by most practising control engineers.
2. *A "global" linearizing effect in terms of the tracking response from the reference r to the output y*: As just discussed, the use of high-gain feedback yields $y \approx r - n$. This holds also for cases where nonlinear effects cause the linear model G to change significantly as we change r. Thus, even though the underlying system is strongly nonlinear (and uncertain) the input–output response from y to r is approximately linear (and certain) with a constant gain of 1.

Example 2.1 Feedback amplifier. *The "global" linearizing effect of negative feedback is the basis for feedback amplifiers, first developed by Harold Black in 1927 for telephone communication (Kline, 1993). In the feedback amplifier, we want to magnify the input signal r by a factor α by sending it through an amplifier G with a large gain. In an open-loop (feedforward) arrangement $y = Gr$ and we must adjust the amplifier such that $G = \alpha$. Black's idea was to leave the high-gain amplifier unchanged, and instead modify the input signal r by subtracting $(1/\alpha)y$, where y is the measured output signal. This corresponds to inserting a controller $K_2 = 1/\alpha$ in the negative feedback path (e.g. see Figure 4.4(d) on page 147) to get $y = G(r - K_2 y)$. The closed-loop response becomes $y = \frac{G}{1+GK_2} r$ and for $|GK_2| \gg 1$ (which requires $|G| \gg \alpha$) we get $y \approx \frac{1}{K_2} r = \alpha \cdot r$, as desired. Note that the closed-loop gain α is set by the feedback network $(K_2 = 1/\alpha)$ and is independent of amplifier (G) parameter changes. Furthermore, within the system's closed-loop bandwidth, all signals (with any magnitude or frequency) are amplified by the same amount α, and this property is independent of the amplifier dynamics $G(s)$. Apparently, Black's claimed improvements, with simple negative feedback, over the then-standard feedforward approach, seemed so unlikely that his patent application was initially rejected.*

Remark. *In Black's design, the amplifier gain must be much larger than the desired closed-loop amplification (i.e. $|G| \gg \alpha$). This seems unnecessary, because with feedforward control, it is sufficient to require $|G| = \alpha$. Indeed, the requirement $|G| \gg \alpha$ can be avoided, if we add integral action to the loop. This may be done by use of a "two degrees-of-freedom" controller where we add a controller K_1 before the plant (amplifier) to get $y = GK_1(r - K_2 y)$ (see Figure 4.4 on page 147). The closed-loop response becomes $y = \frac{GK_1}{1+GK_1K_2} r$, and for $|GK_1K_2| \gg 1$ (which requires $|GK_1| \gg \alpha$) we get $y \approx \frac{1}{K_2} r = \alpha r$. The requirement $|GK_1K_2| \gg 1$ only needs to hold at those frequencies for which amplification is desired, and may be obtained by choosing K_1 as a simple PI (proportional–integral) controller with a proportional gain of 1; that is, $K_1 = 1 + \frac{1}{\tau_I s}$ where τ_I is the adjustable integral time.*

Of course, the "global" linearizing effect of negative feedback assumes that high-gain feedback is possible and does not result in closed-loop instability. The latter is well known with audio amplifiers as "singing", "ringing", "squalling" or "howling". In the next section, we consider conditions for closed-loop stability.

2.3 Closed-loop stability

A critical issue in designing feedback controllers is to achieve stability. As noted earlier, if the feedback gain is too large, then the controller may "overreact" and the closed-loop system becomes unstable. This is illustrated next by a simple example.

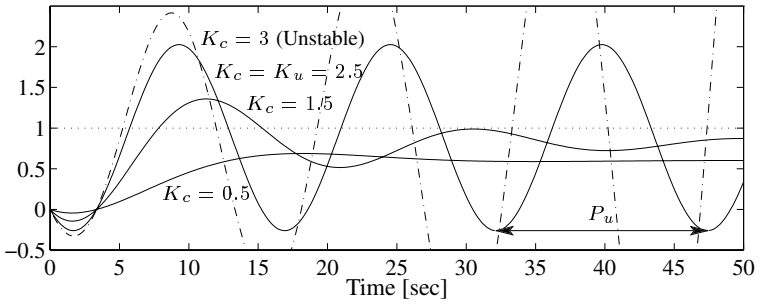

Figure 2.6: Effect of proportional gain K_c on the closed-loop response $y(t)$ for the inverse response process

Example 2.2 Inverse response process. *Consider the plant (time in seconds)*

$$\boxed{G(s) = \frac{3(-2s+1)}{(10s+1)(5s+1)}} \tag{2.31}$$

This is one of two main example processes used in this chapter to illustrate the techniques of classical control. The model has a right-half plane (RHP) zero at $s = 0.5$ rad/s. This imposes a fundamental limitation on control, and high controller gains will induce closed-loop instability.

This is illustrated for a proportional (P) controller $K(s) = K_c$ in Figure 2.6, where the response $y = Tr = GK_c(1 + GK_c)^{-1}r$ to a step change in the reference ($r(t) = 1$ for $t > 0$) is shown for four different values of K_c. The system is seen to be stable for $K_c < 2.5$, and unstable for $K_c > 2.5$. The controller gain at the limit of instability, $K_u = 2.5$, is sometimes called the ultimate gain and for this value the system is seen to cycle continuously with a period $P_u = 15.2$ s, corresponding to the frequency $\omega_u \triangleq 2\pi/P_u = 0.42$ rad/s.

Two methods are commonly used to determine closed-loop stability:

1. The poles of the closed-loop system are evaluated. That is, the roots of $1 + L(s) = 0$ are found, where L is the transfer function around the loop. The system is stable *if and only if* all the closed-loop poles are in the open left-half plane (LHP) (i.e. poles on the imaginary axis are considered "unstable"). The poles are also equal to the eigenvalues of the state-space A-matrix, and this is usually how the poles are computed numerically.
2. The frequency response (including negative frequencies) of $L(j\omega)$ is plotted in the complex plane and the number of encirclements it makes of the critical point -1 is counted. By *Nyquist's stability criterion* (for which a detailed statement is given in Theorem 4.9) closed-loop stability is inferred by equating the number of encirclements to the number of open-loop unstable poles (RHP-poles).

   For open-loop stable systems where $\angle L(j\omega)$ falls with frequency such that $\angle L(j\omega)$ crosses -180° only once (from above at frequency ω_{180}), one may equivalently use *Bode's*

stability condition which says that the closed-loop system is stable if and only if the loop gain $|L|$ is less than 1 at this frequency; that is

$$\text{Stability} \quad \Leftrightarrow \quad |L(j\omega_{180})| < 1 \tag{2.32}$$

where ω_{180} is the phase crossover frequency defined by $\angle L(j\omega_{180}) = -180°$.

Method 1, which involves computing the poles, is best suited for numerical calculations. However, time delays must first be approximated as rational transfer functions, e.g. Padé approximations. Method 2, which is based on the frequency response, has a nice graphical interpretation, and may also be used for systems with time delays. Furthermore, it provides useful measures of relative stability and forms the basis for several of the robustness tests used later in this book.

Example 2.3 Stability of inverse response process with proportional control. *Let us determine the condition for closed-loop stability of the plant G in (2.31) with proportional control; that is, with $K(s) = K_c$ (a constant) and loop transfer function $L(s) = K_c G(s)$.*

1. *The system is stable if and only if all the closed-loop poles are in the LHP. The poles are solutions to $1 + L(s) = 0$ or equivalently the roots of*

$$(10s+1)(5s+1) + K_c 3(-2s+1) = 0$$

$$\Leftrightarrow \quad 50s^2 + (15 - 6K_c)s + (1 + 3K_c) = 0 \tag{2.33}$$

But since we are only interested in the half plane location *of the poles, it is not necessary to solve (2.33). Rather, one may consider the coefficients a_i of the characteristic equation $a_n s^n + \cdots + a_1 s + a_0 = 0$ in (2.33), and use the Routh–Hurwitz test to check for stability. For second-order systems, this test says that we have stability if and only if all the coefficients have the same sign. This yields the following stability conditions:*

$$(15 - 6K_c) > 0; \quad (1 + 3K_c) > 0$$

or equivalently $-1/3 < K_c < 2.5$. With negative feedback ($K_c \geq 0$) only the upper bound is of practical interest, and we find that the maximum allowed gain ("ultimate gain") is $K_u = 2.5$ which agrees with the simulation in Figure 2.6. The poles at the onset of instability may be found by substituting $K_c = K_u = 2.5$ into (2.33) to get $50s^2 + 8.5 = 0$, i.e. $s = \pm j\sqrt{8.5/50} = \pm j0.412$. Thus, at the onset of instability we have two poles on the imaginary axis, and the system will be continuously cycling with a frequency $\omega = 0.412$ rad/s corresponding to a period $P_u = 2\pi/\omega = 15.2$ s. This agrees with the simulation results in Figure 2.6.

2. *Stability may also be evaluated from the frequency response of $L(s)$. A graphical evaluation is most enlightening. The Bode plots of the plant (i.e. $L(s)$ with $K_c = 1$) are shown in Figure 2.7. From these one finds the frequency ω_{180} where $\angle L$ is $-180°$ and then reads off the corresponding gain. This yields $|L(j\omega_{180})| = K_c|G(j\omega_{180})| = 0.4K_c$, and we get from (2.32) that the system is stable if and only if $|L(j\omega_{180})| < 1 \Leftrightarrow K_c < 2.5$ (as found above). Alternatively, the phase crossover frequency may be obtained analytically from*

$$\angle L(j\omega_{180}) = -\arctan(2\omega_{180}) - \arctan(5\omega_{180}) - \arctan(10\omega_{180}) = -180°$$

which gives $\omega_{180} = 0.412$ rad/s as found in the pole calculation above. The loop gain at this frequency is

$$|L(j\omega_{180})| = K_c \frac{3 \cdot \sqrt{(2\omega_{180})^2 + 1}}{\sqrt{(5\omega_{180})^2 + 1} \cdot \sqrt{(10\omega_{180})^2 + 1}} = 0.4K_c$$

which is the same as found from the graph in Figure 2.7. The stability condition $|L(j\omega_{180})| < 1$ then yields $K_c < 2.5$ as expected.

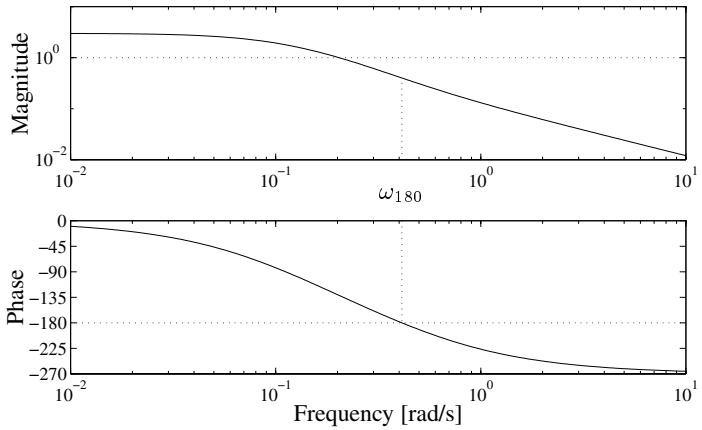

Figure 2.7: Bode plots for $L(s) = K_c \frac{3(-2s+1)}{(10s+1)(5s+1)}$ with $K_c = 1$

2.4 Evaluating closed-loop performance

Although closed-loop stability is an important issue, the real objective of control is to improve performance; that is, to make the output $y(t)$ behave in a more desirable manner. Actually, the possibility of inducing instability is one of the disadvantages of feedback control which has to be traded off against performance improvement. The objective of this section is to discuss ways of evaluating closed-loop performance.

2.4.1 Typical closed-loop responses

The following example, which considers proportional plus integral (PI) control of the stable inverse response process in (2.31), illustrates what type of closed-loop performance one might expect.

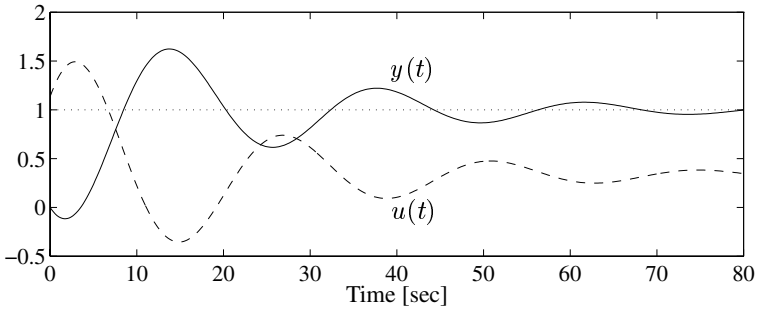

Figure 2.8: Closed-loop response to a unit step change in reference for the stable inverse response process (2.31) with PI control

Example 2.4 PI control of the inverse response process. *We have already studied the use of a proportional controller for the process in (2.31). We found that a controller gain of $K_c = 1.5$ gave a reasonably good response, except for a steady-state offset (see Figure 2.6). The reason for this offset is the non-zero steady-state sensitivity function, $S(0) = \frac{1}{1+K_c G(0)} = 0.18$ (where $G(0) = 3$ is the steady-state gain of the plant). From $e = -Sr$ in (2.20) it follows that for $r = 1$ the steady-state control error is -0.18 (as is confirmed by the simulation in Figure 2.6). To remove the steady-state offset we add integral action in the form of a PI controller*

$$K(s) = K_c \left(1 + \frac{1}{\tau_I s}\right) \tag{2.34}$$

The settings for K_c and τ_I can be determined from the classical tuning rules of Ziegler and Nichols (1942):

$$K_c = K_u/2.2, \quad \tau_I = P_u/1.2 \tag{2.35}$$

where K_u is the maximum (ultimate) P controller gain and P_u is the corresponding period of oscillations. In our case $K_u = 2.5$ and $P_u = 15.2$ s (as observed from the simulation in Figure 2.6), and we get $K_c = 1.14$ and $\tau_I = 12.7$ s. Alternatively, K_u and P_u can be obtained analytically from the model $G(s)$,

$$K_u = 1/|G(j\omega_u)|, \quad P_u = 2\pi/\omega_u \tag{2.36}$$

where ω_u is defined by $\angle G(j\omega_u) = -180^\circ$.

The closed-loop response, with PI control, to a step change in reference is shown in Figure 2.8. The output $y(t)$ has an initial inverse response due to the RHP-zero, but it then rises quickly and $y(t) = 0.9$ at $t = 8.0$ s (the rise time). The response is quite oscillatory and it does not settle to within $\pm 5\%$ of the final value until after $t = 65$ s (the settling time). The overshoot (height of peak relative to the final value) is about 62% which is much larger than one would normally like for reference tracking. The overshoot is due to controller tuning, and could have been avoided by reducing the controller gain. The decay ratio, which is the ratio between subsequent peaks, is about 0.35 which is also a bit large.

Exercise 2.1 * *Use (2.36) to compute K_u and P_u for the process in (2.31).*

In summary, for this example, the Ziegler–Nichols PI tunings are somewhat "aggressive" and give a closed-loop system with smaller stability margins and a more oscillatory response than would normally be regarded as acceptable. For disturbance rejection the controller settings may be more reasonable, and one can add a prefilter to improve the response for reference tracking, resulting in a two degrees-of-freedom controller. However, this will not change the stability robustness of the system.

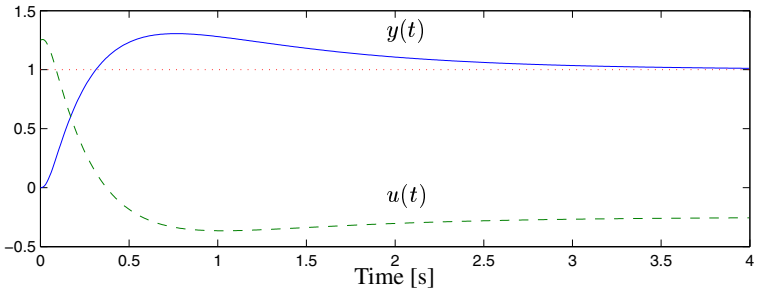

Figure 2.9: Closed-loop response to a unit step change in reference for the unstable process (2.37) with PI control

Example 2.5 PI control of unstable process. *Consider the unstable process,*

$$G(s) = \frac{4}{(s-1)(0.02s+1)^2} \tag{2.37}$$

Without control ($K = 0$), the output in response to any input change will eventually go out of bounds. To stabilize, we use a PI controller (2.34) with settings[3]

$$K_c = 1.25, \quad \tau_I = 1.5 \tag{2.38}$$

The resulting stable closed-loop response to a step change in the reference is shown in Figure 2.9. The response is not oscillatory and the selected tunings are robust with a large gain margin of 18.7 (see Section 2.4.3). The output $y(t)$ has some overshoot (about 30%), which is unavoidable for an unstable process. We note with interest that the input $u(t)$ starts out positive, but that the final steady-state value is negative. That is, the input has an inverse response. This is expected for an unstable process, since the transfer function KS (from the plant output to the plant input) must have a RHP-zero, see page 146.

2.4.2 Time domain performance

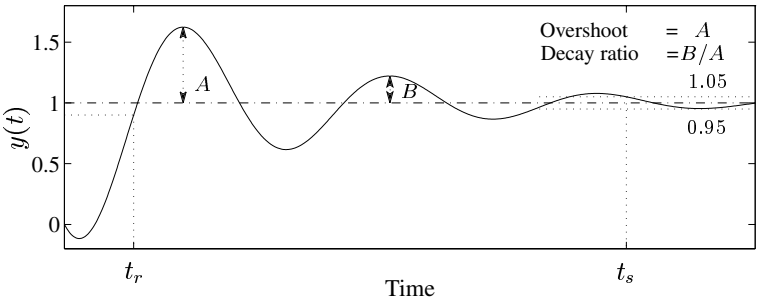

Figure 2.10: Characteristics of closed-loop response to step in reference

Step response analysis. The above examples illustrate the approach often taken by engineers when evaluating the performance of a control system. That is, one simulates the response to a step in the reference input, and considers the following characteristics (see Figure 2.10):

- *Rise time (t_r):* the time it takes for the output to first reach 90% of its final value, which is usually required to be small.
- *Settling time (t_s):* the time after which the output remains within $\pm\epsilon\%$ of its final value (typically $\epsilon = 5$), which is usually required to be small.
- *Overshoot:* the peak value divided by the final value, which should typically be 1.2 (20%) or less.
- *Decay ratio:* the ratio of the second and first peaks, which should typically be 0.3 or less.
- *Steady-state offset:* the difference between the final value and the desired final value, which is usually required to be small.

[3] The PI controller for this unstable process is almost identical to the H-infinity ($\mathcal{H}_\infty$) S/KS controller obtained using the weights $w_u = 1$ and $w_P = 1/M + \omega_B^*/s$ with $M = 1.5$ and $\omega_B^* = 10$ in (2.112) and (2.113); see Exercise 2.5 (page 65)

The rise time and settling time are measures of the *speed of the response*, whereas the overshoot, decay ratio and steady-state offset are related to the *quality of the response.* Another measure of the quality of the response is:

- *Total variation (TV):* the total up and down movement of the signal (input or output), which should be as small as possible. The computation of total variation is illustrated in Figure 2.11. In Matlab, `TV = sum(abs(diff(y)))`.

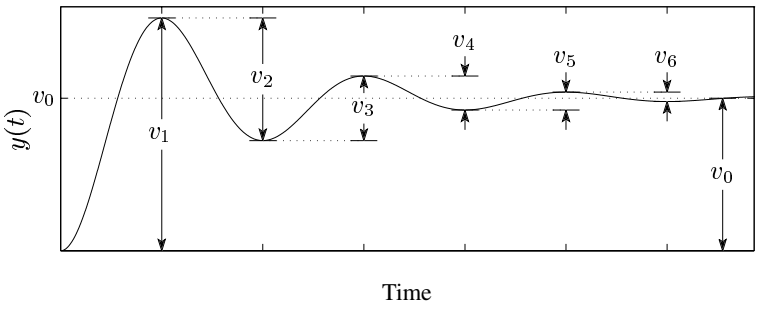

Figure 2.11: Total variation is $\mathrm{TV} = \sum_{i=1}^{\infty} |v_i|$

The above measures address the output response, $y(t)$. In addition, one should consider the magnitude of the manipulated input (control signal, u), which usually should be as small and smooth as possible. One measure of "smoothness" is to have a small total variation. Note that attempting to reduce the total variation of the input signal is equivalent to adding a penalty on input movement, as is commonly done when using model predictive control (MPC). If there are important disturbances, then the response to these should also be considered. Finally, one may investigate in simulation how the controller works if the plant model parameters are different from their nominal values.

Remark 1 Another way of quantifying time domain performance is in terms of some norm of the error signal $e(t) = y(t) - r(t)$. For example, one might use the integral squared error (ISE), or its square root which is the 2-norm of the error signal, $\|e(t)\|_2 = \sqrt{\int_0^\infty |e(\tau)|^2 d\tau}$. In this way, the various objectives related to both the speed and quality of response are combined into one number. Actually, in most cases minimizing the 2-norm seems to give a reasonable trade-off between the various objectives listed above. Another advantage of the 2-norm is that the resulting optimization problems (such as minimizing ISE) are numerically easy to solve. One can also take input magnitudes into account by considering, for example, $J = \sqrt{\int_0^\infty (Q|e(t)|^2 + R|u(t)|^2) dt}$ where Q and R are positive constants. This is similar to linear quadratic (LQ) optimal control, but in LQ control one normally considers an impulse rather than a step change in $r(t)$.

Remark 2 The step response is equal to the integral of the corresponding impulse response, e.g. set $u(\tau) = 1$ in (4.11). Some thought then reveals that one can compute the total variation as the integrated absolute area (1-norm) of the corresponding impulse response (Boyd and Barratt, 1991, p. 98). That is, let $y = Tr$, then the total variation in y for a step change in r is

$$\mathrm{TV} = \int_0^\infty |g_T(\tau)| d\tau \triangleq \|g_T(t)\|_1 \tag{2.39}$$

where $g_T(t)$ is the impulse response of T, i.e. $y(t)$ resulting from an impulse change in $r(t)$.

2.4.3 Frequency domain performance

The frequency response of the loop transfer function, $L(j\omega)$, or of various closed-loop transfer functions, may also be used to characterize closed-loop performance. Typical Bode plots of L, T and S are shown in Figure 2.14. One advantage of the frequency domain compared to a step response analysis is that it considers a broader class of signals (sinusoids of any frequency). This makes it easier to characterize feedback properties, and in particular system behaviour in the crossover (bandwidth) region. We will now describe some of the important frequency domain measures used to assess performance, e.g. gain and phase margins, the maximum peaks of S and T, and the various definitions of crossover and bandwidth frequencies used to characterize speed of response.

Gain and phase margins

Let $L(s)$ denote the loop transfer function of a system which is closed-loop stable under negative feedback. A typical Bode plot and a typical Nyquist plot of $L(j\omega)$ illustrating the gain margin (GM) and phase margin (PM) are given in Figures 2.12 and 2.13, respectively. From Nyquist's stability condition, the closeness of the curve $L(j\omega)$ to the point -1 in the complex plane is a good measure of how close a stable closed-loop system is to instability. We see from Figure 2.13 that GM measures the closeness of $L(j\omega)$ to -1 along the real axis, whereas PM is a measure along the unit circle.

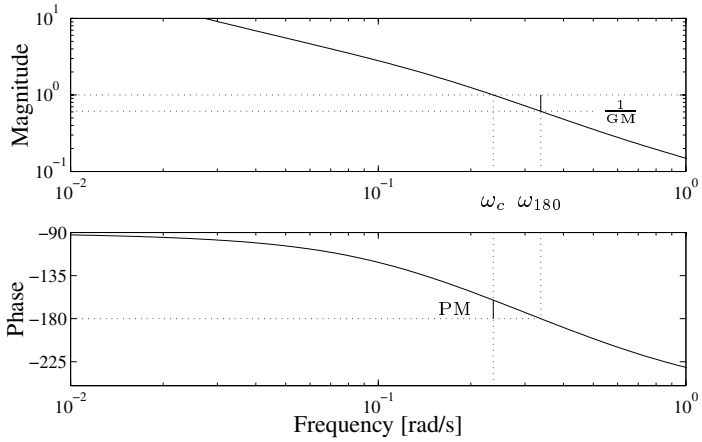

Figure 2.12: Typical Bode plot of $L(j\omega)$ with PM and GM indicated

More precisely, if the Nyquist plot of L crosses the negative real axis between -1 and 0, then the (upper) *gain margin* is defined as

$$\mathrm{GM} = 1/|L(j\omega_{180})| \tag{2.40}$$

where the *phase crossover frequency* ω_{180} is where the Nyquist curve of $L(j\omega)$ crosses the negative real axis between -1 and 0, i.e.

$$\angle L(j\omega_{180}) = -180^\circ \tag{2.41}$$

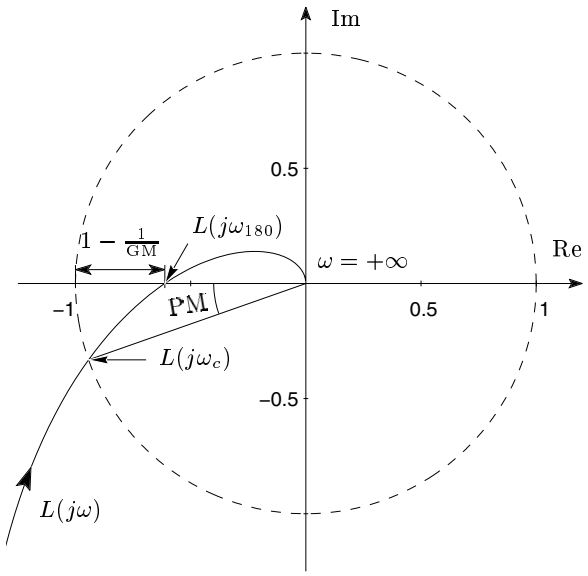

Figure 2.13: Typical Nyquist plot of $L(j\omega)$ for stable plant with PM and GM indicated. Closed-loop instability occurs if $L(j\omega)$ encircles the critical point -1.

If there is more than one such crossing between -1 and 0, then we take the closest crossing to -1, corresponding to the largest value of $|L(j\omega_{180})|$. For some systems, e.g. for low-order minimum-phase plants, there is no such crossing and GM $= \infty$. The GM is the factor by which the loop gain $|L(j\omega)|$ may be increased before the closed-loop system becomes unstable. The GM is thus a direct safeguard against steady-state gain uncertainty (error). Typically, we require $\mathrm{GM} > 2$. On a Bode plot with a logarithmic axis for $|L|$, we have that GM is the vertical distance (in dB) from the unit magnitude line down to $|L(j\omega_{180})|$, see Figure 2.12. Note that $20\log_{10}\mathrm{GM}$ is the GM in dB.

In some cases, e.g. for an unstable plant, the Nyquist plot of L crosses the negative real axis between $-\infty$ and -1, and a *lower gain margin* (or gain reduction margin) can be similarly defined,

$$\mathrm{GM}_L = 1/|L(j\omega_{L180})| \tag{2.42}$$

where ω_{L180} is the frequency where the Nyquist curve of $L(j\omega)$ crosses the negative real axis between $-\infty$ and -1. If there is more than one such crossing, then we take the closest crossing to -1, corresponding to the smallest value of $|L(j\omega_{180})|$. For many systems, e.g. for most stable plants, there is no such crossing and $\mathrm{GM}_L = 0$. The value of GM_L is the factor by which the loop gain $|L(j\omega)|$ may be *decreased* before the closed-loop system becomes unstable.

The *phase margin* is defined as

$$\mathrm{PM} = \angle L(j\omega_c) + 180^\circ \tag{2.43}$$

where the *gain crossover frequency* ω_c is the frequency where $|L(j\omega)|$ crosses 1, i.e.

$$|L(j\omega_c)| = 1 \tag{2.44}$$

If there is more than one such crossing, then the one giving the smallest value of PM is taken. The PM tells us how much negative phase (phase lag) we can add to $L(s)$ at frequency ω_c before the phase at this frequency becomes -180° which corresponds to closed-loop instability (see Figure 2.13). Typically, we require PM larger than 30° or more. The PM is a direct safeguard against time delay uncertainty; the system becomes unstable if we add a time delay of

$$\theta_{\max} = \mathrm{PM}/\omega_c \tag{2.45}$$

Note that the units must be consistent, and so if ω_c is in [rad/s] then PM must be in radians. It is also important to note that by decreasing the value of ω_c (lowering the closed-loop bandwidth, resulting in a slower response) the system can tolerate larger time delay errors.

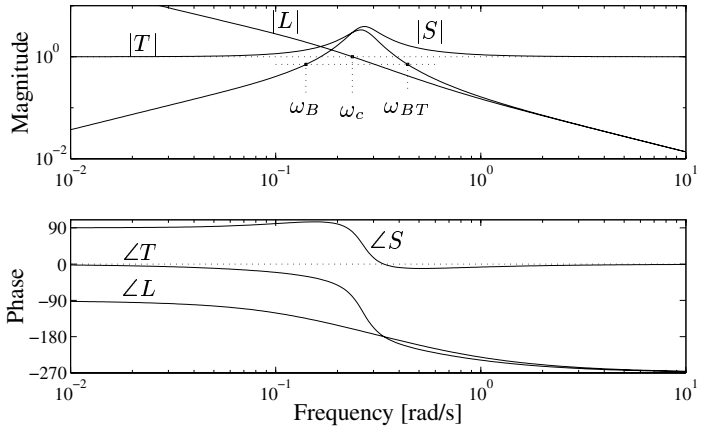

Figure 2.14: Bode magnitude and phase plots of $L = GK$, S and T when $G(s) = \frac{3(-2s+1)}{(10s+1)(5s+1)}$, and $K(s) = 1.136(1 + \frac{1}{12.7s})$ (a Ziegler–Nichols PI controller)

Example 2.4 (page 28) continued. *For the PI-controlled inverse response process example, the corresponding Bode plots for L, S and T are shown in Figure 2.14. From the plot of $L(j\omega)$, we find that the phase margin (PM) is 19.4° (0.34 rad), the gain margin (GM) is 1.63 and ω_c is 0.236 rad/s. The allowed time delay error is then $\theta_{\max} = 0.34$ rad$/0.236$ rad/s $= 1.44$ s. These margins are too small according to common rules of thumb. As defined later in the text, the peak value of $|S|$ is $M_S = 3.92$, and the peak value of $|T|$ is $M_T = 3.35$, which again are high according to normal design rules.*

Example 2.5 (page 30) continued. *The Bode plots of L, S and T for the PI-controlled unstable process are shown in Figure 2.15. The gain margin (GM), lower gain margin (GM_L), phase margin (PM) and peak values of S (M_S) and T (M_T) are*

$$GM = 18.7, GM_L = 0.21, PM = 59.5^o, M_S = 1.19, M_T = 1.38$$

In this case, the phase of $L(j\omega)$ crosses -180° twice. First, $\angle L$ crosses -180° at a low frequency (ω about 0.9) where $|L|$ is about 4.8, and we have that the lower gain margin is $GM_L = 1/4.8 = 0.21$. Second, $\angle L$ crosses -180° at a high frequency (ω about 40) where $|L|$ is about 0.054, and we have that the (upper) gain margin is GM$= 1/0.054 = 18.7$. Thus, instability is induced by decreasing the loop gain by a factor 4.8 or increasing it by a factor 18.7.

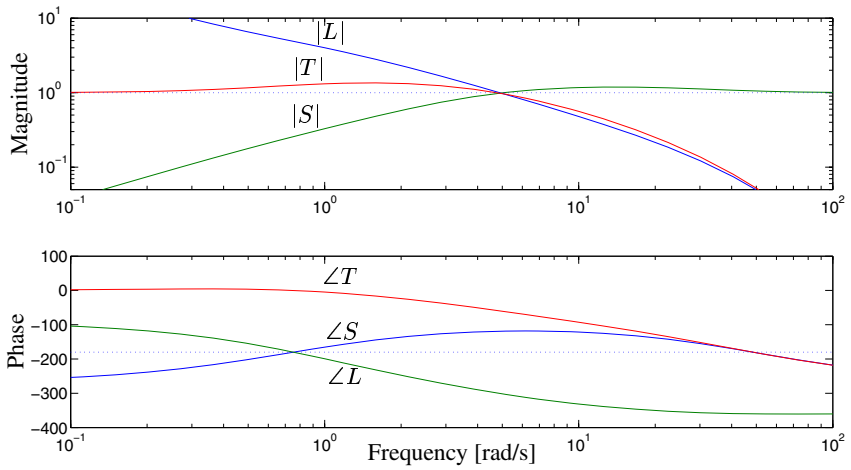

Figure 2.15: Bode magnitude and phase plots of $L = GK$, S and T for PI control of unstable process, $G(s) = \frac{4}{(s-1)(0.02s+1)^2}$, $K(s) = 1.25(1 + \frac{1}{1.5s})$

Exercise 2.2 *Prove that the maximum additional delay for which closed-loop stability is maintained is given by (2.45).*

Exercise 2.3 * *Derive the approximation for $K_u = 1/|G(j\omega_u)|$ given in (5.96) for a first-order delay system.*

Stability margins are measures of how close a stable closed-loop system is to instability. From the above arguments we see that the GM and PM provide stability margins for gain and delay uncertainty. More generally, to maintain closed-loop stability, the Nyquist stability condition tells us that the number of encirclements of the critical point -1 by $L(j\omega)$ must not change. Thus, the closeness of the frequency response $L(j\omega)$ to the critical point -1 is a good measure of closeness to instability. The GMs represent the closeness along the negative real axis, and the PM along the unit circle. As discussed next, the actual closest distance is equal to $1/M_S$, where M_S is the peak value of the sensitivity $|S(j\omega)|$. As expected, the GM and PM are closely related to M_S, and since $|S|$ is also a measure of performance, they are therefore also useful in terms of *performance*. In summary, specifications on the GM and PM (e.g. GM > 2 and PM $> 30^\circ$) are used to provide the appropriate trade-off between performance and stability robustness.

Maximum peak criteria

The maximum peaks of the sensitivity and complementary sensitivity functions are defined as

$$M_S = \max_\omega |S(j\omega)|; \quad M_T = \max_\omega |T(j\omega)| \tag{2.46}$$

(Note that $M_S = \|S\|_\infty$ and $M_T = \|T\|_\infty$ in terms of the $\mathcal{H}_\infty$ norm introduced later.) Since $S + T = 1$, using (A.51), it follows that at any frequency

$$\big|\, |S| - |T| \,\big| \le |S + T| = 1$$

so M_S and M_T differ at most by 1. A large value of M_S therefore occurs if and only if M_T is large. For a stable plant, the peak value for $|S|$ is usually higher than for $|T|$ ($M_S > M_T$) and occurs at a higher frequency (see Figure 2.14). For unstable plants, M_T is usually larger than M_S (see Figure 2.15). Note that these are not general rules.

Typically, it is required that M_S is less than about 2 (6 dB) and M_T is less than about 1.25 (2 dB). A large value of M_S or M_T (larger than about 4) indicates poor performance as well as poor robustness. An upper bound on M_T has been a common design specification in classical control and the reader may be familiar with the use of M-circles on a Nyquist plot or a Nichols chart used to determine M_T from $L(j\omega)$.

We now give some justification for why we may want to bound the value of M_S. Without control ($u = 0$), we have $e = y - r = G_d d - r$, and with feedback control $e = S(G_d d - r)$. Thus, feedback control improves performance in terms of reducing $|e|$ at all frequencies where $|S| < 1$. Usually, $|S|$ is small at low frequencies: for example, $|S(0)| = 0$ for systems with integral action. But because all real systems are strictly proper we must at high frequencies have that $L \to 0$ or equivalently $S \to 1$. At intermediate frequencies one cannot avoid in practice a peak value, M_S, larger than 1 (e.g. see the remark below). Thus, there is an intermediate frequency range where feedback control degrades performance, and the value of M_S is a measure of the worst-case performance degradation. One may also view M_S as a robustness measure. To maintain closed-loop stability, we want $L(j\omega)$ to stay away from the critical -1 point. The smallest distance between $L(j\omega)$ and -1 is M_S^{-1}, and therefore for robustness, the smaller M_S, the better. In summary, both for stability and performance we want M_S close to 1.

There is a close relationship between these maximum peaks and the GM and PM. Specifically, for a given M_S we are guaranteed

$$\mathrm{GM} \geq \frac{M_S}{M_S - 1}; \qquad \mathrm{PM} \geq 2\arcsin\left(\frac{1}{2M_S}\right) \geq \frac{1}{M_S}\ [\mathrm{rad}] \tag{2.47}$$

For example, with $M_S = 2$ we are guaranteed $\mathrm{GM} \geq 2$ and $\mathrm{PM} \geq 29.0^\circ$. Similarly, for a given value of M_T we are guaranteed

$$\mathrm{GM} \geq 1 + \frac{1}{M_T}; \qquad \mathrm{PM} \geq 2\arcsin\left(\frac{1}{2M_T}\right) \geq \frac{1}{M_T}\ [\mathrm{rad}] \tag{2.48}$$

and specifically with $M_T = 2$ we have $\mathrm{GM} \geq 1.5$ and $\mathrm{PM} \geq 29.0^\circ$.

Proof of (2.47) and (2.48): To derive the GM inequalities notice that $L(j\omega_{180}) = -1/\mathrm{GM}$ (since $\mathrm{GM} = 1/|L(j\omega_{180})|$ and L is real and negative at ω_{180}), from which we get

$$T(j\omega_{180}) = \frac{-1}{\mathrm{GM} - 1}; \quad S(j\omega_{180}) = \frac{1}{1 - \frac{1}{\mathrm{GM}}} \tag{2.49}$$

and the GM results follow. To derive the PM inequalities in (2.47) and (2.48) consider Figure 2.16 where we have $|S(j\omega_c)| = 1/|1 + L(j\omega_c)| = 1/|-1 - L(j\omega_c)|$ and we obtain

$$|S(j\omega_c)| = |T(j\omega_c)| = \frac{1}{2\sin(\mathrm{PM}/2)} \tag{2.50}$$

and the inequalities follow. Alternative formulae, which are sometimes used, follow from the identity $2\sin(\mathrm{PM}/2) = \sqrt{2(1 - \cos(\mathrm{PM}))}$. □

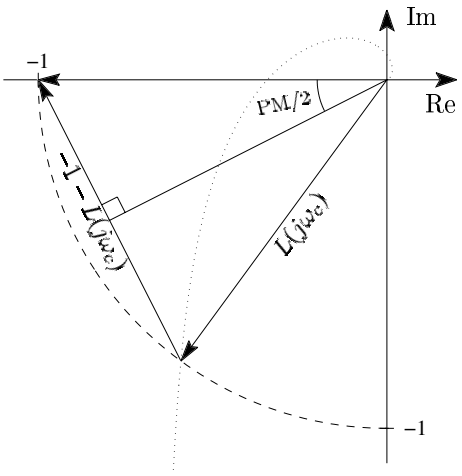

Figure 2.16: Nyquist plot of vector $L(j\omega)$. At frequency ω_c we see that $|1 + L(j\omega_c)| = 2\sin(\mathrm{PM}/2)$.

Remark. Since GM > 1, we note with interest that (2.49) requires $|S|$ to be larger than 1 at frequency ω_{180}. This means that provided ω_{180} exists, i.e. $L(j\omega)$ has more than -180° phase lag at some frequency (which is the case for any real system), then the peak of $|S(j\omega)|$ must exceed 1.

In conclusion, we see that specifications on the peaks of $|S(j\omega)|$ or $|T(j\omega)|$ (M_S or M_T) can make specifications on the GM and PM unnecessary. For instance, requiring $M_S < 2$ implies the common rules of thumb $\mathrm{GM} > 2$ and $\mathrm{PM} > 30^\circ$.

2.4.4 Relationship between time and frequency domain peaks

For a change in reference r, the output is $y(s) = T(s)r(s)$. Is there any relationship between the frequency domain peak of $T(j\omega)$, M_T, and any characteristic of the time domain step response, e.g. the overshoot or the total variation? To answer this consider a prototype second-order system with complementary sensitivity function

$$T(s) = \frac{1}{\tau^2 s^2 + 2\tau\zeta s + 1} \tag{2.51}$$

For underdamped systems with $\zeta < 1$ the poles are complex and yield oscillatory step responses. With $r(t) = 1$ (a unit step change) the values of the overshoot and total variation for $y(t)$ are given, together with M_T and M_S, as a function of ζ in Table 2.1. From Table 2.1, we see that the total variation TV correlates quite well with M_T. This is further confirmed by (A.137) and (2.39) which together yield the following general bounds:

$$M_T \ \leq \mathrm{TV} \leq (2n+1)M_T \tag{2.52}$$

Here n is the order of $T(s)$, which is 2 for our prototype system in (2.51). Given that the response of many systems can be crudely approximated by fairly low-order systems, the bound in (2.52) suggests that M_T may provide a reasonable approximation to the total variation. This provides some justification for the use of M_T in classical control to evaluate the quality of the response.

Table 2.1: Step response characteristics and frequency peaks of prototype second-order system (2.51), see also Table 2.2

	Time domain, $y(t)$		Frequency domain	
ζ	Overshoot	Total variation	M_T	M_S
2.0	1	1	1	1.05
1.5	1	1	1	1.08
1.0	1	1	1	1.15
0.8	1.02	1.03	1	1.22
0.6	1.09	1.21	1.04	1.35
0.4	1.25	1.68	1.36	1.66
0.2	1.53	3.22	2.55	2.73
0.1	1.73	6.39	5.03	5.12
0.01	1.97	63.7	50.0	50.0

Table 2.2: **Matlab program to generate Table 2.1**

```
% Uses the Control toolbox
tau=1;zeta=0.1;t=0:0.01:100;
T = tf(1,[tau*tau 2*tau*zeta 1]); S = 1-T;
[A,B,C,D]=ssdata(T); y = step(A,B,C,D,1,t);
overshoot=max(y),tv=sum(abs(diff(y)))
Mt=norm(T,inf,1e-4),Ms=norm(S,inf,1e-4)
```

2.4.5 Bandwidth and crossover frequency

The concept of bandwidth is very important in understanding the benefits and trade-offs involved when applying feedback control. Above we considered peaks of closed-loop transfer functions, M_S and M_T, which are related to the quality of the response. However, for performance we must also consider the speed of the response, and this leads to considering the bandwidth frequency of the system. In general, a large bandwidth corresponds to a smaller rise time, since high-frequency signals are more easily passed on to the outputs. A high bandwidth also indicates a system which is sensitive to noise. Conversely, if the bandwidth is small, the time response will generally be slow, and the system will usually be more robust.

Loosely speaking, *bandwidth* may be defined as the frequency range $[\omega_1, \omega_2]$ over which control is effective. In most cases we require tight control at steady-state so $\omega_1 = 0$, and we then simply call $\omega_2 = \omega_B$ the bandwidth.

The word "effective" may be interpreted in different ways, and this may give rise to different definitions of bandwidth. The interpretation we use is that control is *effective* if we obtain some *benefit* in terms of performance. For tracking performance the error is $e = y - r = -Sr$ and we get that feedback is effective (in terms of improving performance) as long as the relative error $|e|/|r| = |S|$ is reasonably small, which we may define to be $|S| \leq 0.707$.[4] We then get the following definition:

Definition 2.1 *The (closed-loop) bandwidth, ω_B, is the frequency where $|S(j\omega)|$ first crosses $1/\sqrt{2} = 0.707$ (≈ -3 dB) from below.*

Remark. Another interpretation is to say that control is *effective* if it significantly *changes* the output

[4] The reason for choosing the value 0.707 when defining the bandwidth ω_B is that, for the simple case of a first-order closed-loop response with $S = s/(s+a)$, the low-frequency asymptote s/a of S crosses magnitude 1 at frequency $\omega = a$, and at this frequency $|S(j\omega)| = 1/\sqrt{2} = 0.707$.

response. For tracking performance, the output is $y = Tr$ and since without control $T = 0$, we may say that control is effective as long as T is reasonably large, which we may define to be larger than 0.707. This leads to an alternative definition which has been traditionally used to define the bandwidth of a control system: *The bandwidth in terms of T, ω_{BT}, is the highest frequency at which $|T(j\omega)|$ crosses $1/\sqrt{2} = 0.707$ (≈ -3 dB) from above.* However, we would argue that this alternative definition, although being closer to how the term is used in some other fields, is less useful for feedback control.

The *gain crossover frequency*, ω_c, defined as the frequency where $|L(j\omega_c)|$ first crosses 1 from above, is also sometimes used to define closed-loop bandwidth. It has the advantage of being simple to compute and usually gives a value between ω_B and ω_{BT}. Specifically, for systems with PM $< 90^\circ$ (most practical systems) we have

$$\omega_B < \omega_c < \omega_{BT} \tag{2.53}$$

Proof of (2.53): Note that $|L(j\omega_c)| = 1$ so $|S(j\omega_c)| = |T(j\omega_c)|$. Thus, when PM $= 90^\circ$ we get $|S(j\omega_c)| = |T(j\omega_c)| = 0.707$ (see (2.50)), and we have $\omega_B = \omega_c = \omega_{BT}$. For PM $< 90^\circ$ we get $|S(j\omega_c)| = |T(j\omega_c)| > 0.707$, and since ω_B is the frequency where $|S(j\omega)|$ crosses 0.707 from below we must have $\omega_B < \omega_c$. Similarly, since ω_{BT} is the frequency where $|T(j\omega)|$ crosses 0.707 from above, we must have $\omega_{BT} > \omega_c$. □

From this we have that the situation is generally as follows: Up to the frequency ω_B, $|S|$ is less than 0.7 and control is effective in terms of improving performance. In the frequency range $[\omega_B, \omega_{BT}]$ control still affects the response, but does not improve performance – in most cases we find that in this frequency range $|S|$ is larger than 1 and control degrades performance. Finally, at frequencies higher than ω_{BT} we have $S \approx 1$ and control has no significant effect on the response. The situation just described is illustrated in Example 2.7 below (see Figure 2.18).

Example 2.4 (pages 28 and 34) continued. *The plant $G(s) = \frac{3(-2s+1)}{(10s+1)(5s+1)}$ has a RHP-zero and the Ziegler–Nichols PI tunings ($K_c = 1.14, \tau_I = 12.7$) are quite aggressive with GM $= 1.63$ and PM $= 19.4^o$. The bandwidth and crossover frequencies are $\omega_B = 0.14, \omega_c = 0.24$ and $\omega_{BT} = 0.44$, which is in agreement with (2.53).*

Example 2.6 *Consider the simple case of a first-order closed-loop system,*

$$L(s) = \frac{k}{s}, \quad S(s) = \frac{s}{s+k}; \quad T(s) = \frac{k}{s+k}$$

In this ideal case, all bandwidth and crossover frequencies are identical: $\omega_c = \omega_B = \omega_{BT} = k$. Furthermore, the phase of L remains constant at -90^o, so PM $= 90^o$, $\omega_{180} = \infty$ (or really undefined) and GM $= \infty$.

Example 2.7 Comparison of ω_B and ω_{BT} as indicators of performance. *An example where ω_{BT} is a poor indicator of performance is the following (we are* not *suggesting this as a good controller design!):*

$$L = \frac{-s+z}{s(\tau s + \tau z + 2)}; \quad T = \frac{-s+z}{s+z}\frac{1}{\tau s+1}; \quad z = 0.1,\ \tau = 1 \tag{2.54}$$

For this system, both L and T have a RHP-zero at $z = 0.1$, and we have $GM = 2.1$, $PM = 60.1^\circ$, $M_S = 1.93$ and $M_T = 1$. We find that $\omega_B = 0.036$ and $\omega_c = 0.054$ are both less than $z = 0.1$ (as one should expect because speed of response is limited by the presence of RHP-zeros), whereas $\omega_{BT} = 1/\tau = 1.0$ is ten times larger than z. The closed-loop response to a unit step change in the reference is shown in Figure 2.17. The rise time is 31.0 s, which is close to $1/\omega_B = 28.0$ s, but very

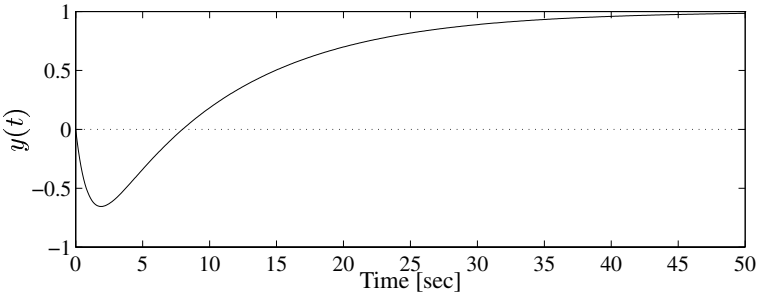

Figure 2.17: Step response for system $T = \frac{-s+0.1}{s+0.1}\frac{1}{s+1}$

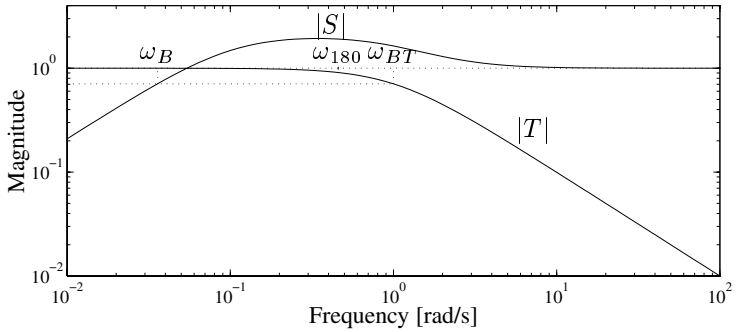

Figure 2.18: Plots of $|S|$ and $|T|$ for system $T = \frac{-s+0.1}{s+0.1}\frac{1}{s+1}$

different from $1/\omega_{BT} = 1.0$ *s, illustrating that* ω_B *is a better indicator of closed-loop performance than* ω_{BT}.

The magnitude Bode plots of S *and* T *are shown in Figure 2.18. We see that* $|T| \approx 1$ *up to about* ω_{BT}. *However, in the frequency range from* ω_B *to* ω_{BT} *the phase of* T *(not shown) drops from about* -40° *to about* -220°, *so in practice tracking is out of phase and control is poor in this frequency range.*

In conclusion, ω_B (which is defined in terms of $|S|$) and ω_c (in terms of $|L|$) are good indicators of closed-loop performance, while ω_{BT} (in terms of $|T|$) may be misleading in some cases. The reason is that we want $T \approx 1$ in order to have good performance, and it is not sufficient that $|T| \approx 1$; we must also consider its phase. On the other hand, for good performance we want S close to 0, and this will be the case if $|S| \approx 0$ irrespective of the phase of S.

2.5 Controller design

Many methods exist for controller design and some of these will be discussed in Chapter 9. In addition to heuristic rules and on-line tuning we can distinguish between three main approaches to controller design:

1. **Shaping of transfer functions.** In this approach the designer specifies the *magnitude* of some transfer function(s) as a function of frequency, and then finds a controller which gives the desired shape(s).
   (a) **Loop shaping.** This is the classical approach in which the magnitude of the open-loop transfer function, $L(j\omega)$, is shaped. Usually no optimization is involved and the designer aims to obtain $|L(j\omega)|$ with desired bandwidth, slopes, etc. We will look at this approach in detail later in Section 2.6. However, classical loop shaping is difficult to apply for complicated systems, and one may then instead use the Glover–McFarlane $\mathcal{H}_\infty$ loop-shaping design presented in Chapter 9. The method consists of a second step where optimization is used to make an initial loop-shaping design more robust.
   (b) **Shaping of closed-loop transfer functions, such as S, T and KS.** One analytical approach is the internal model control (IMC) design procedure, where one aims to specify directly $T(s)$. This works well for simple systems and is discussed in Section 2.7. However, optimization is more generally used, resulting in various $\mathcal{H}_\infty$ optimal control problems such as mixed weighted sensitivity; see Section 2.8 and later chapters.
2. **The signal-based approach.** This involves time domain problem formulations resulting in the minimization of a norm of a transfer function. Here one considers a particular disturbance or reference change and then one tries to optimize the closed-loop response. The "modern" state-space methods from the 1960's, such as linear quadratic Gaussian (LQG) control, are based on this signal-oriented approach. In LQG the input signals are assumed to be stochastic (or alternatively impulses in a deterministic setting) and the expected value of the output variance (or the 2-norm) is minimized. These methods may be generalized to include frequency-dependent weights on the signals leading to what is called the Wiener–Hopf (or $\mathcal{H}_2$ norm) design method.

   By considering sinusoidal signals, frequency by frequency, a signal-based $\mathcal{H}_\infty$ optimal control methodology can be derived in which the $\mathcal{H}_\infty$ norm of a combination of closed-loop transfer functions is minimized. This approach has attracted significant interest, and may be combined with model uncertainty representations to yield quite complex robust performance problems requiring μ-synthesis, an important topic which will be addressed in later chapters.

   In approaches 1 and 2, the overall design process is iterative between controller design and performance (or cost) evaluation. If performance is not satisfactory then one must either adjust the controller parameters directly (e.g. by reducing K_c from the value obtained by the Ziegler–Nichols rules) or adjust some weighting factor in the objective function used to synthesize the controller.
3. **Numerical optimization.** This often involves attempts to optimize directly the true objectives, such as minimizing the rise time subject to satisfying given values for the stability margins, etc. Computationally, such optimization problems may be difficult to solve, especially if one does not have convexity in the controller parameters. Also, by effectively including performance evaluation and controller design in a single-step procedure, the problem formulation is far more critical than in iterative two-step approaches.

The above *off-line* methods are used to precompute a feedback controller which is later implemented on the plant. This is the main focus of this book. In addition, there exist computational methods where the optimization problem is solved *on-line*. These methods

are well suited for certain nonlinear problems where an explicit feedback controller does not exist or is difficult to obtain. For example, in the process industry, *model predictive control* is used to handle problems with constraints on the inputs and outputs. On-line optimization approaches are expected to become more popular in the future as faster computers and more efficient and reliable computational algorithms are developed.

2.6 Loop shaping

In the classical loop-shaping approach to feedback controller design, "loop shape" refers to the magnitude of the loop transfer function $L = GK$ as a function of frequency. An understanding of how K can be selected to shape this loop gain provides invaluable insight into the multivariable techniques and concepts which will be presented later in the book, and so we will discuss loop shaping in some detail in this section.

2.6.1 Trade-offs in terms of L

Recall (2.20), which yields the closed-loop response in terms of the control error $e = y - r$:

$$e = -\underbrace{(I+L)^{-1}}_{S} r + \underbrace{(I+L)^{-1}}_{S} G_d d - \underbrace{(I+L)^{-1}L}_{T} n \tag{2.55}$$

For "perfect control" we want $e = y - r = 0$; that is, we would like

$$e \approx 0 \cdot d + 0 \cdot r + 0 \cdot n$$

The first two requirements in this equation, namely disturbance rejection and command tracking, are obtained with $S \approx 0$, or equivalently, $T \approx I$. Since $S = (I + L)^{-1}$, this implies that the loop transfer function L must be large in magnitude. On the other hand, the requirement for zero noise transmission implies that $T \approx 0$, or equivalently, $S \approx I$, which is obtained with $L \approx 0$. This illustrates the fundamental nature of feedback design which always involves a trade-off between conflicting objectives; in this case between large loop gains for disturbance rejection and tracking, and small loop gains to reduce the effect of noise.

It is also important to consider the magnitude of the control action u (which is the input to the plant). We want u small because this causes less wear and saves input energy, and also because u is often a disturbance to other parts of the system (e.g. consider opening a window in your office to adjust your comfort and the undesirable disturbance this will impose on the air conditioning system for the building). In particular, we usually want to avoid fast changes in u. The control action is given by $u = K(r - y_m)$ and we find as expected that a small u corresponds to small controller gains and a small $L = GK$.

The most important design objectives which necessitate trade-offs in feedback control are summarized below:

1. Performance, good disturbance rejection: needs large controller gains, i.e. L large.
2. Performance, good command following: L large.
3. Stabilization of unstable plant: L large.
4. Mitigation of measurement noise on plant outputs: L small.
5. Small magnitude of input signals: K small and L small.

6. Physical system must be strictly proper: L has to approach 0 at high frequencies.
7. Stability (stable plant): L small.

Fortunately, the conflicting design objectives mentioned above are generally in different frequency ranges, and we can meet most of the objectives by using a large loop gain ($|L| > 1$) at low frequencies below crossover, and a small gain ($|L| < 1$) at high frequencies above crossover.

2.6.2 Fundamentals of loop-shaping design

By *loop shaping* we mean a design procedure that involves explicitly shaping the magnitude of the loop transfer function, $|L(j\omega)|$. Here $L(s) = G(s)K(s)$ where $K(s)$ is the feedback controller to be designed and $G(s)$ is the product of all other transfer functions around the loop, including the plant, the actuator and the measurement device. Essentially, to get the benefits of feedback control we want the loop gain, $|L(j\omega)|$, to be as large as possible within the bandwidth region. However, due to time delays, RHP-zeros, unmodelled high-frequency dynamics and limitations on the allowed manipulated inputs, the loop gain has to drop below 1 at and above some frequency which we call the crossover frequency ω_c. Thus, disregarding stability for the moment, it is desirable that $|L(j\omega)|$ falls sharply with frequency. To measure how $|L|$ falls with frequency we consider the logarithmic slope $N = d\ln|L|/d\ln\omega$. For example, a slope $N = -1$ implies that $|L|$ drops by a factor of 10 when ω increases by a factor of 10. If the gain is measured in decibels (dB) then a slope of $N = -1$ corresponds to -20 dB/ decade. The value of $-N$ at high frequencies is often called the *roll-off* rate.

The design of $L(s)$ is most crucial and difficult in the crossover region between ω_c (where $|L| = 1$) and ω_{180} (where $\angle L = -180^\circ$). For stability, we at least need the loop gain to be less than 1 at frequency ω_{180}, i.e. $|L(j\omega_{180})| < 1$. Thus, to get a high bandwidth (fast response) we want ω_c and therefore ω_{180} large; that is, we want the phase lag in L to be small. Unfortunately, this is not consistent with the desire that $|L(j\omega)|$ should fall sharply. For example, the loop transfer function $L = 1/s^n$ (which has a slope $N = -n$ on a log–log plot) has a phase $\angle L = -n \cdot 90^\circ$. Thus, to have a PM of 45° we need $\angle L > -135^\circ$, and the slope of $|L|$ cannot exceed $N = -1.5$.

In addition, if the slope is made steeper at lower or higher frequencies, then this will add unwanted phase lag at intermediate frequencies. As an example, consider $L_1(s)$ given in (2.14) with the Bode plot shown in Figure 2.3 on page 20. Here the slope of the asymptote of $|L|$ is -1 at the gain crossover frequency (where $|L_1(j\omega_c)| = 1$), which by itself gives -90° phase lag. However, due to the influence of the steeper slopes of -2 at lower and higher frequencies, there is a "penalty" of about -35° at crossover, so the actual phase of L_1 at ω_c is approximately -125°.

The situation becomes even worse for cases with delays or RHP-zeros in $L(s)$ which add undesirable phase lag to L without contributing to a desirable negative slope in L. At the gain crossover frequency ω_c, the additional phase lag from delays and RHP-zeros may in practice be -30° or more.

In summary, a desired loop shape for $|L(j\omega)|$ typically has a slope of about -1 in the crossover region, and a slope of -2 or higher beyond this frequency; that is, the roll-off is 2 or larger. Also, with a proper controller, which is required for any real system, we must have that $L = GK$ rolls off at least as fast as G. At low frequencies, the desired shape of $|L|$ depends on what disturbances and references we are designing for. For example, if we are considering step changes in the references or disturbances which affect the outputs as steps,

then a slope for $|L|$ of -1 at low frequencies is acceptable. If the references or disturbances require the outputs to change in a ramp-like fashion then a slope of -2 is required. In practice, integrators are included in the controller to get the desired low-frequency performance, and for offset-free reference tracking the rule is that

- *$L(s)$ must contain at least one integrator for each integrator in $r(s)$.*

Proof: Let $L(s) = \widehat{L}(s)/s^{n_I}$ where $\widehat{L}(0)$ is non-zero and finite and n_I is the number of integrators in $L(s)$ – sometimes n_I is called the *system type*. Consider a reference signal of the form $r(s) = 1/s^{n_r}$. For example, if $r(t)$ is a unit step, then $r(s) = 1/s$ ($n_r = 1$), and if $r(t)$ is a ramp then $r(s) = 1/s^2$ ($n_r = 2$). The final value theorem for Laplace transforms is

$$\lim_{t\to\infty} e(t) = \lim_{s\to 0} se(s) \tag{2.56}$$

In our case, the control error is

$$e(s) = -\frac{1}{1+L(s)}r(s) = -\frac{s^{n_I-n_r}}{s^{n_I}+\widehat{L}(s)} \tag{2.57}$$

and to get zero offset (i.e. $e(t\to\infty) = 0$) we must from (2.56) require that $n_I \geq n_r$, and the rule follows. □

In conclusion, one can define the desired loop transfer function in terms of the following specifications:

1. The gain crossover frequency, ω_c, where $|L(j\omega_c)| = 1$.
2. The shape of $L(j\omega)$, e.g. in terms of the slope of $|L(j\omega)|$ in certain frequency ranges. Typically, we desire a slope of about $N = -1$ around crossover, and a larger roll-off at higher frequencies. The desired slope at lower frequencies depends on the nature of the disturbance or reference signal.
3. The system type, defined as the number of pure integrators in $L(s)$.

In Section 2.6.4, we discuss how to specify the loop shape when disturbance rejection is the primary objective of control. Loop-shaping design is typically an iterative procedure where the designer shapes and reshapes $|L(j\omega)|$ after computing the PM and GM, the peaks of closed-loop frequency responses (M_T and M_S), selected closed-loop time responses, the magnitude of the input signal, etc. The procedure is illustrated next by an example.

Example 2.8 Loop-shaping design for the inverse response process. *We will now design a loop-shaping controller for the example process in (2.31) which has a RHP-zero at $s = 0.5$. The RHP-zero cannot be cancelled by the controller, because otherwise the system is internally unstable. Thus L must contain the RHP-zeros of G. In addition, the RHP-zero limits the achievable bandwidth and so the crossover region (defined as the frequencies between ω_c and ω_{180}) will be at about 0.5 rad/s. We require the system to have one integrator (type 1 system), and therefore a reasonable approach is to let the loop transfer function have a slope of -1 at low frequencies, and then to roll off with a higher slope at frequencies beyond 0.5 rad/s. The plant and our choice for the loop shape is*

$$G(s) = \frac{3(-2s+1)}{(10s+1)(5s+1)}; \quad L(s) = 3K_c\frac{(-2s+1)}{s(2s+1)(0.33s+1)} \tag{2.58}$$

The frequency response (Bode plots) of L is shown in Figure 2.19 for $K_c = 0.05$. The controller gain K_c was selected to get reasonable stability margins (PM and GM). The asymptotic slope of $|L|$ is -1 up to 3 rad/s where it changes to -2. The controller corresponding to the loop shape in (2.58) is

$$K(s) = K_c\frac{(10s+1)(5s+1)}{s(2s+1)(0.33s+1)}, \quad K_c = 0.05 \tag{2.59}$$

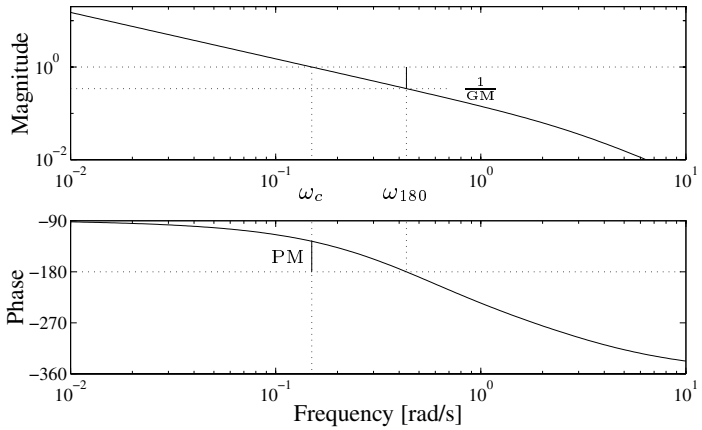

Figure 2.19: Frequency response of $L(s)$ in (2.58) for loop-shaping design with $K_c = 0.05$ ($GM = 2.92$, $PM = 54^\circ$, $\omega_c = 0.15$, $\omega_{180} = 0.43$, $M_S = 1.75$, $M_T = 1.11$)

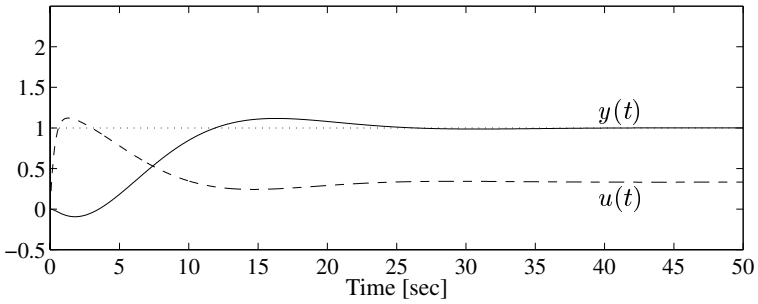

Figure 2.20: Response to step in reference for loop-shaping design (2.59)

The controller has zeros at the locations of the plant poles. This is desired in this case because we do not want the slope of the loop shape to drop at the break frequencies $1/10 = 0.1$ *rad/s and* $1/5 = 0.2$ *rad/s just before crossover. The phase of* L *is* -90° *at low frequency, and at* $\omega = 0.5$ *rad/s the additional contribution from the term* $\frac{-2s+1}{2s+1}$ *in (2.58) is* -90°*, so for stability we need* $\omega_c < 0.5$ *rad/s. The choice* $K_c = 0.05$ *yields* $\omega_c = 0.15$ *rad/s corresponding to* $GM = 2.92$ *and* $PM = 54^\circ$*. The corresponding time response is shown in Figure 2.20. It is seen to be much better than the responses with either the simple PI controller in Figure 2.8 (page 28) or with the P controller in Figure 2.6 (page 26). Figure 2.20 also shows that the magnitude of the input signal remains less than* 1 *in magnitude most of the time. This means that the controller gain is not too large at high frequencies. The magnitude Bode plot for the controller (2.59) is shown in Figure 2.21. It is interesting to note that in the crossover region around* $\omega = 0.5$ *rad/s the controller gain is quite constant, around* 1 *in magnitude, which is similar to the "best" gain found using a P controller (see Figure 2.6).*

Limitations imposed by RHP-zeros and time delays

Based on the above loop-shaping arguments we can now examine how the presence of delays and RHP-zeros limits the achievable control performance. We have already argued that if

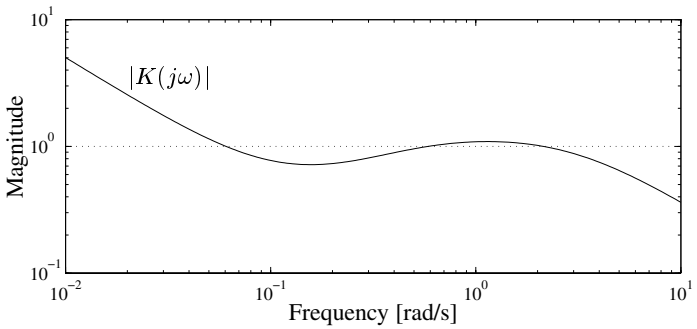

Figure 2.21: Magnitude Bode plot of controller (2.59) for loop-shaping design

we want the loop shape to have a slope of -1 around crossover (ω_c), with preferably a steeper slope before and after crossover, then the phase lag of L at ω_c will necessarily be at least -90°, even when there are no RHP-zeros or delays. Therefore, if we assume that for performance and robustness we want a PM of about 35° or more, then the additional phase contribution from any delays and RHP-zeros at frequency ω_c cannot exceed about -55°.

First consider a time delay θ. It yields an additional phase contribution of $-\theta\omega$, which at frequency $\omega = 1/\theta$ is -1 rad = -57° (which is slightly more than -55°). Thus, for acceptable control performance we need $\omega_c < 1/\theta$, approximately.

Next consider a real RHP-zero at $s = z$. To avoid an increase in slope caused by this zero we place a pole at $s = -z$ such that the loop transfer function contains the term $\frac{-s+z}{s+z}$, the form of which is referred to as all-pass since its magnitude equals 1 at all frequencies. The phase contribution from the all-pass term at $\omega = z/2$ is $-2\arctan(0.5) = -53^\circ$ (which is very close to -55°), so for acceptable control performance we need $\omega_c < z/2$, approximately.

2.6.3 Inverse-based controller design

In Example 2.6.2, we made sure that $L(s)$ contained the RHP-zero of $G(s)$, but otherwise the specified $L(s)$ was independent of $G(s)$. This suggests the following possible approach for a minimum-phase plant (i.e. one with no RHP-zeros or time delays). We select a loop shape which has a slope of -1 throughout the frequency range, namely

$$L(s) = \frac{\omega_c}{s} \tag{2.60}$$

where ω_c is the desired gain crossover frequency. This loop shape yields a PM of 90° and an infinite GM since the phase of $L(j\omega)$ never reaches -180°. The controller corresponding to (2.60) is

$$K(s) = \frac{\omega_c}{s} G^{-1}(s) \tag{2.61}$$

That is, the controller inverts the plant and adds an integrator ($1/s$). This is an old idea, and is also the essential part of the internal model control (IMC) design procedure (Morari and Zafiriou, 1989) (page 55), which has proved successful in many applications. However, there are at least three good reasons why this inverse-based controller may not be a good choice:

1. RHP-zeros or a time delay in $G(s)$ cannot be inverted.
2. The controller will not be realizable if $G(s)$ has a pole excess of two or larger, and may in any case yield large input signals. These problems may be partly fixed by adding high-frequency dynamics to the controller.
3. The loop shape resulting from (2.60) and (2.61) is *not* generally desirable, unless the references and disturbances affect the outputs as steps. This is illustrated by the following example.

Example 2.9 Disturbance process. *We now introduce our second SISO example control problem in which disturbance rejection is an important objective in addition to command tracking. We assume that the plant has been appropriately scaled as outlined in Section 1.4.*

Problem formulation. *Consider the disturbance process described by*

$$\boxed{G(s) = \frac{200}{10s+1}\frac{1}{(0.05s+1)^2}, \quad G_d(s) = \frac{100}{10s+1}} \tag{2.62}$$

with time in seconds (a block diagram is shown in Figure 2.23 below). The control objectives are:

1. *Command tracking: The rise time (to reach 90% of the final value) should be less than 0.3 s and the overshoot should be less than 5%.*
2. *Disturbance rejection: The output in response to a unit step disturbance should remain within the range $[-1, 1]$ at all times, and it should return to 0 as quickly as possible ($|y(t)|$ should at least be less than 0.1 after 3 s).*
3. *Input constraints: $u(t)$ should remain within the range $[-1, 1]$ at all times to avoid input saturation (this is easily satisfied for most designs).*

Analysis. *Since $G_d(0) = 100$ we have that without control the output response to a unit disturbance ($d = 1$) will be 100 times larger than what is deemed to be acceptable. The magnitude $|G_d(j\omega)|$ is lower at higher frequencies, but it remains larger than 1 up to $\omega_d \approx 10$ rad/s (where $|G_d(j\omega_d)| = 1$). Thus, feedback control is needed up to frequency ω_d, so we need ω_c to be approximately equal to 10 rad/s for disturbance rejection. On the other hand, we do not want ω_c to be larger than necessary because of sensitivity to noise and stability problems associated with high-gain feedback. We will thus aim at a design with $\omega_c \approx 10$ rad/s.*

Inverse-based controller design. *We will consider the inverse-based design as given by (2.60) and (2.61) with $\omega_c = 10$. Since $G(s)$ has a pole excess of three this yields an unrealizable controller, and therefore we choose to approximate the plant term $(0.05s+1)^2$ by $(0.1s+1)$ and then in the controller we let this term be effective over one decade, i.e. we use $(0.1s+1)/(0.01s+1)$ to give the realizable design*

$$K_0(s) = \frac{\omega_c}{s}\frac{10s+1}{200}\frac{0.1s+1}{0.01s+1}, \; L_0(s) = \frac{\omega_c}{s}\frac{0.1s+1}{(0.05s+1)^2(0.01s+1)}, \; \omega_c = 10 \tag{2.63}$$

The response to a step reference is excellent as shown in Figure 2.22(a). The rise time is about 0.16 s and there is no overshoot so the specifications are more than satisfied. However, the response to a step disturbance (Figure 2.22(b)) is much too sluggish. Although the output stays within the range $[-1, 1]$, it is still 0.75 at $t = 3$ s (whereas it should be less than 0.1). Because of the integral action the output does eventually return to zero, but it does not drop below 0.1 until after 23 s.

The above example illustrates that the simple inverse-based design method, where L has a slope of about $N = -1$ at all frequencies, does not always yield satisfactory designs. In the example, reference tracking was excellent, but disturbance rejection was poor. The objective of the next section is to understand why the disturbance response was so poor, and to propose a more desirable loop shape for disturbance rejection.

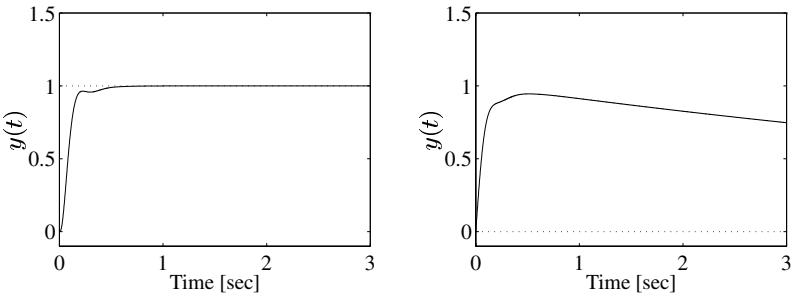

(a) Tracking response (b) Disturbance response

Figure 2.22: Responses with "inverse-based" controller $K_0(s)$ for the disturbance process

2.6.4 Loop shaping for disturbance rejection

At the outset we assume that the disturbance has been scaled such that at each frequency $|d(\omega)| \leq 1$, and the main control objective is to achieve $|e(\omega)| < 1$. With feedback control we have $e = y = SG_d d$, so to achieve $|e(\omega)| < 1$ for $|d(\omega)| = 1$ (the worst-case disturbance) we require $|SG_d(j\omega)| < 1, \forall\omega$, or equivalently,

$$|1 + L| > |G_d| \quad \forall\omega \tag{2.64}$$

At frequencies where $|G_d| > 1$, this is approximately the same as requiring $|L| > |G_d|$. However, in order to minimize the input signals, thereby reducing the sensitivity to noise and avoiding stability problems, we do not want to use larger loop gains than necessary (at least at frequencies around crossover). A reasonable initial loop shape $L_{\min}(s)$ is then one that just satisfies the condition

$$|L_{\min}| \approx |G_d| \tag{2.65}$$

where the subscript min signifies that $L_{\min}$ is the smallest loop gain to satisfy $|e(\omega)| < 1$. Since $L = GK$, the controller must satisfy

$$|K| > |K_{\min}| \approx |G^{-1}G_d| \tag{2.66}$$

Note that this bound assumes that the models G and G_d are scaled such that the worst-case disturbance d is of unit magnitude and the desired control error e is less than 1. The implications of the bound are as follows:

- For disturbance rejection a good choice for the controller is one which contains the dynamics (G_d) of the disturbance and inverts the dynamics (G) of the inputs (at least at frequencies just before crossover).
- For disturbances entering directly at the plant output, $G_d = 1$, we get $|K_{\min}| = |G^{-1}|$, so an inverse-based design provides the best trade-off between performance (disturbance rejection) and minimum use of feedback.
- For disturbances entering directly at the plant input (which is a common situation in practice – often referred to as a load disturbance), we have $G_d = G$ and we get $|K_{\min}| = 1$, so a simple proportional controller with unit gain yields a good trade-off between output performance and input usage.

- Notice that a reference change may be viewed as a disturbance directly affecting the output. This follows from (1.18), from which we get that a maximum reference change $r = R$ may be viewed as a disturbance $d = 1$ with $G_d(s) = -R$ where R is usually a constant. This explains why selecting K to be like G^{-1} (an inverse-based controller) yields good responses to step changes in the reference.

In addition to satisfying $|L| \approx |G_d|$ (see (2.65)) at frequencies around crossover, the desired loop shape $L(s)$ may be modified as follows:

1. Increase the loop gain at low frequencies to improve the performance. For example, we could use
$$|K| = k \cdot \left| \frac{s + \omega_I}{s} \right| \cdot \left| G^{-1} G_d \right| \tag{2.67}$$
where $k > 1$ is used to speed up the response, and the integrator term is added to get zero steady-state offset to a step disturbance.
2. Around crossover make the slope N of $|L|$ to be about -1. This is to achieve good transient behaviour with acceptable GM and PM.
3. Let $L(s)$ roll off faster at higher frequencies (beyond the bandwidth) in order to reduce the use of manipulated inputs, to make the controller realizable and to reduce the effects of noise.

The above requirements are concerned with the magnitude, $|L(j\omega)|$. In addition, the dynamics (phase) of $L(s)$ must be selected such that the closed-loop system is stable. When selecting $L(s)$ to satisfy $|L| \approx |G_d|$ one should replace $G_d(s)$ by the corresponding minimum-phase transfer function with the same magnitude; that is, time delays and RHP-zeros in $G_d(s)$ should not be included in $L(s)$ as this will impose undesirable limitations on feedback. On the other hand, any time delays or RHP-zeros in $G(s)$ must be included in $L = GK$ because RHP pole–zero cancellations between $G(s)$ and $K(s)$ yield internal instability; see Chapter 4. The final feedback controller has the form

$$K(s) = kw(s)G(s)^{-1}G_d(s) \tag{2.68}$$

where $w(s)$ incorporates the various shaping and stabilizing ideas introduced above. Usually, $w(s)$ is also selected with the aim of getting a simple final controller $K(s)$.

Remark. The idea of including a disturbance model in the controller is well known and is more rigorously presented in, for example, research on the internal model principle (Wonham, 1974), or the internal model control design for disturbances (Morari and Zafiriou, 1989). However, our development is simple and sufficient for gaining the insight needed for later chapters.

Example 2.10 Loop-shaping design for the disturbance process. *Consider again the plant described by (2.62). The plant can be represented by the block diagram in Figure 2.23, and we see that the disturbance enters at the plant input in the sense that G and G_d share the same dominating dynamics as represented by the term $200/(10s + 1)$.*

Step 1. Initial design. *From (2.65) we know that a good initial loop shape looks like $|L_{\min}| = |G_d| = \left| \frac{100}{10s+1} \right|$ at frequencies up to crossover. The corresponding controller is $K(s) = G^{-1}L_{\min} = 0.5(0.05s + 1)^2$. This controller is not proper (i.e. it has more zeros than poles), but since the term $(0.05s + 1)^2$ only comes into effect at $1/0.05 = 20$ rad/s, which is beyond the desired gain crossover frequency $\omega_c = 10$ rad/s, we may replace it by a constant gain of 1 resulting in a proportional controller*

$$K_1(s) = 0.5 \tag{2.69}$$

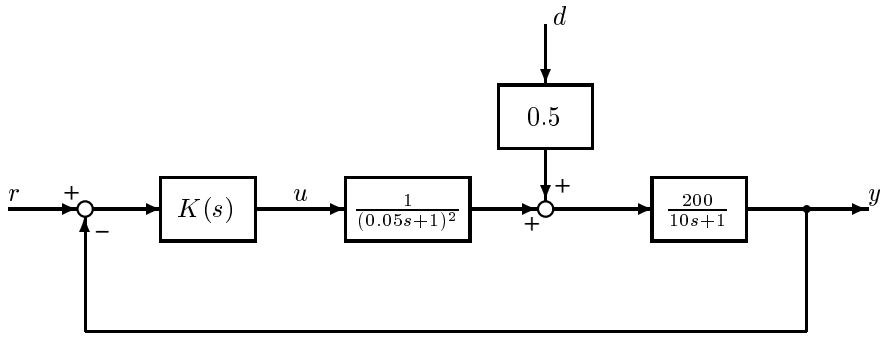

Figure 2.23: Block diagram representation of the disturbance process in (2.62)

The magnitude of the corresponding loop transfer function, $|L_1(j\omega)|$, and the response ($y_1(t)$) to a step change in the disturbance are shown in Figure 2.24. This simple controller works surprisingly well, and for $t < 3$ s the response to a step change in the disturbance is not much different from that with the more complicated inverse-based controller $K_0(s)$ of (2.63) as shown earlier in Figure 2.22. However, there is no integral action and $y_1(t) \to 1$ as $t \to \infty$.

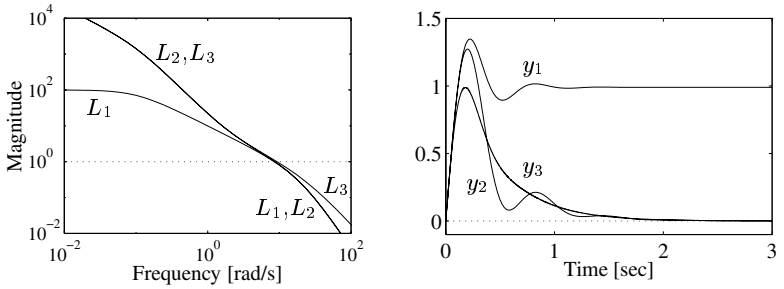

(a) Loop gains (b) Disturbance responses

Figure 2.24: Loop shapes and disturbance responses for controllers K_1, K_2 and K_3 for the disturbance process

Step 2. More gain at low frequency. *To get integral action we multiply the controller by the term $\frac{s+\omega_I}{s}$, see (2.67), where ω_I is the frequency up to which the term is effective (the asymptotic value of the term is 1 for $\omega > \omega_I$). For performance we want large gains at low frequencies, so we want ω_I to be large, but in order to maintain an acceptable PM (which is 44.7° for controller K_1) the term should not add too much negative phase at frequency ω_c, so ω_I should not be too large. A reasonable value is $\omega_I = 0.2\omega_c$ for which the phase contribution from $\frac{s+\omega_I}{s}$ is $\arctan(1/0.2) - 90^\circ = -11^\circ$ at ω_c. In our case $\omega_c \approx 10$ rad/s, so we select the following controller:*

$$K_2(s) = 0.5\frac{s+2}{s} \tag{2.70}$$

The resulting disturbance response (y_2) shown in Figure 2.24(b) satisfies the requirement that $|y(t)| < 0.1$ at time $t = 3$ s, but $y(t)$ exceeds 1 for a short time. Also, the response is slightly oscillatory as might be expected since the PM is only 31° and the peak values for $|S|$ and $|T|$ are $M_S = 2.28$ and $M_T = 1.89$.

Step 3. High-frequency correction. *To increase the PM and improve the transient response we supplement the controller with "derivative action" by multiplying $K_2(s)$ by a lead–lag term which is effective over one decade starting at* 20 *rad/s:*

$$K_3(s) = 0.5\frac{s+2}{s}\,\frac{0.05s+1}{0.005s+1} \tag{2.71}$$

This gives a PM of 51°*, and peak values* $M_S = 1.43$ *and* $M_T = 1.23$*. From Figure 2.24(b), it is seen that the controller* $K_3(s)$ *reacts quicker than* $K_2(s)$ *and the disturbance response* $y_3(t)$ *stays below* 1.

Table 2.3: Alternative loop-shaping designs for the disturbance process

						Reference		Disturbance	
	GM	PM	ω_c	M_S	M_T	t_r	$y_{\max}$	$y_{\max}$	$y(t=3)$
Spec.$\rightarrow$			≈ 10			≤ 0.3	≤ 1.05	≤ 1	≤ 0.1
K_0	9.95	72.9°	11.4	1.34	1	0.16	1.00	0.95	0.75
K_1	4.04	44.7°	8.48	1.83	1.33	0.21	1.24	1.35	0.99
K_2	3.24	30.9°	8.65	2.28	1.89	0.19	1.51	1.27	0.001
K_3	19.7	50.9°	9.27	1.43	1.23	0.16	1.24	0.99	0.001

Table 2.3 summarizes the results for the four loop-shaping designs; the inverse-based design K_0 *for reference tracking and the three designs* K_1, K_2 *and* K_3 *for disturbance rejection. Although controller* K_3 *satisfies the requirements for disturbance rejection, it is* not *satisfactory for reference tracking; the overshoot is* 24% *which is significantly higher than the maximum value of* 5%*. On the other hand, the inverse-based controller* K_0 *inverts the term* $1/(10s+1)$ *which is also in the disturbance model, and therefore yields a very sluggish response to disturbances (the output is still* 0.75 *at* $t = 3$ *s whereas it should be less than* 0.1*).*

In summary, for this process none of the controller designs meet all the objectives for both reference tracking and disturbance rejection. The solution is to use a two degrees-of-freedom controller as discussed next.

2.6.5 Two degrees-of-freedom design

For reference tracking we typically want the controller to look like $\frac{1}{s}G^{-1}$, see (2.61), whereas for disturbance rejection we want the controller to look like $\frac{1}{s}G^{-1}G_d$, see (2.67). We cannot generally achieve both of these simultaneously with a single (feedback) controller.

The solution is to use a two degrees-of-freedom controller where the reference signal r and output measurement y_m are treated independently by the controller, rather than operating on their difference $r-y_m$ as in a one degree-of-freedom controller. There exist several alternative implementations of a two degrees-of-freedom controller. The most general form is shown in Figure 1.3(b) on page 12 where the controller has two inputs (r and y_m) and one output (u). However, the controller is often split into two separate blocks. One form was shown in Figure 2.5, but here we will use the form in Figure 2.25 where K_y denotes the feedback part of the controller and K_r the reference prefilter. The feedback controller K_y is used to reduce the effect of uncertainty (disturbances and model error) whereas the prefilter K_r shapes the commands r to improve tracking performance. In general, it is optimal to design the combined two degrees-of-freedom controller K in one step. However, in practice K_y is often designed first for disturbance rejection, and then K_r is designed to improve reference tracking. This is the approach taken here.

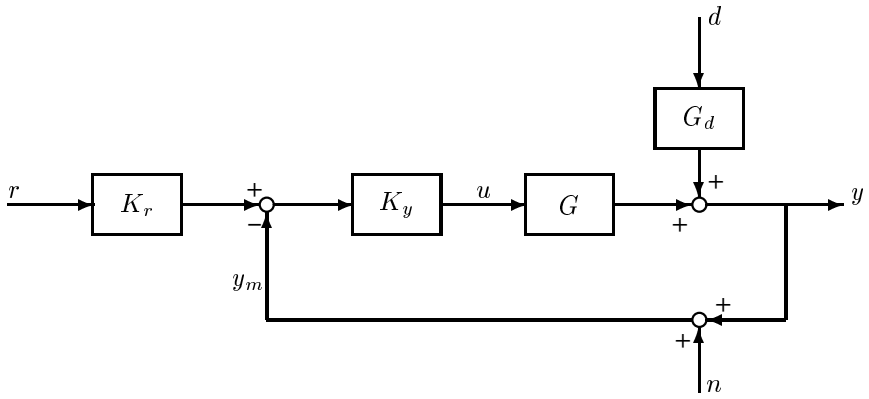

Figure 2.25: Two degrees-of-freedom controller

Let $T = L(1 + L)^{-1}$ (with $L = GK_y$) denote the complementary sensitivity function for the feedback system. Then for a one degree-of-freedom controller $y = Tr$, whereas for a two degrees-of-freedom controller $y = TK_r r$. If the desired transfer function for reference tracking (often denoted the reference model) is $T_{\rm ref}$, then the corresponding ideal reference prefilter K_r satisfies $TK_r = T_{\rm ref}$, or

$$K_r(s) = T^{-1}(s)T_{\rm ref}(s) \tag{2.72}$$

Thus, in theory we may design $K_r(s)$ to get any desired tracking response $T_{\rm ref}(s)$. However, in practice it is not so simple because the resulting $K_r(s)$ may be unstable (if $G(s)$ has RHP-zeros) or unrealizable, and also $TK_r \neq T_{\rm ref}$ if $G(s)$ and thus $T(s)$ is not known exactly.

Remark. A convenient practical choice of prefilter is the lead–lag network

$$K_r(s) = \frac{\tau_{\rm lead}s + 1}{\tau_{\rm lag}s + 1} \tag{2.73}$$

Here we select $\tau_{\rm lead} > \tau_{\rm lag}$ if we want to speed up the response, and $\tau_{\rm lead} < \tau_{\rm lag}$ if we want to slow down the response. If one does not require fast reference tracking, which is the case in many process control applications, a simple lag is often used (with $\tau_{\rm lead} = 0$).

Example 2.11 Two degrees-of-freedom design for the disturbance process. *In Example 2.10 we designed a loop-shaping controller $K_3(s)$ for the plant in (2.62) which gave good performance with respect to disturbances. However, the command tracking performance was not quite acceptable as is shown by y_3 in Figure 2.26. The rise time is 0.16 s which is better than the required value of 0.3 s, but the overshoot is 24% which is significantly higher than the maximum value of 5%. To improve upon this we can use a two degrees-of-freedom controller with $K_y = K_3$, and we design $K_r(s)$ based on (2.72) with reference model $T_{\rm ref} = 1/(0.1s + 1)$ (a first-order response with no overshoot). To get a low-order $K_r(s)$, we either may use the actual $T(s)$ and then use a low-order approximation of $K_r(s)$, or we may start with a low-order approximation of $T(s)$. We will do the latter. From the step response y_3 in Figure 2.26 we approximate the response by two parts: a fast response with time constant 0.1 s and gain 1.5, and a slower response with time constant 0.5 s and gain -0.5 (the sum of the gains is 1). Thus we use $T(s) \approx \frac{1.5}{0.1s+1} - \frac{0.5}{0.5s+1} = \frac{(0.7s+1)}{(0.1s+1)(0.5s+1)}$, from which (2.72) yields $K_r(s) = \frac{0.5s+1}{0.7s+1}$. Following closed-loop simulations we modified this slightly to arrive at the design*

$$K_{r3}(s) = \frac{0.5s + 1}{0.65s + 1} \cdot \frac{1}{0.03s + 1} \tag{2.74}$$

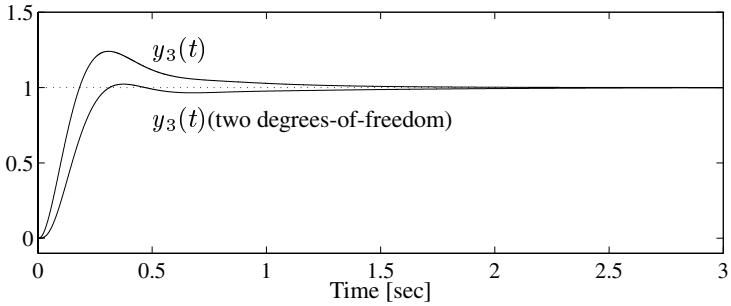

Figure 2.26: Tracking responses with the one degree-of-freedom controller (K_3) and the two degrees-of-freedom controller (K_3, K_{r3}) for the disturbance process

where the term $1/(0.03s + 1)$ *was included to avoid the initial peaking of the input signal* $u(t)$ *above* 1. *The tracking response with this two degrees-of-freedom controller is shown in Figure 2.26. The rise time is* 0.25 *s which is better than the requirement of* 0.3 *s, and the overshoot is only* 2.3% *which is better than the requirement of* 5%. *The disturbance response is the same as curve* y_3 *in Figure 2.24. In conclusion, we are able to satisfy all specifications using a low-order two degrees-of-freedom controller.*

Loop shaping applied to a flexible structure

The following example shows how the loop-shaping procedure for disturbance rejection can be used to design a one degree-of-freedom controller for a very different kind of plant.

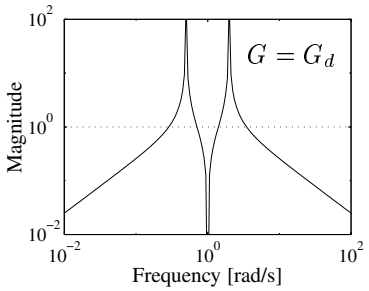

(a) Magnitude plot of $|G| = |G_d|$

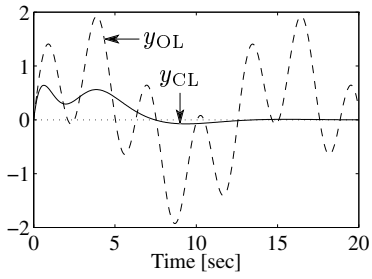

(b) Open-loop and closed-loop disturbance responses with $K = 1$

Figure 2.27: Flexible structure in (2.75)

Example 2.12 Loop shaping for a flexible structure. *Consider the following model of a flexible structure with a disturbance occurring at the plant input:*

$$G(s) = G_d(s) = \frac{2.5s(s^2 + 1)}{(s^2 + 0.5^2)(s^2 + 2^2)} \tag{2.75}$$

From the Bode magnitude plot in Figure 2.27(a) we see that $|G_d(j\omega)| \gg 1$ *around the resonance frequencies of* 0.5 *and* 2 *rad/s, so control is needed at these frequencies. The dashed line in Figure 2.27(b) shows the open-loop response to a unit step disturbance. The output is seen to cycle*

between -2 *and* 2 *(outside the allowed range* -1 *to* 1*), which confirms that control is needed. From (2.66) a controller which meets the specification* $|y(\omega)| \leq 1$ *for* $|d(\omega)| = 1$ *is given by* $|K_{\min}(j\omega)| = |G^{-1}G_d| = 1$*. Indeed the controller*

$$K(s) = 1 \tag{2.76}$$

turns out to be a good choice as is verified by the closed-loop disturbance response (solid line) in Figure 2.27(b); the output goes up to about 0.5 *and then returns to zero. The fact that the choice* $L(s) = G(s)$ *gives closed-loop stability is not immediately obvious since* $|G|$ *has four gain crossover frequencies. However, instability cannot occur because the plant is "passive" with* $\angle G > -180^\circ$ *at all frequencies.*

2.6.6 Conclusions on loop shaping

The loop-shaping procedure outlined and illustrated by the examples above is well suited for relatively simple problems, as might arise for stable plants where $L(s)$ crosses the negative real axis only once. Although the procedure may be extended to more complicated systems the effort required by the engineer is considerably greater. In particular, it may be very difficult to achieve stability.

Fortunately, there exist alternative methods where the burden on the engineer is much less. One such approach is the Glover–McFarlane $\mathcal{H}_\infty$ loop-shaping procedure which is discussed in detail in Chapter 9. It is essentially a two-step procedure, where in the first step the engineer, as outlined in this section, decides on a loop shape, $|L|$ (denoted the "shaped plant" G_s), and in the second step an optimization provides the necessary phase corrections to get a stable and robust design. The method is applied to the disturbance process in Example 9.3 on page 368.

An alternative to shaping the open-loop transfer function $L(s)$ is to shape closed-loop transfer functions. This is discussed next in Sections 2.7 and 2.8.

2.7 IMC design procedure and PID control for stable plants

Specifications directly on the *open-loop transfer function* $L = GK$, as in the loop-shaping design procedures of the previous section, make the design process transparent as it is clear how changes in $L(s)$ affect the controller $K(s)$ and vice versa. An apparent problem with this approach, however, is that it does not consider directly the *closed-loop transfer functions*, such as S and T, which determine the final response. The following approximations apply:

$$\begin{array}{lll} |L(j\omega)| \gg 1 & \Rightarrow & S \approx L^{-1}; \quad T \approx 1 \\ |L(j\omega)| \ll 1 & \Rightarrow & S \approx 1; \qquad T \approx L \end{array}$$

but in the important crossover region where $|L(j\omega)|$ is close to 1, one cannot infer anything about S and T from the magnitude of the loop shape, $|L(j\omega)|$.

An alternative design strategy is to shape directly the relevant closed-loop transfer functions. In this section, we present such a strategy in the form of internal model control (IMC), with a focus on the design of PID controllers. The more general approach of shaping closed-loop transfer functions using $\mathcal{H}_\infty$ optimal control is discussed in the next section.

The IMC design method (e.g. Morari and Zafiriou, 1989) is simple and has proven to be successful in applications. The idea is to specify the desired closed-loop response and solve for the resulting controller. This simple idea, also known as "direct synthesis", results in an "inverse-based" controller design. The key step is to specify a good closed-loop response. To do so, one needs to understand what closed-loop responses are achievable and desirable.

The first step in the IMC procedure for a stable plant is to factorize the plant model into an invertible minimum-phase part (G_m) and a non-invertible all-pass part (G_a). A time delay θ and non-minimum-phase (RHP) zeros z_i cannot be inverted, because the inverse would be non-causal and unstable, respectively. We therefore have

$$G(s) = G_m G_a \tag{2.77}$$

$$G_a(s) = e^{-\theta s} \prod_i \frac{-s + z_i}{s + z_i}, \quad \mathrm{Re}(z_i) > 0; \theta > 0 \tag{2.78}$$

The second step is to specify the desired closed-loop transfer function T from references to outputs, $y = Tr$. There is no way we can prevent T from including the non-minimum-phase elements of G_a, so we specify

$$T(s) = f(s) G_a(s) \tag{2.79}$$

where $f(s)$ is a low-pass filter selected by the designer, typically of the form $f(s) = 1/(\tau_c s + 1)^n$. The rest is algebra. We have from (2.19) that

$$T = GK(1 + GK)^{-1} \tag{2.80}$$

so combining (2.77), (2.79) and (2.80), and solving for the controller, yields

$$K = G^{-1} \frac{T}{1 - T} = G_m^{-1} \frac{1}{f^{-1} - G_a} \tag{2.81}$$

We note that the controller inverts the minimum-phase part G_m of the plant.

Example 2.13 *We apply the IMC design method to a stable second-order plus time delay process*

$$G(s) = k \frac{e^{-\theta s}}{\tau_0^2 s^2 + 2\tau_0 \zeta s + 1} \tag{2.82}$$

where ζ is the damping factor. $|\zeta| < 1$ gives an underdamped process with oscillations. We consider a stable process where τ_0 and ζ are non-negative. Factorization yields $G_a(s) = e^{-\theta s}$, $G_m(s) = \frac{k}{\tau_0^2 s^2 + 2\tau_0 \zeta s + 1}$. We select a first-order filter $f(s) = 1/(\tau_c s + 1)$. From (2.79) this specifies that we desire, following the unavoidable time delay, a simple first-order tracking response with time constant τ_c:

$$T(s) = \frac{1}{\tau_c s + 1} e^{-\theta s} \tag{2.83}$$

From (2.81), the resulting controller becomes

$$K(s) = G_m^{-1} \frac{1}{f^{-1} - G_a} = \frac{\tau_0^2 s^2 + 2\tau_0 \zeta s + 1}{k} \frac{1}{\tau_c s + 1 - e^{-\theta s}} \tag{2.84}$$

where τ_c is a tuning parameter. This controller is not rational and cannot be written in standard state-space form. However, it can be easily realized in discrete form as a "Smith predictor". Alternatively, we can approximate the time delay and derive a rational controller. For example, we may use a first-order Taylor approximation $e^{-\theta s} \approx 1 - \theta s$. This gives

$$K(s) = \frac{\tau_0^2 s^2 + 2\tau_0 \zeta s + 1}{k} \frac{1}{(\tau_c + \theta) s} \tag{2.85}$$

which can be implemented as a PID controller.

PID control. The PID controller, with three adjustable parameters, is the most widely used control algorithm in industry. There are many variations, but the most common is probably the "ideal" (or parallel) form

$$K_{\rm PID}(s) = K_c \left(1 + \frac{1}{\tau_I s} + \tau_D s\right) \tag{2.86}$$

where the parameters are the gain K_c, integral time τ_I and derivative time τ_D. Another common implementation is the *cascade form*

$$K_{\rm PID,cascade}(s) = \widetilde{K}_c \frac{\widetilde{\tau}_I s + 1}{\widetilde{\tau}_I s} \left(\widetilde{\tau}_D s + 1\right) \tag{2.87}$$

The cascade form is somewhat less general than (2.86) as it does not allow for complex zeros. To translate the cascade PID settings in (2.87) to the ideal form in (2.86), we introduce the factor $\alpha = 1 + \widetilde{\tau}_D/\widetilde{\tau}_I$, and we have

$$K_c = \widetilde{K}_c \cdot \alpha,\ \tau_I = \widetilde{\tau}_I \cdot \alpha,\ \tau_D = \widetilde{\tau}_D/\alpha \tag{2.88}$$

As indicated, the reverse translation is not always possible.

With derivative action, the practical implementation is not as given in (2.86) and (2.87). First, with τ_D non-zero, the controllers in (2.86) and (2.87) are improper. In practice, one needs to add a filter to the controller itself or to the controller input (measurement). The filter is typically of the form $\frac{1}{\epsilon\tau_D s+1}$ with ϵ about 0.1. In most cases, the addition of this filter will not noticeably change the closed-loop response. Second, to avoid "derivative kick" the reference signal is usually not differentiated, which in effect corresponds to a two degrees-of-freedom implementation. In summary, a typical practical implementation of the PID controller (2.86) is

$$u = K_c \left[\left(1 + \frac{1}{\tau_I s}\right)(r - y_m) - \frac{\tau_D s}{\epsilon\tau_D s + 1} y_m\right] \tag{2.89}$$

where u is the plant input, y_m the plant measurement and r the reference.

Example 2.13 continued. *The IMC controller (2.85) for the second-order process (2.82) can be realized as an ideal PID controller (2.86) with*

$$K_c = \frac{1}{k}\frac{2\tau_0\zeta}{\tau_c + \theta}, \quad \tau_I = 2\tau_0\zeta, \quad \tau_D = 0.5\tau_0/\zeta \tag{2.90}$$

For $\zeta < 1$ we have complex zeros in the controller and it cannot be realized in the cascade PID form (2.87). However, for overdamped plants with $\zeta > 1$, we can write the model (2.82) in the form

$$G(s) = k\frac{e^{-\theta s}}{(\tau_1 s + 1)(\tau_2 s + 1)} \tag{2.91}$$

resulting from (2.85) in the controller $K(s) = \frac{(\tau_1 s+1)(\tau_2 s+1)}{k}\frac{1}{(\tau_c+\theta)s}$. Comparing with (2.87), the cascade PID settings become

$$\widetilde{K}_c = \frac{1}{k}\frac{\tau_1}{\tau_c + \theta}, \quad \widetilde{\tau}_I = \tau_1, \quad \widetilde{\tau}_D = \tau_2 \tag{2.92}$$

Using (2.88), the corresponding ideal PID settings become

$$K_c = \frac{1}{k}\frac{(\tau_1 + \tau_2)}{\tau_c + \theta}, \quad \tau_I = \tau_1 + \tau_2, \quad \tau_D = \frac{\tau_2}{1 + \tau_2/\tau_1} \tag{2.93}$$

We note that the PID settings are simpler if we use the cascade form.

SIMC (Skogestad/Simple IMC) PID design for first- or second-order plus delay process. Skogestad (2003) has derived simple rules for model reduction and PID tuning based on the above ideas. He claims these are "probably the best simple PID tuning rules in the world" ☺ . In process control, it is common to approximate the process with a first-order plus time delay model,

$$G(s) = \frac{k}{\tau s + 1} e^{-\theta s} \tag{2.94}$$

Specifying a first-order reference tracking response and using a first-order approximation of the time delay then gives $K_c = \frac{1}{k}\frac{\tau}{\tau_c+\theta}$ and $\tau_I = \tau$ (set $\tau_1 = \tau$ and $\tau_2 = 0$ in (2.93)). These settings are derived for step references and also work well for step disturbances entering directly at the plant output. However, for nearly integrating processes with large τ, say $\tau \geq 8\theta$, step disturbances entering at the plant input will affect the output in a ramp-like fashion. To counteract this, one may modify (increase) the integral action by decreasing τ_I. However, to avoid undesired closed-loop oscillations, τ_I cannot be decreased too much, and Skogestad (2003) recommends the following SIMC PI settings for the plant model (2.94):

$$\boxed{K_c = \frac{1}{k}\frac{\tau}{\tau_c + \theta}, \quad \tau_I = \min\left(\tau, 4(\tau_c + \theta)\right)} \tag{2.95}$$

For PI control there is no difference between the ideal (2.86) and cascade (2.87) forms. The use of *derivative action* (PID control) is uncommon in process control applications, where most plants are stable with simple overdamped responses. This is because the performance improvement is usually too small to justify the added complexity and the increased sensitivity to measurement noise. One exception is for a "dominant" second-order process,

$$G(s) = k\frac{e^{-\theta s}}{(\tau_1 s + 1)(\tau_2 s + 1)} \tag{2.96}$$

where "dominant" means roughly speaking that $\tau_2 > \theta$. We derived cascade PID settings for this model in (2.92). Again, to improve the performance for integrating disturbances, we need to modify the integral time for an integrating process. Thus, for the plant model (2.96) the recommended SIMC settings with the cascade PID controller (2.87) are

$$\boxed{\widetilde{K}_c = \frac{1}{k}\frac{\tau_1}{\tau_c + \theta}, \quad \widetilde{\tau}_I = \min\left(\tau_1, 4(\tau_c + \theta)\right), \quad \widetilde{\tau}_D = \tau_2} \tag{2.97}$$

The corresponding settings for the ideal-form PID controller are obtained using (2.88), but are more complicated.

The settings in (2.95) and (2.97) follow directly from the model, except for the single tuning parameter τ_c that affects the controller gain (and the integral time for near-integrating processes). The choice of the tuning parameter τ_c is based on a trade-off between output performance (favoured by a small τ_c) and robustness and input usage (favoured by a large τ_c). For robust and "fast" control, Skogestad (2003) recommends $\boxed{\tau_c = \theta}$, which for the model (2.96) gives a sensitivity peak $M_S \approx 1.7$, gain margin GM ≈ 3 and crossover frequency $\omega_c = 0.5/\theta$.

Model reduction and effective delay. To derive a model in the form (2.94) or (2.96), where θ is the *effective delay*, Skogestad (2003) provides some simple analytic rules for

model reduction. These are based on the approximations $e^{-\theta s} \approx 1 - \theta s$ (for approximating a RHP-zero as a delay) and $e^{-\theta s} \approx 1/(1+\theta s)$ (for approximating a lag as a delay). The lag approximation is conservative, because in terms of control a delay is worse than a lag of equal magnitude. Thus, when approximating the largest lag, Skogestad (2003) recommends the use of the simple *half rule*:

- **Half rule.** *The largest neglected lag (denominator) time constant is distributed equally to the effective delay and the smallest retained time constant.*

To illustrate, let the original model be in the form

$$G_0(s) = \frac{\prod_j (-T_{j0}^{\text{inv}} s + 1)}{\prod_i (\tau_{i0} s + 1)} e^{-\theta_0 s} \tag{2.98}$$

where the lags τ_{i0} are ordered according to their magnitude, and $T_{j0}^{\text{inv}} = 1/z_{j0} > 0$ denote the inverse response (negative numerator) time constants corresponding to the RHP-zeros located at $s = z_{j0}$. Then, according to the half rule, to obtain a first-order model $G(s) = e^{-\theta s}/(\tau_1 s + 1)$ (for PI control), we use

$$\tau_1 = \tau_{10} + \frac{\tau_{20}}{2}; \quad \theta = \theta_0 + \frac{\tau_{20}}{2} + \sum_{i \geq 3} \tau_{i0} + \sum_j T_{j0}^{\text{inv}} + \frac{h}{2} \tag{2.99}$$

and, to obtain a second-order model (2.96) (for PID control), we use

$$\tau_1 = \tau_{10}; \quad \tau_2 = \tau_{20} + \frac{\tau_{30}}{2}; \quad \theta = \theta_0 + \frac{\tau_{30}}{2} + \sum_{i \geq 4} \tau_{i0} + \sum_j T_{j0}^{\text{inv}} + \frac{h}{2} \tag{2.100}$$

where h is the sampling period (for cases with digital implementation). The main objective of the empirical half rule is to maintain the robustness of the proposed PI and PID tuning rules, which with $\tau_c = \theta$ give M_S about 1.7. This is discussed by Skogestad (2003), who also provides additional rules for approximating positive numerator time constants (LHP-zeros).

Example 2.14 *The process*

$$G_0(s) = \frac{2}{(s+1)(0.2s+1)}$$

is approximated using the half rule as a first-order with time delay process, $G(s) = ke^{-\theta s+1}/(\tau s+1)$, with $k = 2, \theta = 0.2/2 = 0.1$ and $\tau = 1 + 0.2/2 = 1.1$. Choosing $\tau_c = \theta = 0.1$ the SIMC PI settings (2.95) become $K_c = \frac{1}{2}\frac{1.1}{2 \cdot 0.1} = 2.75$ and $\tau_I = \min(1.1, 4 \cdot 2 \cdot 0.1) = 0.8$.

In this case, we may also consider using a second-order model (2.96) with $k = 2, \tau_1 = 1, \tau_2 = 0.2, \theta = 0$ (no approximation). Since $\theta = 0$, we cannot choose $\tau_c = \theta$ as it would yield an infinite controller gain. However, the controller gain is limited by other factors, such as the allowed input magnitude, measurement noise and unmodelled dynamics. Because of such factors, let us assume that the largest allowed controller gain is $\widetilde{K}_c = 10$. From (2.97) this corresponds to $\tau_c = 0.05$, and we get $\widetilde{\tau}_I = \min(1, 4 \cdot 0.05) = 0.2$ and $\widetilde{\tau}_D = \tau_2 = 0.2$. Using (2.88), the corresponding ideal PID settings are $K_c = 20, \tau_I = 0.4$ and $\tau_D = 0.1$.

Example 2.15 *Consider the process*

$$G(s) = 3\frac{(-0.8s+1)}{(6s+1)(2.5s+1)^2(0.4s+1)} e^{-1.2s}$$

Using the half rule, the process is approximated as a first-order time delay model with

$$k = 3,\ \tau_1 = 6 + 2.5/2 = 7.25,\ \theta = 1.2 + 0.8 + 2.5/2 + 2.5 + 0.4 = 6.15$$

or as a second-order time delay model with

$$k = 3,\ \tau_1 = 6,\ \tau_2 = 2.5 + 2.5/2 = 3.75,\ \theta = 1.2 + 0.8 + 2.5/2 + 0.4 = 3.65$$

The PI settings based on the first-order model are (choosing $\tau_c = \theta = 6.15$)

$$K_c = \frac{1}{3}\frac{7.25}{2 \cdot 7.15} = 0.169, \quad \tau_I = \min(7.25, 8 \cdot 6.15) = 7.25$$

and the cascade PID settings based on the second-order model are (choosing $\tau_c = \theta = 3.65$)

$$\widetilde{K}_c = 0.274, \quad \widetilde{\tau}_I = 6, \quad \widetilde{\tau}_D = 3.75$$

We note that a PI controller results from a first-order model, and a PID controller from a second-order model. Since the effective delay θ is the main limiting factor in terms of control performance, its value gives invaluable insight into the inherent controllability of the process. With the effective delay computed using the half rule, it follows that PI control performance is limited by (half of) the magnitude of the second-largest time constant τ_2, whereas PID control performance is limited by (half of) the magnitude of the third-largest time constant, τ_3.

Example 2.16 *Let us finally consider the "disturbance process" in (2.62)*

$$G(s) = \frac{200}{10s+1}\frac{1}{(0.05s+1)^2}$$

Using the half rule, the process is approximated as a first-order time delay model with $k = 200, \tau_1 = 10.025$ and $\theta = 0.075$. The recommended choice for "fast" control is $\tau_c = \theta = 0.075$. However, on page 47 it was stated that we aim for a gain crossover frequency of about $w_c = 10$ [rad/s]. Since we desire a first-order closed-loop response, this corresponds to $\tau_c = 1/\omega_c = 0.1$. With $\tau_c = 0.1$ the corresponding SIMC PI settings are $K_c = \frac{1}{200}\frac{10.025}{(0.1+0.075)} = 0.286$ and $\tau_I = \min(10.025, 4 \cdot (0.1 + 0.075)) = 0.7$. This is an almost-integrating process, and we note that we reduce the integral time from 10.025 (which would be good for tracking step references) to 0.7 in order to get acceptable performance for input disturbances.

To improve further the performance, we use the half rule to obtain a second-order model ($k = 200, \tau_1 = 10, \tau_2 = 0.075, \theta = 0.025$) and choose $\omega_c = 0.1$ to derive SIMC PID settings ($\widetilde{K}_c = 0.4, \widetilde{\tau}_I = 0.5, \widetilde{\tau}_D = 0.075$). Interestingly, the corresponding controller

$$K(s) = 0.4\frac{s+2}{s}(0.075s+1)$$

is almost identical to the final controller K_3 in (2.71), designed previously using loop-shaping ideas.

2.8 Shaping closed-loop transfer functions

In Section 2.6, we discussed the shaping of the magnitude of the open-loop transfer function $L(s)$. In this section, we introduce the reader to the shaping of the magnitudes of *closed-loop* transfer functions, where we synthesize a controller by minimizing an $\mathcal{H}_\infty$ performance objective. The topic is discussed further in Section 3.5.7 and in more detail in Chapter 9. Such a design strategy automates the actual controller design, leaving the engineer with the task of selecting reasonable bounds ("weights") on the desired closed-loop transfer functions. Before explaining how this may be done in practice, we discuss the terms $\mathcal{H}_\infty$ and $\mathcal{H}_2$.

2.8.1 The terms $\mathcal{H}_\infty$ and $\mathcal{H}_2$

The $\mathcal{H}_\infty$ norm of a stable scalar transfer function $f(s)$ is simply the peak value of $|f(j\omega)|$ as a function of frequency, i.e.

$$\|f(s)\|_\infty \triangleq \max_\omega |f(j\omega)| \tag{2.101}$$

Remark. Strictly speaking, we should here replace "max" (the maximum value) by "sup" (the supremum, the least upper bound). This is because the maximum may only be approached as $w \to \infty$ and may therefore not actually be achieved. However, for engineering purposes there is no difference between "sup" and "max".

The terms $\mathcal{H}_\infty$ norm and $\mathcal{H}_\infty$ control are intimidating at first, and a name conveying the engineering significance of $\mathcal{H}_\infty$ would have been better. After all, we are simply talking about a design method which aims to press down the peak(s) of one or more selected transfer functions. However, the term $\mathcal{H}_\infty$, which is purely mathematical, has now established itself in the control community. To make the term less forbidding, an explanation of its background may help. First, the symbol ∞ comes from the fact that the maximum magnitude over frequency may be written as

$$\max_\omega |f(j\omega)| = \lim_{p\to\infty} \left(\int_{-\infty}^{\infty} |f(j\omega)|^p d\omega \right)^{1/p}$$

Essentially, by raising $|f|$ to an infinite power we pick out its peak value. Next, the symbol $\mathcal{H}$ stands for "Hardy space", and $\mathcal{H}_\infty$ in the context of this book is the set of transfer functions with bounded ∞-norm, which is simply the set of *stable and proper* transfer functions.

Similarly, the symbol $\mathcal{H}_2$ stands for the Hardy space of transfer functions with bounded 2-norm, which is the set of *stable and strictly proper* transfer functions. The $\mathcal{H}_2$ norm of a strictly proper stable scalar transfer function is defined as

$$\|f(s)\|_2 \triangleq \left(\frac{1}{2\pi} \int_{-\infty}^{\infty} |f(j\omega)|^2 d\omega \right)^{1/2} \tag{2.102}$$

The factor $1/\sqrt{2\pi}$ is introduced to get consistency with the 2-norm of the corresponding impulse response; see (4.120). Note that the $\mathcal{H}_2$ norm of a semi-proper (or bi-proper) transfer function (where $\lim_{s\to\infty} f(s)$ is a non-zero constant) is infinite, whereas its $\mathcal{H}_\infty$ norm is finite. An example of a semi-proper transfer function (with an infinite $\mathcal{H}_2$ norm) is the sensitivity function $S = (I + GK)^{-1}$.

2.8.2 Weighted sensitivity

As already discussed, the sensitivity function S is a very good indicator of closed-loop performance, both for SISO and MIMO systems. The main advantage of considering S is that because we ideally want S small, it is sufficient to consider just its magnitude $|S|$; that is, we need not worry about its phase. Typical specifications in terms of S include:

1. Minimum bandwidth frequency ω_B^* (defined as the frequency where $|S(j\omega)|$ crosses 0.707 from below).
2. Maximum tracking error at selected frequencies.
3. System type, or alternatively the maximum steady-state tracking error, A.

4. Shape of S over selected frequency ranges.
5. Maximum peak magnitude of S, $\|S(j\omega)\|_\infty \leq M$.

The peak specification prevents amplification of noise at high frequencies, and also introduces a margin of robustness; typically we select $M = 2$. Mathematically, these specifications may be captured by an upper bound, $1/|w_P(s)|$, on the magnitude of S, where $w_P(s)$ is a weight selected by the designer. The subscript P stands for *performance* since S is mainly used as a performance indicator, and the performance requirement becomes

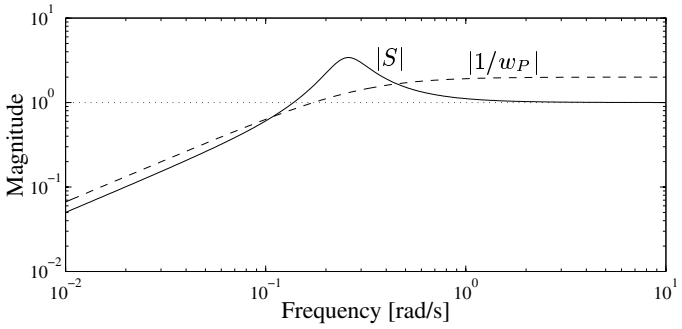

(a) Sensitivity S and performance weight w_P

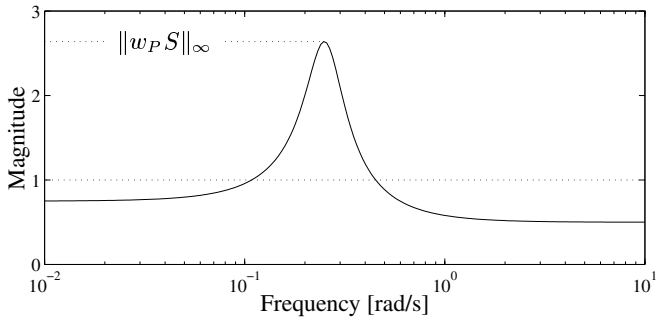

(b) Weighted sensitivity $w_P S$

Figure 2.28: Case where $|S|$ exceeds its bound $1/|w_P|$, resulting in $\|w_P S\|_\infty > 1$

$$|S(j\omega)| < 1/|w_P(j\omega)|, \ \forall\omega \tag{2.103}$$

$$\Leftrightarrow \quad |w_P S| < 1, \ \forall\omega \quad \Leftrightarrow \quad \boxed{\|w_P S\|_\infty < 1} \tag{2.104}$$

The last equivalence follows from the definition of the $\mathcal{H}_\infty$ norm, and in words the performance requirement is that the $\mathcal{H}_\infty$ norm of the weighted sensitivity, $w_P S$, must be less than 1. In Figure 2.28(a), an example is shown where the sensitivity, $|S|$, exceeds its upper bound, $1/|w_P|$, at some frequencies. The resulting weighted sensitivity, $|w_P S|$, therefore exceeds 1 at the same frequencies as is illustrated in Figure 2.28(b). Note that we usually do *not* use a log-scale for the magnitude when plotting *weighted* transfer functions, such as $|w_P S|$.

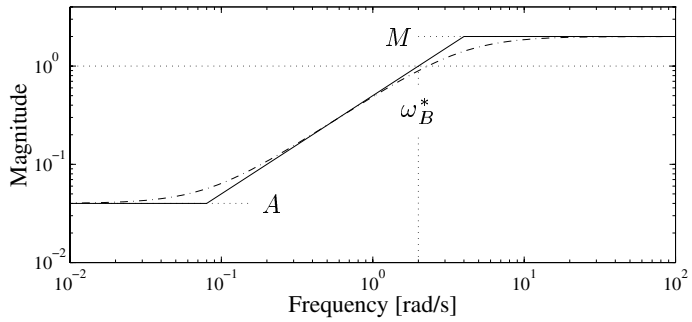

Figure 2.29: Inverse of performance weight: exact and asymptotic plot of $1/|w_P(j\omega)|$ in (2.105)

Weight selection. An asymptotic plot of a typical upper bound, $1/|w_P|$, is shown in Figure 2.29. The weight illustrated may be represented by

$$\boxed{w_P(s) = \frac{s/M + \omega_B^*}{s + \omega_B^* A}} \tag{2.105}$$

and we see that $1/|w_P(j\omega)|$ (the upper bound on $|S|$) is equal to A (typically $A \approx 0$) at low frequencies, is equal to $M \geq 1$ at high frequencies, and the asymptote crosses 1 at the frequency ω_B^*, which is approximately the bandwidth requirement.

Remark. For this weight the loop shape $L = \omega_B^*/s$ yields an S which exactly matches the bound (2.104) at frequencies below the bandwidth and easily satisfies (by a factor M) the bound at higher frequencies.

In some cases, in order to improve performance, we may require a steeper slope for L (and S) below the bandwidth, and then a higher-order weight may be selected. A weight which goes as $(w_B/s)^n$ at frequencies below crossover is

$$\boxed{w_P(s) = \frac{(s/M^{1/n} + \omega_B^*)^n}{(s + \omega_B^* A^{1/n})^n}} \tag{2.106}$$

Exercise 2.4 *For $n = 2$, make an asymptotic plot of $1/|w_P|$ in (2.106) and compare with the asymptotic plot of $1/|w_P|$ in (2.105).*

The insights gained in the previous section on loop-shaping design are very useful for selecting weights. For example, for disturbance rejection we must satisfy $|SG_d(j\omega)| < 1$ at all frequencies (assuming the variables have been scaled to be less than 1 in magnitude). It then follows that a good initial choice for the performance weight is to let $|w_P(j\omega)|$ look like $|G_d(j\omega)|$ at frequencies where $|G_d| > 1$. In other cases, one may first obtain an initial controller using another design procedure, such as LQG, and the resulting sensitivity $|S(j\omega)|$ may then be used to select a performance weight for a subsequent $\mathcal{H}_\infty$ design.

2.8.3 Stacked requirements: mixed sensitivity

The specification $\|w_P S\|_\infty < 1$ puts a lower bound on the bandwidth, but not an upper one, and nor does it allow us to specify the roll-off of $L(s)$ above the bandwidth. To do this

one can make demands on another closed-loop transfer function, e.g. on the complementary sensitivity $T = I - S = GKS$. For instance, one might specify an upper bound $1/|w_T|$ on the magnitude of T to make sure that L rolls off sufficiently fast at high frequencies. Also, to achieve robustness or to restrict the magnitude of the input signals, $u = KS(r - G_d d)$, one may place an upper bound, $1/|w_u|$, on the magnitude of KS. To combine these "mixed sensitivity" specifications, a "stacking approach" is usually used, resulting in the following overall specification:

$$\|N\|_\infty = \max_\omega \bar{\sigma}(N(j\omega)) < 1; \quad N = \begin{bmatrix} w_P S \\ w_T T \\ w_u K S \end{bmatrix} \tag{2.107}$$

Here we use the maximum singular value, $\bar{\sigma}(N(j\omega))$, to measure the size of the matrix N at each frequency. For SISO systems, N is a vector and $\bar{\sigma}(N)$ is the usual Euclidean vector norm:

$$\bar{\sigma}(N) = \sqrt{|w_P S|^2 + |w_T T|^2 + |w_u K S|^2} \tag{2.108}$$

After selecting the form of N and the weights, the $\mathcal{H}_\infty$ optimal controller is obtained by solving the problem

$$\min_K \|N(K)\|_\infty \tag{2.109}$$

where K is a stabilizing controller. A good tutorial introduction to $\mathcal{H}_\infty$ control is given by Kwakernaak (1993).

Remark 1 The stacking procedure is selected for mathematical convenience as it does not allow us to specify exactly the bounds on the individual transfer functions as described above. For example, assume that $\phi_1(K)$ and $\phi_2(K)$ are two functions of K (which might represent $\phi_1(K) = w_P S$ and $\phi_2(K) = w_T T$) and that we want to achieve

$$|\phi_1| < 1 \quad \text{and} \quad |\phi_2| < 1 \tag{2.110}$$

This is similar to, but not quite the same as, the stacked requirement

$$\bar{\sigma} \begin{bmatrix} \phi_1 \\ \phi_2 \end{bmatrix} = \sqrt{|\phi_1|^2 + |\phi_2|^2} < 1 \tag{2.111}$$

Objectives (2.110) and (2.111) are very similar when either $|\phi_1|$ or $|\phi_2|$ is small, but in the "worst" case when $|\phi_1| = |\phi_2|$, we get from (2.111) that $|\phi_1| \leq 0.707$ and $|\phi_2| \leq 0.707$. That is, there is a possible "error" in each specification equal to at most a factor $\sqrt{2} \approx 3$ dB. In general, with n stacked requirements the resulting error is at most $\sqrt{n}$. This inaccuracy in the specifications is something we are probably willing to sacrifice in the interests of mathematical convenience. In any case, the specifications are in general rather rough, and are effectively knobs for the engineer to select and adjust until a satisfactory design is reached.

Remark 2 Let $\gamma_{\min} = \min_K \|N(K)\|_\infty$ denote the optimal $\mathcal{H}_\infty$ norm. An important property of $\mathcal{H}_\infty$ optimal controllers is that they yield a flat frequency response; that is, $\bar{\sigma}(N(j\omega)) = \gamma_{\min}$ at all frequencies. The practical implication is that, except for at most a factor $\sqrt{n}$, the transfer functions resulting from a solution to (2.109) will be close to $\gamma_{\min}$ times the bounds selected by the designer. This gives the designer a mechanism for directly shaping the magnitudes of $\bar{\sigma}(S)$, $\bar{\sigma}(T)$, $\bar{\sigma}(KS)$, and so on.

Example 2.17 $\mathcal{H}_\infty$ mixed sensitivity design for the disturbance process. *Consider again the plant in (2.62), and consider an $\mathcal{H}_\infty$ mixed sensitivity S/KS design in which*

$$N = \begin{bmatrix} w_P S \\ w_u K S \end{bmatrix} \tag{2.112}$$

Appropriate scaling of the plant has been performed so that the inputs should be about 1 or less in magnitude, and we therefore select a simple input weight $w_u = 1$. The performance weight is chosen, in the form of (2.105), as

$$w_{P1}(s) = \frac{s/M + \omega_B^*}{s + \omega_B^* A}; \quad M = 1.5,\ \omega_B^* = 10, \quad A = 10^{-4} \tag{2.113}$$

A value of $A = 0$ would ask for integral action in the controller, but to get a stable weight and to prevent numerical problems in the algorithm used to synthesize the controller, we have moved the integrator slightly by using a small non-zero value for A. This has no practical significance in terms of control performance. The value $\omega_B^* = 10$ has been selected to achieve approximately the desired crossover frequency ω_c of 10 rad/s. The $\mathcal{H}_\infty$ problem is solved with the Robust Control toolbox in Matlab using the commands in Table 2.4.

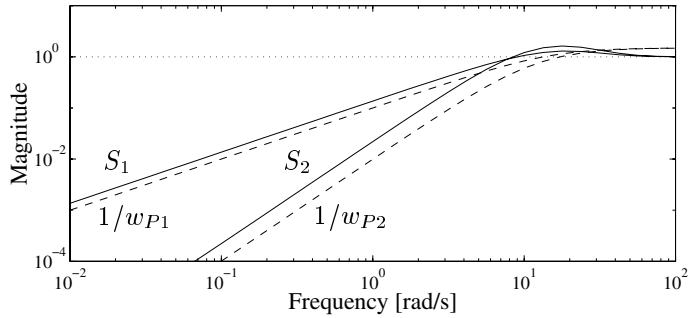

Figure 2.30: Inverse of performance weight (dashed line) and resulting sensitivity function (solid line) for two $\mathcal{H}_\infty$ designs (1 and 2) for the disturbance process

Table 2.4: **Matlab program to synthesize $\mathcal{H}_\infty$ controller for Example 2.17**

```
% Uses the Robust Control toolbox
G=tf(200,conv([10 1],conv([0.05 1],[0.05 1])));   % Plant is G.
M=1.5; wb=10; A=1.e-4;
Wp = tf([1/M wb], [1 wb*A]); Wu = 1;              % Weights.
% Find H-infinity optimal controller:
[khinf,ghinf,gopt] = mixsyn(G,Wp,Wu,[]);
Marg = allmargin(G*khinf)                         % Gain and phase margins
```

For this problem, we achieved an optimal $\mathcal{H}_\infty$ norm of 1.37, so the weighted sensitivity requirements are not quite satisfied (see design 1 in Figure 2.30 where the curve for $|S_1|$ is slightly above that for $1/|w_{P1}|$). Nevertheless, the design seems good with $\|S\|_\infty = M_S = 1.30$, $\|T\|_\infty = M_T = 1$, $GM = 8$, $PM = 71.19^\circ$ and $\omega_c = 7.22$ rad/s, and the tracking response is very good as shown by curve y_1 in Figure 2.31(a). (The design is actually very similar to the loop-shaping design for references, K_0, which was an inverse-based controller.)

However, we see from curve y_1 in Figure 2.31(b) that the disturbance response is very sluggish. If disturbance rejection is the main concern, then from our earlier discussion in Section 2.6.4 this

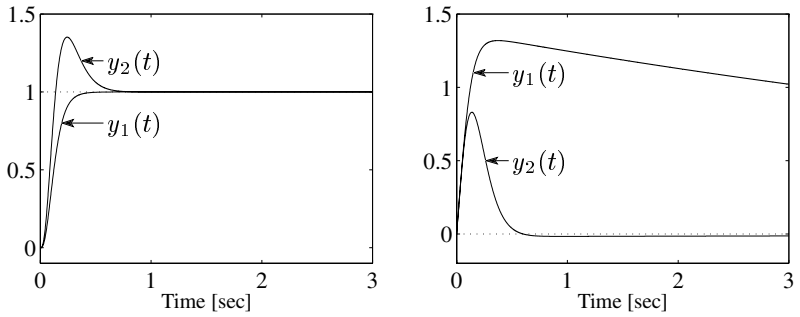

(a) Tracking response (b) Disturbance response

Figure 2.31: Closed-loop step responses for two alternative $\mathcal{H}_\infty$ designs (1 and 2) for the disturbance process in Example 2.17

motivates the need for a performance weight that specifies higher gains at low frequencies. We therefore try

$$w_{P2}(s) = \frac{(s/M^{1/2} + \omega_B^*)^2}{(s + \omega_B^* A^{1/2})^2}, \quad M = 1.5, \omega_B^* = 10, A = 10^{-4} \tag{2.114}$$

The inverse of this weight is shown in Figure 2.30, and is seen from the dashed line to cross 1 *in magnitude at about the same frequency as weight* w_{P1}*, but it specifies tighter control at lower frequencies. With the weight* w_{P2}*, we get a design with an optimal* $\mathcal{H}_\infty$ *norm of* 2.19*, yielding* $M_S = 1.62$*,* $M_T = 1.42$*,* $GM = 4.77$*,* $PM = 43.8^\circ$ *and* $\omega_c = 11.28$ *rad/s. (The design is actually very similar to the loop-shaping design for disturbances,* K_3*.) The disturbance response is very good, whereas the tracking response has a somewhat high overshoot; see curve* y_2 *in Figure 2.31(a).*

In conclusion, design 1 *is best for reference tracking whereas design* 2 *is best for disturbance rejection. To get a design with both good tracking and good disturbance rejection we need a two degrees-of-freedom controller, as was discussed in Example 2.11 (page 52).*

Exercise 2.5 $\mathcal{H}_\infty$ **design for unstable plant.** *Obtain* S/KS $\mathcal{H}_\infty$ *controllers for the unstable process (2.37) using* $w_u = 1$ *and the performance weights in (2.113) (design 1) and (2.114) (design 2). Plot the frequency response of the controller for design 1 together with the PI controller (2.38) to confirm that the two controllers are almost identical. You will find that the response with the design 2 (second-order weight) is faster, but on the other hand robustness margins are not quite as good:*

	$\gamma_{\min} = \|N\|_\infty$	ω_c	M_S	M_T	GM	GM_L	PM
Design 1:	*3.24*	*4.96*	*1.17*	*1.35*	*18.48*	*0.20*	*61.7°*
Design 2:	*5.79*	*8.21*	*1.31*	*1.56*	*11.56*	*0.23*	*48.5°*

2.9 Conclusion

The main purpose of this chapter has been to present the classical ideas and techniques of feedback control. We have concentrated on SISO systems so that insights into the necessary design trade-offs, and the design approaches available, can be properly developed before MIMO systems are considered. We also introduced the $\mathcal{H}_\infty$ problem based on weighted sensitivity, for which typical performance weights are given in (2.105) and (2.106).

3

INTRODUCTION TO MULTIVARIABLE CONTROL

In this chapter, we introduce the reader to multi-input multi-output (MIMO) systems. It is almost "a book within the book" because a lot of topics are discussed in more detail in later chapters. Topics include transfer functions for MIMO systems, multivariable frequency response analysis and the singular value decomposition (SVD), relative gain array (RGA), multivariable control, and multivariable right-half plane (RHP) zeros. The need for a careful analysis of the effect of uncertainty in MIMO systems is motivated by two examples. Finally, we describe a general control configuration that can be used to formulate control problems. The chapter should be accessible to readers who have attended a classical SISO control course.

3.1 Introduction

We consider a MIMO plant with m inputs and l outputs. Thus, the basic transfer function model is $y(s) = G(s)u(s)$, where y is an $l \times 1$ vector, u is an $m \times 1$ vector and $G(s)$ is an $l \times m$ transfer function matrix.

If we make a change in the first input, u_1, then this will generally affect all the outputs, $y_1, y_2, \ldots, y_l$; that is, there is *interaction* between the inputs and outputs. A non-interacting plant would result if u_1 only affects y_1, u_2 only affects y_2, and so on.

The main difference between a scalar (SISO) system and a MIMO system is the presence of *directions* in the latter. Directions are relevant for vectors and matrices, but not for scalars. However, despite the complicating factor of directions, most of the ideas and techniques presented in the previous chapter on SISO systems may be extended to MIMO systems. The singular value decomposition (SVD) provides a useful way of quantifying multivariable directionality, and we will see that most SISO results involving the absolute value (magnitude) may be generalized to multivariable systems by considering the maximum singular value. An exception to this is Bode's stability condition which has no generalization in terms of singular values. This is related to the fact that it is difficult to find a good measure of phase for MIMO transfer functions.

The chapter is organized as follows. We start by presenting some rules for determining multivariable transfer functions from block diagrams. Although most of the formulae for scalar systems apply, we must exercise some care since matrix multiplication is not commutative: that is, in general $GK \neq KG$. Then we introduce the singular value decomposition and show how it may be used to study directions in multivariable systems.

We also give a brief introduction to multivariable control and decoupling. We then consider a simple plant with a multivariable RHP-zero and show how the effect of this zero may be shifted from one output channel to another. After this we discuss robustness, and study two example plants, each 2×2, which demonstrate that the simple gain and phase margins used for SISO systems do not generalize easily to MIMO systems. Finally, we consider a general control problem formulation.

At this point, the reader may find it useful to browse through Appendix A where some important mathematical tools are described. Exercises to test understanding of this mathematics are given at the end of this chapter.

3.2 Transfer functions for MIMO systems

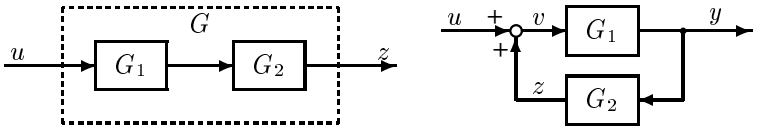

(a) Cascade system (b) Positive feedback system

Figure 3.1: Block diagrams for the cascade rule and the feedback rule

The following three rules are useful when evaluating transfer functions for MIMO systems.

1. **Cascade rule.** *For the cascade (series) interconnection of G_1 and G_2 in Figure 3.1(a), the overall transfer function matrix is $G = G_2 G_1$.*

Remark. The order of the transfer function matrices in $G = G_2 G_1$ (first G_2 and then G_1) is the reverse of the order in which they appear in the block diagram of Figure 3.1(a) (first G_1 and then G_2). This has led some authors to use block diagrams in which the inputs enter at the right hand side. However, in this case the order of the transfer function blocks in a feedback path will be reversed compared with their order in the formula, so no fundamental benefit is obtained.

2. **Feedback rule.** *With reference to the positive feedback system in Figure 3.1(b), we have $v = (I - L)^{-1} u$ where $L = G_2 G_1$ is the transfer function around the loop.*
3. **Push-through rule.** *For matrices of appropriate dimensions*

$$G_1 (I - G_2 G_1)^{-1} = (I - G_1 G_2)^{-1} G_1 \tag{3.1}$$

Proof: Equation (3.1) is verified by premultiplying both sides by $(I - G_1 G_2)$ and postmultiplying both sides by $(I - G_2 G_1)$. □

Exercise 3.1 * *Derive the cascade and feedback rules.*

The cascade and feedback rules can be combined into the following MIMO rule for evaluating closed-loop transfer functions from block diagrams.

> **MIMO rule:** *Start from the output and write down the blocks as you meet them when moving backwards (against the signal flow) towards the input. If you exit*

from a feedback loop then include a term $(I - L)^{-1}$ for positive feedback (or $(I + L)^{-1}$ for negative feedback) where L is the transfer function around that loop (evaluated against the signal flow starting at the point of exit from the loop). Parallel branches should be treated independently and their contributions added together.

Care should be taken when applying this rule to systems with nested loops. For such systems it is probably safer to write down the signal equations and eliminate internal variables to get the transfer function of interest. The rule is best understood by considering an example.

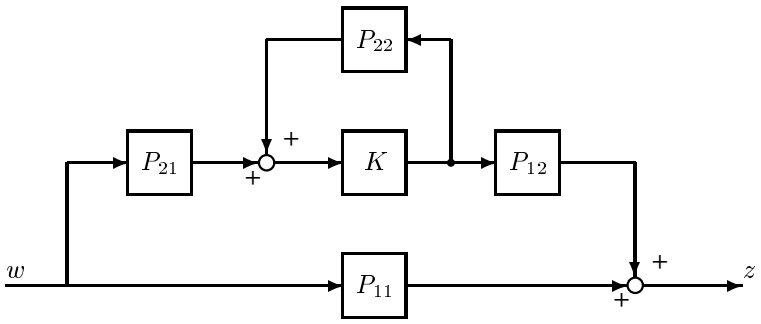

Figure 3.2: Block diagram corresponding to (3.2)

Example 3.1 *The transfer function for the block diagram in Figure 3.2 is given by*

$$z = (P_{11} + P_{12}K(I - P_{22}K)^{-1}P_{21})w \tag{3.2}$$

To derive this from the MIMO rule above we start at the output z and move backwards towards w. There are two branches, one of which gives the term P_{11} directly. In the other branch we move backwards and meet P_{12} and then K. We then exit from a feedback loop and get a term $(I - L)^{-1}$ (positive feedback) with $L = P_{22}K$, and finally we meet P_{21}.

Exercise 3.2 *Use the MIMO rule to derive the transfer functions from u to y and from u to z in Figure 3.1(b). Use the push-through rule to rewrite the two transfer functions.*

Exercise 3.3 * *Use the MIMO rule to show that (2.19) corresponds to the negative feedback system in Figure 2.4.*

Negative feedback control systems

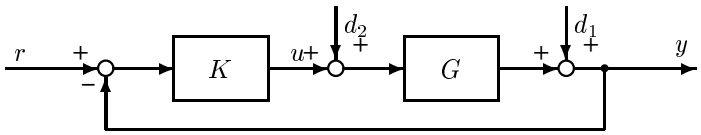

Figure 3.3: Conventional negative feedback control system

For the negative feedback system in Figure 3.3, we define L to be the loop transfer function as seen when breaking the loop at the *output* of the plant. Thus, for the case where the loop

consists of a plant G and a feedback controller K we have

$$L = GK \tag{3.3}$$

The sensitivity and complementary sensitivity are then defined as

$$S \triangleq (I + L)^{-1}; \quad T \triangleq I - S = L(I + L)^{-1} \tag{3.4}$$

In Figure 3.3, T is the transfer function from r to y, and S is the transfer function from d_1 to y; also see (2.17) to (2.21) which apply to MIMO systems.

S and T are sometimes called the *output sensitivity* and *output complementary sensitivity*, respectively, and to make this explicit one may use the notation $L_O \equiv L$, $S_O \equiv S$ and $T_O \equiv T$. This is to distinguish them from the corresponding transfer functions evaluated at the *input* to the plant.

We define L_I to be the loop transfer function as seen when breaking the loop at the *input* to the plant with negative feedback assumed. In Figure 3.3

$$L_I = KG \tag{3.5}$$

The *input* sensitivity and *input* complementary sensitivity functions are then defined as

$$S_I \triangleq (I + L_I)^{-1}; \quad T_I \triangleq I - S_I = L_I(I + L_I)^{-1} \tag{3.6}$$

In Figure 3.3, $-T_I$ is the transfer function from d_2 to u. Of course, for SISO systems $L_I = L$, $S_I = S$ and $T_I = T$.

Exercise 3.4 *In Figure 3.3, what transfer function does S_I represent? Evaluate the transfer functions from d_1 and d_2 to $r - y$.*

The following relationships are useful:

$$(I + L)^{-1} + L(I + L)^{-1} = S + T = I \tag{3.7}$$

$$G(I + KG)^{-1} = (I + GK)^{-1}G \tag{3.8}$$

$$GK(I + GK)^{-1} = G(I + KG)^{-1}K = (I + GK)^{-1}GK \tag{3.9}$$

$$T = L(I + L)^{-1} = (I + (L)^{-1})^{-1} \tag{3.10}$$

Note that the matrices G and K in (3.7)–(3.10) need not be square whereas $L = GK$ is square: (3.7) follows trivially by factorizing out the term $(I + L)^{-1}$ from the right; (3.8) says that $GS_I = SG$ and follows from the push-through rule; (3.9) also follows from the push-through rule; (3.10) can be derived from the identity $M_1^{-1}M_2^{-1} = (M_2M_1)^{-1}$.

Similar relationships, but with G and K interchanged, apply for the transfer functions evaluated at the plant input. To assist in remembering (3.7)–(3.10) note that G comes first (because the transfer function is evaluated at the output) and then G and K alternate in sequence. A given transfer matrix never occurs twice in sequence. For example, the closed-loop transfer function $G(I+GK)^{-1}$ does *not* exist (unless G is repeated in the block diagram, but then these G's would actually represent two different physical entities).

Remark 1 The above identities are clearly useful when deriving transfer functions analytically, but they are also useful for numerical calculations involving state-space realizations, e.g. $L(s) = C(sI - A)^{-1}B + D$. For example, assume we have been given a state-space realization for $L = GK$ with n states (so A is an $n \times n$ matrix) and we want to find the state-space realization of T. Then we can first form $S = (I + L)^{-1}$ with n states, and then multiply it by L to obtain $T = SL$ with $2n$ states. However, a minimal realization of T has only n states. This may be obtained numerically using model reduction, but it is preferable to find it directly using $T = I - S$, see (3.7).

Remark 2 Note also that the right identity in (3.10) can only be used to compute the state-space realization of T if that of L^{-1} exists, so L must be semi-proper with $D \neq 0$ (which is rarely the case in practice). On the other hand, since L is square, we can always compute the frequency response of $L(j\omega)^{-1}$ (except at frequencies where $L(s)$ has $j\omega$-axis poles), and then obtain $T(j\omega)$ from (3.10).

Remark 3 In Appendix A.7 we present some factorizations of the sensitivity function which will be useful in later applications. For example, (A.147) relates the sensitivity of a perturbed plant, $S' = (I + G'K)^{-1}$, to that of the nominal plant, $S = (I + GK)^{-1}$. We have

$$S' = S(I + E_O T)^{-1}, \quad E_O \triangleq (G' - G)G^{-1} \tag{3.11}$$

where E_O is an output multiplicative perturbation representing the difference between G and G', and T is the nominal complementary sensitivity function.

3.3 Multivariable frequency response analysis

The transfer function $G(s)$ is a function of the Laplace variable s and can be used to represent a dynamic system. However, if we fix $s = s_0$ then we may view $G(s_0)$ simply as an $l \times m$ complex matrix (with m inputs and l outputs), which can be analyzed using standard tools in matrix algebra. In particular, the choice $s_0 = j\omega$ is of interest since $G(j\omega)$ represents the response to a sinusoidal signal of frequency ω.

3.3.1 Obtaining the frequency response from $G(s)$

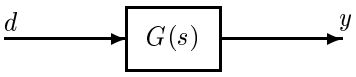

Figure 3.4: System $G(s)$ with input d and output y

The frequency domain is ideal for studying directions in multivariable systems at any given frequency. Consider the system $G(s)$ in Figure 3.4 with input $d(s)$ and output $y(s)$:

$$y(s) = G(s)d(s) \tag{3.12}$$

(We denote the input here by d rather than by u to avoid confusion with the matrix U used below in the singular value decomposition.) In Section 2.1 we considered the sinusoidal response of scalar systems. These results may be directly generalized to multivariable systems by considering the elements g_{ij} of the matrix G. We have

- $g_{ij}(j\omega)$ represents the sinusoidal response from input j to output i.

To be more specific, we apply to input channel j a scalar sinusoidal signal given by

$$d_j(t) = d_{j0}\sin(\omega t + \alpha_j) \tag{3.13}$$

This input signal is persistent: that is, it has been applied since $t = -\infty$. Then the corresponding persistent output signal in channel i is also a sinusoid with the same frequency

$$y_i(t) = y_{i0}\sin(\omega t + \beta_i) \tag{3.14}$$

where the amplification (gain) and phase shift may be obtained from the complex number $g_{ij}(j\omega)$ as follows:

$$\frac{y_{io}}{d_{jo}} = |g_{ij}(j\omega)|, \quad \beta_i - \alpha_j = \angle g_{ij}(j\omega) \tag{3.15}$$

In *phasor notation*, see (2.5) and (2.10), we may compactly represent the sinusoidal time response described in (3.13)–(3.15) by

$$y_i(\omega) = g_{ij}(j\omega)d_j(\omega) \tag{3.16}$$

where

$$d_j(\omega) = d_{jo}e^{j\alpha_j}, \quad y_i(\omega) = y_{io}e^{j\beta_i} \tag{3.17}$$

Here the use of ω (and not $j\omega$) as the argument of $d_j(\omega)$ and $y_i(\omega)$ implies that these are complex numbers, representing at each frequency ω the magnitude and phase of the sinusoidal signals in (3.13) and (3.14).

The overall response to simultaneous input signals of the same frequency in several input channels is, by the superposition principle for linear systems, equal to the sum of the individual responses, and we have from (3.16)

$$y_i(\omega) = g_{i1}(j\omega)d_1(\omega) + g_{i2}(j\omega)d_2(\omega) + \cdots = \sum_j g_{ij}(j\omega)d_j(\omega) \tag{3.18}$$

or in matrix form

$$\boxed{y(\omega) = G(j\omega)d(\omega)} \tag{3.19}$$

where

$$d(\omega) = \begin{bmatrix} d_1(\omega) \\ d_2(\omega) \\ \vdots \\ d_m(\omega) \end{bmatrix} \quad \text{and} \quad y(\omega) = \begin{bmatrix} y_1(\omega) \\ y_2(\omega) \\ \vdots \\ y_l(\omega) \end{bmatrix} \tag{3.20}$$

represent the vectors of sinusoidal input and output signals.

Example 3.2 *Consider a* 2×2 *multivariable system where we simultaneously apply sinusoidal signals of the same frequency* ω *to the two input channels:*

$$d(t) = \begin{bmatrix} d_1(t) \\ d_2(t) \end{bmatrix} = \begin{bmatrix} d_{10}\sin(\omega t + \alpha_1) \\ d_{20}\sin(\omega t + \alpha_2) \end{bmatrix} \quad \text{or} \quad d(\omega) = \begin{bmatrix} d_{10}e^{j\alpha_1} \\ d_{20}e^{j\alpha_2} \end{bmatrix} \tag{3.21}$$

The corresponding output signal is

$$y(t) = \begin{bmatrix} y_1(t) \\ y_2(t) \end{bmatrix} = \begin{bmatrix} y_{10}\sin(\omega t + \beta_1) \\ y_{20}\sin(\omega t + \beta_2) \end{bmatrix} \quad \text{or} \quad y(\omega) = \begin{bmatrix} y_{10}e^{j\beta_1} \\ y_{20}e^{j\beta_2} \end{bmatrix} \tag{3.22}$$

$y(\omega)$ *is obtained by multiplying the complex matrix* $G(j\omega)$ *by the complex vector* $d(\omega)$*, as given in (3.19).*

3.3.2 Directions in multivariable systems

For a SISO system, $y = Gd$, the gain at a given frequency is simply

$$\frac{|y(\omega)|}{|d(\omega)|} = \frac{|G(j\omega)d(\omega)|}{|d(\omega)|} = |G(j\omega)| \tag{3.23}$$

The gain depends on the frequency ω, but since the system is linear it is independent of the input magnitude $|d(\omega)|$.

Things are not quite as simple for MIMO systems where the input and output signals are both vectors, and we need to "sum up" the magnitudes of the elements in each vector by use of some norm, as discussed in Appendix A.5.1. If we select the vector 2-norm, the usual measure of length, then at a given frequency ω the magnitude of the vector input signal is

$$\|d(\omega)\|_2 = \sqrt{\sum_j |d_j(\omega)|^2} = \sqrt{d_{10}^2 + d_{20}^2 + \cdots} \tag{3.24}$$

and the magnitude of the vector output signal is

$$\|y(\omega)\|_2 = \sqrt{\sum_i |y_i(\omega)|^2} = \sqrt{y_{10}^2 + y_{20}^2 + \cdots} \tag{3.25}$$

The *gain* of the system $G(s)$ for a particular input signal $d(\omega)$ is then given by the ratio

$$\frac{\|y(\omega)\|_2}{\|d(\omega)\|_2} = \frac{\|G(j\omega)d(\omega)\|_2}{\|d(\omega)\|_2} = \frac{\sqrt{y_{10}^2 + y_{20}^2 + \cdots}}{\sqrt{d_{10}^2 + d_{20}^2 + \cdots}} \tag{3.26}$$

Again the gain depends on the frequency ω, and again it is independent of the input magnitude $\|d(\omega)\|_2$. However, for a MIMO system there are additional degrees of freedom and the gain depends also on the *direction* of the input d.[1] The maximum gain as the direction of the input is varied is the maximum singular value of G,

$$\max_{d \neq 0} \frac{\|Gd\|_2}{\|d\|_2} = \max_{\|d\|_2 = 1} \|Gd\|_2 = \bar{\sigma}(G) \tag{3.27}$$

whereas the minimum gain is the minimum singular value of G,

$$\min_{d \neq 0} \frac{\|Gd\|_2}{\|d\|_2} = \min_{\|d\|_2 = 1} \|Gd\|_2 = \underline{\sigma}(G) \tag{3.28}$$

The first identities in (3.27) and (3.28) follow because the gain is independent of the input magnitude for a linear system.

Example 3.3 *For a system with two inputs, $d = \begin{bmatrix} d_{10} \\ d_{20} \end{bmatrix}$, the gain is in general different for the following five inputs:*

$$d_1 = \begin{bmatrix} 1 \\ 0 \end{bmatrix},\ d_2 = \begin{bmatrix} 0 \\ 1 \end{bmatrix},\ d_3 = \begin{bmatrix} 0.707 \\ 0.707 \end{bmatrix},\ d_4 = \begin{bmatrix} 0.707 \\ -0.707 \end{bmatrix},\ d_5 = \begin{bmatrix} 0.6 \\ -0.8 \end{bmatrix}$$

[1] The term *direction* refers to a normalized vector of unit length.

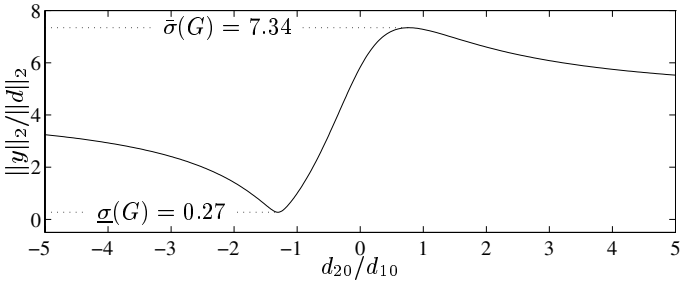

Figure 3.5: Gain $\|Gd\|_2/\|d\|_2$ as a function of d_{20}/d_{10} for G in (3.29)

(which all have the same magnitude $\|d\|_2 = 1$ but are in different directions). For example, for the 2×2 system

$$G = \begin{bmatrix} 5 & 4 \\ 3 & 2 \end{bmatrix} \tag{3.29}$$

(a constant matrix) we compute for the five inputs d_j the following output vectors:

$$y_1 = \begin{bmatrix} 5 \\ 3 \end{bmatrix},\ y_2 = \begin{bmatrix} 4 \\ 2 \end{bmatrix},\ y_3 = \begin{bmatrix} 6.36 \\ 3.54 \end{bmatrix},\ y_4 = \begin{bmatrix} 0.707 \\ 0.707 \end{bmatrix},\ y_5 = \begin{bmatrix} -0.2 \\ 0.2 \end{bmatrix}$$

and the 2-norms of these five outputs (i.e. the gains for the five inputs) are

$$\|y_1\|_2 = 5.83,\ \|y_2\|_2 = 4.47,\ \|y_3\|_2 = 7.30,\ \|y_4\|_2 = 1.00,\ \|y_5\|_2 = 0.28$$

This dependency of the gain on the input direction is illustrated graphically in Figure 3.5 where we have used the ratio d_{20}/d_{10} as an independent variable to represent the input direction. We see that, depending on the ratio d_{20}/d_{10}, the gain varies between 0.27 and 7.34. These are the minimum and maximum singular values of G, respectively.

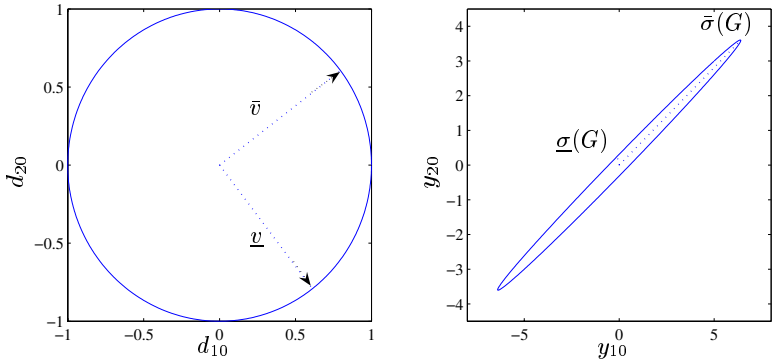

Figure 3.6: Outputs (right plot) resulting from use of $\|d\|_2 = 1$ (unit circle in left plot) for system G in (3.29). The maximum ($\bar{\sigma}(G)$) and minimum ($\underline{\sigma}(G)$) gains are obtained for $d = (\bar{v})$ and $d = (\underline{v})$ respectively.

An alternative plot, which shows the directions of the outputs more clearly, is shown in Figure 3.6. From the shape of the output space (right plot), we see that it is easy to increase both y_{10} and y_{20} simultaneously (gain $\bar{\sigma}(G) = 7.34$), but difficult to increase one and decrease the other (gain $\underline{\sigma}(G) = 0.27$).

3.3.3 Eigenvalues are a poor measure of gain

Before discussing in more detail the singular value decomposition, we want to demonstrate that the magnitudes of the eigenvalues of a transfer function matrix, e.g. $|\lambda_i(G(j\omega))|$, do *not* provide a useful means of generalizing the SISO gain, $|G(j\omega)|$. First of all, eigenvalues can only be computed for square systems, and even then they can be very misleading. To see this, consider the system $y = Gd$ with

$$G = \begin{bmatrix} 0 & 100 \\ 0 & 0 \end{bmatrix} \tag{3.30}$$

which has both eigenvalues λ_i equal to zero. However, to conclude from the eigenvalues that the system gain is zero is clearly misleading. For example, with an input vector $d = [0 \;\; 1]^T$ we get an output vector $y = [100 \;\; 0]^T$.

The "problem" is that the eigenvalues measure the gain for the special case when the inputs and the outputs are in the same direction, namely in the direction of the eigenvectors. To see this let t_i be an eigenvector of G and consider an input $d = t_i$. Then the output is $y = Gt_i = \lambda_i t_i$ where λ_i is the corresponding eigenvalue. We get

$$\|y\|/\|d\| = \|\lambda_i t_i\|/\|t_i\| = |\lambda_i|$$

so $|\lambda_i|$ measures the gain in the direction t_i. This may be useful for stability analysis, but not for performance.

To find useful generalizations of gain of G for the case when G is a matrix, we need the concept of a *matrix norm*, denoted $\|G\|$. Two important properties which must be satisfied for a matrix norm are the *triangle inequality*

$$\|G_1 + G_2\| \leq \|G_1\| + \|G_2\| \tag{3.31}$$

and the *multiplicative property*

$$\|G_1 G_2\| \leq \|G_1\| \cdot \|G_2\| \tag{3.32}$$

(see Appendix A.5 for more details). As we may expect, the magnitude of the largest eigenvalue, $\rho(G) \triangleq |\lambda_{\max}(G)|$ (the spectral radius), does *not* satisfy the properties of a matrix norm; also see (A.116).

In Appendix A.5.2 we introduce several matrix norms, such as the Frobenius norm $\|G\|_F$, the sum norm $\|G\|_{\text{sum}}$, the maximum column sum $\|G\|_{i1}$, the maximum row sum $\|G\|_{i\infty}$, and the maximum singular value $\|G\|_{i2} = \bar{\sigma}(G)$ (the latter three norms are induced by a vector norm, e.g. see (3.27); this is the reason for the subscript i). Actually, the choice of matrix norm among these is not critical because the various norms of an $l \times m$ matrix differ at most by a factor $\sqrt{ml}$, see (A.119)–(A.124). In this book, we will use all of the above norms, each depending on the situation. However, in this chapter we will mainly use the induced 2-norm, $\bar{\sigma}(G)$. Notice that $\bar{\sigma}(G) = 100$ for the matrix in (3.30).

Exercise 3.5 * *Compute the spectral radius and the five matrix norms mentioned above for the matrices in (3.29) and (3.30).*

3.3.4 Singular value decomposition

The singular value decomposition (SVD) is defined in Appendix A.3. Here we are interested in its physical interpretation when applied to the frequency response of a MIMO system $G(s)$ with m inputs and l outputs.

Consider a fixed frequency ω where $G(j\omega)$ is a constant $l \times m$ complex matrix, and denote $G(j\omega)$ by G for simplicity. Any matrix G may be decomposed into its singular value decomposition, and we write

$$G = U\Sigma V^H \tag{3.33}$$

where

Σ is an $l \times m$ matrix with $k = \min\{l, m\}$ non-negative singular values, σ_i, arranged in descending order along its *main diagonal*; the other entries are zero. The singular values are the positive square roots of the eigenvalues of $G^H G$, where G^H is the complex conjugate transpose of G,

$$\sigma_i(G) = \sqrt{\lambda_i(G^H G)} \tag{3.34}$$

U is an $l \times l$ unitary matrix of output singular vectors, u_i,

V is an $m \times m$ unitary matrix of input singular vectors, v_i.

In short, any matrix may be decomposed into an input rotation V, a scaling matrix Σ and an output rotation U. This is illustrated by the SVD of a real 2×2 matrix which can always be written in the form

$$G = \underbrace{\begin{bmatrix} \cos\theta_1 & -\sin\theta_1 \\ \sin\theta_1 & \cos\theta_1 \end{bmatrix}}_{U} \underbrace{\begin{bmatrix} \sigma_1 & 0 \\ 0 & \sigma_2 \end{bmatrix}}_{\Sigma} \underbrace{\begin{bmatrix} \cos\theta_2 & \pm\sin\theta_2 \\ -\sin\theta_2 & \pm\cos\theta_2 \end{bmatrix}^T}_{V^T} \tag{3.35}$$

where the angles θ_1 and θ_2 depend on the given matrix. From (3.35) we see that the matrices U and V involve rotations and that their columns are orthonormal.

The singular values are sometimes called the principal values or principal gains, and the associated directions are called principal directions. In general, the singular values must be computed numerically. For 2×2 matrices, however, analytic expressions for the singular values are given in (A.37).

Caution. It is standard notation to use the symbol U to denote the matrix of *output* singular vectors. This is unfortunate as it is also standard notation to use u (lower case) to represent the *input* signal. The reader should be careful not to confuse these two.

Input and output directions. The column vectors of U, denoted u_i, represent the *output directions* of the plant. They are orthogonal and of unit length (orthonormal), i.e.

$$\|u_i\|_2 = \sqrt{|u_{i1}|^2 + |u_{i2}|^2 + \cdots + |u_{il}|^2} = 1 \tag{3.36}$$

$$u_i^H u_i = 1, \quad u_i^H u_j = 0, \quad i \neq j \tag{3.37}$$

Likewise, the column vectors of V, denoted v_i, are orthogonal and of unit length, and represent the *input directions*. These input and output directions are related through the singular values. To see this, note that since V is unitary we have $V^H V = I$, so (3.33) may be written as $GV = U\Sigma$, which for column i becomes

$$Gv_i = \sigma_i u_i \tag{3.38}$$

where v_i and u_i are vectors, whereas σ_i is a scalar. That is, if we consider an *input* in the direction v_i, then the *output* is in the direction u_i. Furthermore, since $\|v_i\|_2 = 1$ and

$\|u_i\|_2 = 1$ we see that the i'th singular value σ_i directly gives the gain of the matrix G in this direction. In other words

$$\sigma_i(G) = \|Gv_i\|_2 = \frac{\|Gv_i\|_2}{\|v_i\|_2} \tag{3.39}$$

Some advantages of the SVD over the eigenvalue decomposition for analyzing gains and directionality of multivariable plants are:

1. The singular values give better information about the gains of the plant.
2. The plant directions obtained from the SVD are orthogonal.
3. The SVD also applies directly to non-square plants.

Maximum and minimum singular values. As already stated, it can be shown that the largest gain for *any* input direction is equal to the maximum singular value

$$\bar{\sigma}(G) \equiv \sigma_1(G) = \max_{d \neq 0} \frac{\|Gd\|_2}{\|d\|_2} = \frac{\|Gv_1\|_2}{\|v_1\|_2} \tag{3.40}$$

and that the smallest gain for any input direction (excluding the "wasted" inputs in the null space of G for cases with more inputs than outputs[2])

is equal to the minimum singular value

$$\underline{\sigma}(G) \equiv \sigma_k(G) = \min_{d \neq 0} \frac{\|Gd\|_2}{\|d\|_2} = \frac{\|Gv_k\|_2}{\|v_k\|_2} \tag{3.41}$$

where $k = \min\{l, m\}$. Thus, for any vector d, not in the null space of G, we have that

$$\underline{\sigma}(G) \leq \frac{\|Gd\|_2}{\|d\|_2} \leq \bar{\sigma}(G) \tag{3.42}$$

Defining $u_1 = \bar{u}, v_1 = \bar{v}, u_k = \underline{u}$ and $v_k = \underline{v}$, then it follows that

$$G\bar{v} = \bar{\sigma}\bar{u}, \qquad G\underline{v} = \underline{\sigma}\,\underline{u} \tag{3.43}$$

The vector $\bar{v}$ corresponds to the input direction with largest amplification, and $\bar{u}$ is the corresponding output direction in which the inputs are most effective. The directions involving $\bar{v}$ and $\bar{u}$ are sometimes referred to as the "strongest", "high-gain" or "most important" directions. The next most important directions are associated with v_2 and u_2, and so on (see Appendix A.3.5) until the "least important", "weak" or "low-gain" directions which are associated with $\underline{v}$ and $\underline{u}$.

Example 3.3 continued. *Consider again the system (3.29) with*

$$G = \begin{bmatrix} 5 & 4 \\ 3 & 2 \end{bmatrix} \tag{3.44}$$

The SVD of G_1 is

$$G = \underbrace{\begin{bmatrix} 0.872 & 0.490 \\ 0.490 & -0.872 \end{bmatrix}}_{U} \underbrace{\begin{bmatrix} 7.343 & 0 \\ 0 & 0.272 \end{bmatrix}}_{\Sigma} \underbrace{\begin{bmatrix} 0.794 & -0.608 \\ 0.608 & 0.794 \end{bmatrix}^H}_{V^H}$$

[2] For a "fat" matrix G with more inputs than outputs ($m > l$), we can always choose a non-zero input d in the null space of G such that $Gd = 0$.

The largest gain of 7.343 is for an input in the direction $\bar{v} = \begin{bmatrix} 0.794 \\ 0.608 \end{bmatrix}$. *The smallest gain of 0.272 is for an input in the direction* $\underline{v} = \begin{bmatrix} -0.608 \\ 0.794 \end{bmatrix}$. *This confirms the findings on page 73 (see Figure 3.6).*

Note that the directions in terms of the singular vectors are not unique, in the sense that the elements in each pair of vectors (u_i, v_i) may be multiplied by a complex scalar c of magnitude 1 ($|c| = 1$). This is easily seen from (3.38). For example, we may change the sign of the vector $\bar{v}$ (multiply by $c = -1$) provided we also change the sign of the vector $\bar{u}$. Also, if you use Matlab to compute the SVD of the matrix in (3.44) (`g=[5 4; 3 2 ]; [u,s,v]=svd(g)`), then you will probably find that the signs of the elements in U and V are different from those given above.

Since in (3.44) both inputs affect both outputs, we say that the system is *interactive*. This follows from the relatively large off-diagonal elements in G in (3.44). Furthermore, the system is *ill-conditioned*: that is, some combinations of the inputs have a strong effect on the outputs, whereas other combinations have a weak effect on the outputs. This may be quantified by the *condition number*: the ratio between the gains in the strong and weak directions, which for the system in (3.44) is $\gamma = \bar{\sigma}/\underline{\sigma} = 7.343/0.272 = 27.0$.

Example 3.4 Shopping cart. *Consider a shopping cart (supermarket trolley) with fixed wheels which we may want to move in three directions: forwards, sideways and upwards. This is a simple illustrative example where we can easily figure out the principal directions from experience. The strongest direction, corresponding to the largest singular value, will clearly be in the forwards direction. The next direction, corresponding to the second singular value, will be sideways. Finally, the most "difficult" or "weak" direction, corresponding to the smallest singular value, will be upwards (lifting up the cart).*

For the shopping cart the gain depends strongly on the input direction, i.e. the plant is ill-conditioned. Control of ill-conditioned plants is sometimes difficult, and the control problem associated with the shopping cart can be described as follows. Assume we want to push the shopping cart sideways (maybe we are blocking someone). This is rather difficult (the plant has low gain in this direction) so a strong force is needed. However, if there is any uncertainty in our knowledge about the direction the cart is pointing, then some of our applied force will be directed forwards (where the plant gain is large) and the cart will suddenly move forward with an undesired large speed. We thus see that the control of an ill-conditioned plant may be especially difficult if there is input uncertainty which can cause the input signal to "spread" from one input direction to another. We will discuss this in more detail later.

Example 3.5 Distillation process. *Consider the following steady-state model of a distillation column:*

$$G = \begin{bmatrix} 87.8 & -86.4 \\ 108.2 & -109.6 \end{bmatrix} \tag{3.45}$$

The variables have been scaled as discussed in Section 1.4. Thus, since the elements are much larger than 1 *in magnitude this suggests that there will be no problems with input constraints. However, this is somewhat misleading as the gain in the low-gain direction (corresponding to the smallest singular value) is actually only just above* 1. *To see this consider the SVD of* G*:*

$$G = \underbrace{\begin{bmatrix} 0.625 & -0.781 \\ 0.781 & 0.625 \end{bmatrix}}_{U} \underbrace{\begin{bmatrix} 197.2 & 0 \\ 0 & 1.39 \end{bmatrix}}_{\Sigma} \underbrace{\begin{bmatrix} 0.707 & -0.708 \\ -0.708 & -0.707 \end{bmatrix}^H}_{V^H} \tag{3.46}$$

From the first input singular vector, $\bar{v} = [\,0.707 \quad -0.708\,]^T$, *we see that the gain is* 197.2 *when we increase one input and decrease the other input by a similar amount. On the other hand, from the second input singular vector,* $\underline{v} = [\,-0.708 \quad -0.707\,]^T$, *we see that if we change both inputs by the same amount then the gain is only* 1.39. *The reason for this is that the plant is such that the two inputs*

counteract each other. Thus, the distillation process is ill-conditioned, at least at steady-state, and the condition number is $197.2/1.39 = 141.7$. *The physics of this example is discussed in more detail below, and later in this chapter we will consider a simple controller design (see Motivating robustness example no. 2 in Section 3.7.2).*

Example 3.6 Physics of the distillation process. *The model in (3.45) represents two-point (dual) composition control of a distillation column, where the top composition is to be controlled at* $y_D = 0.99$ *(output* y_1*) and the bottom composition at* $x_B = 0.01$ *(output* y_2*), using reflux L (input* u_1*) and boilup V (input* u_2*) as manipulated inputs (see Figure 10.6 on page 408). Note that we have here returned to the convention of using* u_1 *and* u_2 *to denote the manipulated inputs; the output singular vectors will be denoted by* $\bar{u}$ *and* $\underline{u}$.

The $1,1$*-element of the gain matrix* G *is* 87.8. *Thus an increase in* u_1 *by* 1 *(with* u_2 *constant) yields a large steady-state change in* y_1 *of* 87.8*; that is, the outputs are very sensitive to changes in* u_1. *Similarly, an increase in* u_2 *by* 1 *(with* u_1 *constant) yields* $y_1 = -86.4$. *Again, this is a very large change, but in the opposite direction of that for the increase in* u_1. *We therefore see that changes in* u_1 *and* u_2 *counteract each other, and if we increase* u_1 *and* u_2 *simultaneously by* 1*, then the overall steady-state change in* y_1 *is only* $87.8 - 86.4 = 1.4$.

Physically, the reason for this small change is that the compositions in the distillation column are only weakly dependent on changes in the internal flows *(i.e. simultaneous changes in the internal flows* L *and* V*). This can also be seen from the smallest singular value,* $\underline{\sigma}(G) = 1.39$*, which is obtained for inputs in the direction* $\underline{v} = \begin{bmatrix} -0.708 \\ -0.707 \end{bmatrix}$. *From the output singular vector* $\underline{u} = \begin{bmatrix} -0.781 \\ 0.625 \end{bmatrix}$ *we see that the effect is to move the outputs in different directions; that is, to change* $y_1 - y_2$. *Therefore, it takes a large control action to move the compositions in different directions; that is, to make both products purer simultaneously. This makes sense from a physical point of view.*

On the other hand, the distillation column is very sensitive to changes in external flows *(i.e. increase* $u_1 - u_2 = L - V$*). This can be seen from the input singular vector* $\bar{v} = \begin{bmatrix} 0.707 \\ -0.708 \end{bmatrix}$ *associated with the largest singular value, and is a general property of distillation columns where both products are of high purity. The reason for this is that the external distillate flow (which varies as* $V - L$*) has to be about equal to the amount of light component in the feed, and even a small imbalance leads to large changes in the product compositions.*

For dynamic systems the singular values and their associated directions vary with frequency, and for control purposes it is usually the frequency range corresponding to the closed-loop bandwidth which is of main interest. The singular values are usually plotted as a function of frequency in a Bode magnitude plot with a log-scale for frequency and magnitude. Typical plots are shown in Figure 3.7.

Non-square plant

The SVD is also useful for non-square plants. For example, consider a plant with two inputs and three outputs. In this case the third output singular vector, u_3, tells us in which output direction the plant cannot be controlled. Similarly, for a plant with more inputs than outputs, the additional input singular vectors tell us in which directions the input will have no effect.

Example 3.7 *Consider a non-square system with three inputs and two outputs,*

$$G_2 = \begin{bmatrix} 5 & 4 & 1 \\ 3 & 2 & -1 \end{bmatrix}$$

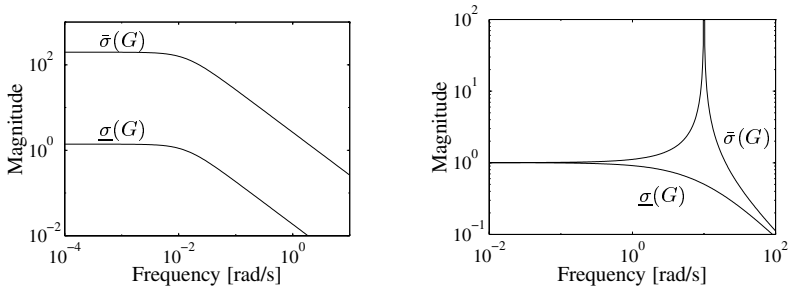

(a) Distillation process in (3.93) (b) Spinning satellite in (3.88)

Figure 3.7: Typical plots of singular values

with SVD

$$G_2 = \underbrace{\begin{bmatrix} 0.877 & 0.481 \\ 0.481 & -0.877 \end{bmatrix}}_{U} \underbrace{\begin{bmatrix} 7.354 & 0 & 0 \\ 0 & 1.387 & 0 \end{bmatrix}}_{\Sigma} \underbrace{\begin{bmatrix} 0.792 & -0.161 & 0.588 \\ 0.608 & 0.124 & -0.785 \\ 0.054 & 0.979 & 0.196 \end{bmatrix}^H}_{V^H}$$

From our definition, the minimum singular value is $\underline{\sigma}(G_2) = 1.387$*, but note that an input* d *in the direction* $v_3 = \begin{bmatrix} 0.588 \\ -0.785 \\ 0.196 \end{bmatrix}$ *is in the null space of* G *and yields a zero output,* $y = Gd = 0$*.*

Exercise 3.6 *For a system with* m *inputs and one output, what is the interpretation of the singular values and the associated input directions (*V*)? What is* U *in this case?*

3.3.5 Singular values for performance

So far we have used the SVD primarily to gain insight into the directionality of MIMO systems. But the maximum singular value is also very useful in terms of frequency domain performance and robustness. We consider performance here.

For SISO systems we earlier found that $|S(j\omega)|$ evaluated as a function of frequency gives useful information about the effectiveness of feedback control. For example, it is the gain from a sinusoidal reference input (or output disturbance) $r(\omega)$[3] to the control error, $|e(\omega)| = |S(j\omega)| \cdots |r(\omega)|$.

For MIMO systems a useful generalization results if we consider the ratio $\|e(\omega)\|_2 / \|r(\omega)\|_2$, where r is the vector of reference inputs, e is the vector of control errors, and $\| \cdot \|_2$ is the vector 2-norm. As explained above, this gain depends on the *direction* of $r(\omega)$ and we have from (3.42) that it is bounded by the maximum and minimum singular value of S,

$$\underline{\sigma}(S(j\omega)) \leq \frac{\|e(\omega)\|_2}{\|r(\omega)\|_2} \leq \bar{\sigma}(S(j\omega)) \tag{3.47}$$

In terms of *performance*, it is reasonable to require that the gain $\|e(\omega)\|_2 / \|r(\omega)\|_2$ remains small for any direction of $r(\omega)$, including the "worst-case" direction which gives a gain of

[3] We use phasor notation here, see page 18, and $|r(\omega)|$ is the magnitude of the sinusoidal signal at frequency ω.

$\bar{\sigma}(S(j\omega))$. Let $1/|w_P(j\omega)|$ (the inverse of the performance weight) represent the maximum allowed magnitude of $\|e\|_2/\|r\|_2$ at each frequency. This results in the following performance requirement:

$$\begin{aligned} \bar{\sigma}(S(j\omega)) < 1/|w_P(j\omega)|,\ \forall\omega \quad &\Leftrightarrow \quad \bar{\sigma}(w_P S) < 1,\ \forall\omega \\ &\Leftrightarrow \quad \|w_P S\|_\infty < 1 \end{aligned} \tag{3.48}$$

where the $\mathcal{H}_\infty$ norm (see also page 60) is defined as the peak of the maximum singular value of the frequency response

$$\|M(s)\|_\infty \triangleq \max_\omega \bar{\sigma}(M(j\omega)) \tag{3.49}$$

Typical performance weights $w_P(s)$ are given in Section 2.8.2, which should be studied carefully.

The singular values of $S(j\omega)$ may be plotted as functions of frequency, as illustrated later in Figure 3.12(a). Typically, they are small at low frequencies where feedback is effective, and they approach 1 at high frequencies because any real system is strictly proper:

$$\omega \to \infty: \quad L(j\omega) \to 0 \quad \Rightarrow \quad S(j\omega) \to I \tag{3.50}$$

The maximum singular value, $\bar{\sigma}(S(j\omega))$, usually has a peak larger than 1 around the crossover frequencies. This peak is undesirable, but it is unavoidable for real systems.

As for SISO systems we define the bandwidth as the frequency up to which feedback is effective. For MIMO systems the bandwidth will depend on directions, and we have a *bandwidth region* between a lower frequency where the maximum singular value, $\bar{\sigma}(S)$, reaches 0.7 (the "low-gain" or "worst-case" direction), and a higher frequency where the minimum singular value, $\underline{\sigma}(S)$, reaches 0.7 (the "high-gain" or "best-case")[4]. If we want to associate a single bandwidth frequency for a multivariable system, then we consider the worst-case (low-gain) direction, and define

- *Bandwidth*, ω_B: Frequency where $\bar{\sigma}(S)$ crosses $\frac{1}{\sqrt{2}} = 0.7$ from below.

It is then understood that the bandwidth is at least ω_B for any direction of the input (reference or disturbance) signal. Since $S = (I + L)^{-1}$, (A.54) yields

$$\underline{\sigma}(L) - 1 \le \frac{1}{\bar{\sigma}(S)} \le \underline{\sigma}(L) + 1 \tag{3.51}$$

Thus at frequencies where feedback is effective (namely where $\underline{\sigma}(L) \gg 1$) we have $\bar{\sigma}(S) \approx 1/\underline{\sigma}(L)$, and at the bandwidth frequency (where $1/\bar{\sigma}(S(j\omega_B)) = \sqrt{2} = 1.41$) we have that $\underline{\sigma}(L(j\omega_B))$ is between 0.41 and 2.41. Thus, the bandwidth is approximately where $\underline{\sigma}(L)$ crosses 1. Finally, at higher frequencies, where for any real system $\underline{\sigma}(L)$ (and $\bar{\sigma}(L)$) is small, we have that $\bar{\sigma}(S) \approx 1$.

3.3.6 Condition number

In Examples 3.4 and 3.5, we noted that the system's gain varied considerably with the input direction. Such systems are said to have strong directionality. Two measures which are used to

[4] The terms "low-gain" and "high-gain" refer to L, whereas the terms "worst-case" and "best-case" refer to the resulting speed of response for the closed-loop system.

quantify the degree of directionality and the level of (two-way) interactions in MIMO systems are the condition number and the relative gain array (RGA), respectively. We first consider the *condition number* of a matrix which is defined as the ratio between the maximum and minimum singular values,

$$\gamma(G) \triangleq \bar{\sigma}(G)/\underline{\sigma}(G) \tag{3.52}$$

A matrix with a large condition number is said to be *ill-conditioned*. For a non-singular (square) matrix $\underline{\sigma}(G) = 1/\bar{\sigma}(G^{-1})$, so $\gamma(G) = \bar{\sigma}(G)\bar{\sigma}(G^{-1})$. It then follows from (A.120) that the condition number is large if both G and G^{-1} have large elements.

The condition number depends strongly on the scaling of the inputs and outputs. To be more specific, if D_1 and D_2 are diagonal scaling matrices, then the condition numbers of the matrices G and D_1GD_2 may be arbitrarily far apart. In general, the matrix G should be scaled on physical grounds, e.g. by dividing each input and output by its largest expected or desired value as discussed in Section 1.4.

One might also consider minimizing the condition number over all possible scalings. This results in the *minimized or optimal condition number* which is defined by

$$\gamma^*(G) = \min_{D_1,D_2} \gamma(D_1GD_2) \tag{3.53}$$

and can be computed using (A.74).

The condition number has been used as an input–output controllability measure, and in particular it has been postulated that a large condition number indicates sensitivity to uncertainty. This is not true in general, but the reverse holds: if the condition number is small, then the multivariable effects of uncertainty are not likely to be serious (see (6.89)).

If the condition number is large (say, larger than 10), then this may *indicate* control problems:

1. A large condition number $\gamma(G) = \bar{\sigma}(G)/\underline{\sigma}(G)$ may be caused by a small value of $\underline{\sigma}(G)$, which is generally undesirable (on the other hand, a large value of $\bar{\sigma}(G)$ need not necessarily be a problem).
2. A large condition number may mean that the plant has a large minimized condition number, or equivalently, it has large RGA elements which indicate fundamental control problems; see below.
3. A large condition number *does* imply that the system is sensitive to "unstructured" (full-block) input uncertainty (e.g. with an inverse-based controller, see (8.136)), but this kind of uncertainty often does not occur in practice. We therefore *cannot* generally conclude that a plant with a large condition number is sensitive to uncertainty, e.g. see the diagonal plant in Example 3.12 (page 89).

3.4 Relative gain array (RGA)

The RGA (Bristol, 1966) of a non-singular square complex matrix G is a square complex matrix defined as

$$\mathrm{RGA}(G) = \Lambda(G) \triangleq G \times (G^{-1})^T \tag{3.54}$$

where $\times$ denotes element-by-element multiplication (the Hadamard or Schur product). With Matlab, we write[5]

```
RGA = G.*pinv(G).'
```

The RGA of a transfer matrix is generally computed as a function of frequency (see Matlab program in Table 3.1). For a 2×2 matrix with elements g_{ij} the RGA is

$$\Lambda(G) = \begin{bmatrix} \lambda_{11} & \lambda_{12} \\ \lambda_{21} & \lambda_{22} \end{bmatrix} = \begin{bmatrix} \lambda_{11} & 1-\lambda_{11} \\ 1-\lambda_{11} & \lambda_{11} \end{bmatrix}; \quad \lambda_{11} = \frac{1}{1 - \frac{g_{12}g_{21}}{g_{11}g_{22}}} \tag{3.55}$$

The RGA is a very useful tool in practical applications. The RGA is treated in detail at three places in this book. First, we give a general introduction in this section (pages 82–90). The use of the RGA for decentralized control is discussed in more detail in Section 10.6 (pages 441–453). Finally, its algebraic properties and extension to non-square matrices are considered in Appendix A.4 (pages 526–529).

3.4.1 Original interpretation: RGA as an interaction measure

We follow Bristol (1966) here, and show that the RGA provides a measure of interactions. Let u_j and y_i denote a particular input–output pair for the multivariable plant $G(s)$, and assume that our task is to use u_j to control y_i. Bristol argued that there will be two extreme cases:

- All other loops open: $u_k = 0, \forall k \neq j$.
- All other loops closed with perfect control: $y_k = 0, \forall k \neq i$.

Perfect control is only possible at steady-state, but it is a good approximation at frequencies within the bandwidth of each loop. We now evaluate "our" gain $\partial y_i / \partial u_j$ for the two extreme cases:

$$\text{Other loops open:} \qquad \left(\frac{\partial y_i}{\partial u_j}\right)_{u_k=0, k\neq j} = g_{ij} \tag{3.56}$$

$$\text{Other loops closed:} \qquad \left(\frac{\partial y_i}{\partial u_j}\right)_{y_k=0, k\neq i} \triangleq \widehat{g}_{ij} \tag{3.57}$$

Here $g_{ij} = [G]_{ij}$ is the ij'th element of G, whereas $\widehat{g}_{ij}$ is the inverse of the ji'th element of G^{-1}

$$\widehat{g}_{ij} = 1/[G^{-1}]_{ji} \tag{3.58}$$

To derive (3.58) we note that

$$y = Gu \quad \Rightarrow \quad \left(\frac{\partial y_i}{\partial u_j}\right)_{u_k=0, k\neq j} = [G]_{ij} \tag{3.59}$$

and interchange the roles of G and G^{-1}, of u and y, and of i and j to get

$$u = G^{-1}y \quad \Rightarrow \quad \left(\frac{\partial u_j}{\partial y_i}\right)_{y_k=0, k\neq i} = [G^{-1}]_{ji} \tag{3.60}$$

[5] The symbol ' in Matlab gives the conjugate transpose (A^H), and we must use .' to get the "regular" transpose (A^T).

and (3.58) follows. Bristol argued that the ratio between the gains in (3.56) and (3.57) is a useful measure of interactions, and defined the ij'th "relative gain" as

$$\lambda_{ij} \triangleq \frac{g_{ij}}{\widehat{g}_{ij}} = [G]_{ij}[G^{-1}]_{ji} \tag{3.61}$$

The RGA is the corresponding matrix of relative gains. From (3.61) we see that $\Lambda(G) = G \times (G^{-1})^T$ where $\times$ denotes element-by-element multiplication (the Schur product). This is identical to our definition of the RGA matrix in (3.54).

Remark. The assumption of $y_k = 0$ ("perfect control of y_k") in (3.57) is satisfied at steady-state ($\omega = 0$) provided we have integral action in the loop, but it will generally not hold exactly at other frequencies. Unfortunately, this has led many authors to dismiss the RGA as being "only useful at steady-state" or "only useful if we use integral action". On the contrary, in most cases it is the value of the RGA at frequencies close to crossover which is most important, and both the gain and the phase of the RGA elements are important. The derivation of the RGA in (3.56) to (3.61) was included to illustrate one useful interpretation of the RGA, but note that our definition of the RGA in (3.54) is purely algebraic and makes no assumption about "perfect control". The general usefulness of the RGA is further demonstrated by the additional general algebraic and control properties of the RGA listed on page 88.

Example 3.8 RGA for 2×2 system. *Consider a 2×2 system with the plant model*

$$y_1 = g_{11}(s)u_1 + g_{12}(s)u_2 \tag{3.62}$$
$$y_2 = g_{21}(s)u_1 + g_{22}(s)u_2 \tag{3.63}$$

Assume that "our" task is to use u_1 to control y_1. First consider the case when the other loop is open, i.e. u_2 is constant. We then have

$$u_2 = 0: \quad y_1 = g_{11}(s)u_1$$

Next consider the case when the other loop is closed with perfect control, i.e. $y_2 = 0$. In this case, u_2 will also change when we change u_1, due to interactions. More precisely, setting $y_2 = 0$ in (3.63) gives

$$u_2 = -\frac{g_{21}(s)}{g_{22}(s)}u_1$$

Substituting this into (3.62) gives

$$y_2 = 0: \quad y_1 = \underbrace{\left(g_{11} - \frac{g_{21}}{g_{22}}g_{21}\right)}_{\widehat{g}_{11}(s)}u_1$$

This means that "our gain" changes from $g_{11}(s)$ to $\widehat{g}_{11}(s)$ as we close the other loop, and the corresponding RGA element becomes

$$\lambda_{11}(s) = \frac{\text{"open-loop gain (with } u_2 = 0)\text{"}}{\text{"closed-loop gain (with } y_2 = 0)\text{"}} = \frac{g_{11}(s)}{\widehat{g}_{11}(s)} = \frac{1}{1 - \frac{g_{12}(s)g_{21}(s)}{g_{11}(s)g_{22}(s)}}$$

Intuitively, for decentralized control, we *prefer* to pair variables u_j and y_i so that λ_{ij} is close to 1 at all frequencies, because this means that the gain from u_j to y_i is unaffected by closing the other loops. More precisely, we have:

> **Pairing rule 1** (page 449): *Prefer pairings such that the rearranged system, with the selected pairings along the diagonal, has an RGA matrix close to identity at frequencies around the closed-loop bandwidth.*

However, one should avoid pairings where the sign of the steady-state gain from u_j to y_i may change depending on the control of the other outputs, because this will yield instability with integral action in the loop. Thus, $g_{ij}(0)$ and $\widehat{g}_{11}(0)$ should have the same sign, and we have:

> **Pairing rule 2** (page 449): *Avoid (if possible) pairing on negative steady-state RGA elements.*

The reader is referred to Section 10.6.4 (page 438) for derivation and further discussion of these pairing rules.

3.4.2 Examples: RGA

Example 3.9 Blending process. *Consider a blending process where we mix sugar (u_1) and water (u_2) to make a given amount ($y_1 = F$) of a soft drink with a given sugar fraction ($y_2 = x$). The balances "mass in = mass out" for total mass and sugar mass are*

$$F_1 + F_2 = F$$

$$F_1 = xF$$

Note that the process itself has no dynamics. Linearization yields

$$dF_1 + dF_2 = dF$$

$$dF_1 = x^* dF + F^* dx$$

With $u_1 = dF_1, u_2 = dF_2, y_1 = dF$ and $y_2 = dx$ we then get the model

$$y_1 = u_1 + u_2$$

$$y_2 = \frac{1 - x^*}{F^*} u_1 - \frac{x^*}{F^*} u_2$$

where $x^* = 0.2$ is the nominal steady-state sugar fraction and $F^* = 2$ kg/s is the nominal amount. The transfer matrix then becomes

$$G(s) = \begin{bmatrix} 1 & 1 \\ \frac{1-x^*}{F^*} & -\frac{x^*}{F^*} \end{bmatrix} = \begin{bmatrix} 1 & 1 \\ 0.4 & -0.1 \end{bmatrix}$$

and the corresponding RGA matrix is (at all frequencies)

$$\Lambda = \begin{bmatrix} x^* & 1 - x^* \\ 1 - x^* & x^* \end{bmatrix} = \begin{bmatrix} 0.2 & 0.8 \\ 0.8 & 0.2 \end{bmatrix}$$

For decentralized control, it then follows from pairing rule 1 ("prefer pairing on RGA elements close to 1") that we should pair on the off-diagonal elements; that is, use u_1 to control y_2 and use u_2 to control y_1. This corresponds to using the largest stream (water, u_2) to control the amount ($y_1 = F$), which is reasonable from a physical point of view. Pairing rule 2 is also satisfied for this choice.

Example 3.10 Steady-state RGA. *Consider a 3×3 plant for which we have at steady-state*

$$G = \begin{bmatrix} 16.8 & 30.5 & 4.30 \\ -16.7 & 31.0 & -1.41 \\ 1.27 & 54.1 & 5.40 \end{bmatrix}, \ \Lambda(G) = \begin{bmatrix} 1.50 & 0.99 & -1.48 \\ -0.41 & 0.97 & 0.45 \\ -0.08 & -0.95 & 2.03 \end{bmatrix} \tag{3.64}$$

For decentralized control, we need to pair on one element in each column or row. It is then clear that the only choice that satisfies pairing rule 2 ("avoid pairing on negative RGA elements") is to pair on the diagonal elements; that is, use u_1 to control y_1, u_2 to control y_2 and u_3 to control y_3.

Remark. *The plant in (3.64) represents the steady-state model of a fluid catalytic cracking (FCC) process. A dynamic model of the FCC process in (3.64) is given in Exercise 6.17 (page 257).*

Some additional examples and exercises, that further illustrate the effectiveness of the steady-state RGA for selecting pairings, are given on page 442.

Example 3.11 Frequency-dependent RGA. *The following model describes a a large pressurized vessel (Skogestad and Wolff, 1991), for example, of the kind found in offshore oil-gas separations. The inputs are the valve positions for liquid (u_1) and vapour (u_2) flow, and the outputs are the liquid volume (y_1) and pressure (y_2).*

$$G(s) = \frac{0.01e^{-5s}}{(s+1.72\cdot 10^{-4})(4.32s+1)} \begin{bmatrix} -34.54(s+0.0572) & 1.913 \\ -30.22s & -9.188(s+6.95\cdot 10^{-4}) \end{bmatrix} \quad (3.65)$$

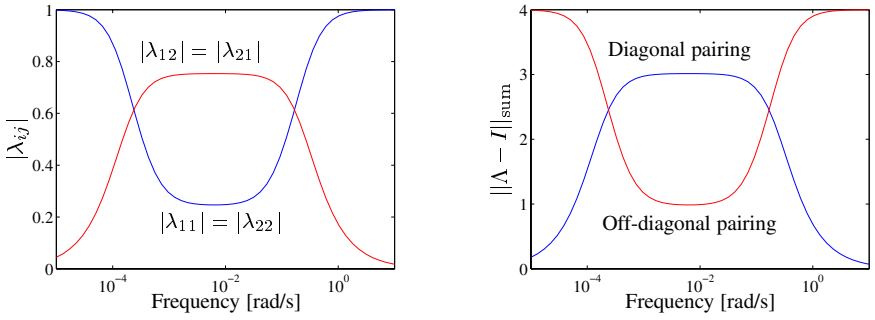

(a) Magnitude of RGA elements

(b) RGA number

Figure 3.8: Frequency-dependent RGA for $G(s)$ in (3.65)

The RGA matrix $\Lambda(s)$ depends on frequency. At steady-state ($s = 0$) the 2,1 element of $G(s)$ is zero, so $\Lambda(0) = I$. Similarly, at high frequencies the 1,2 element is small relative to the other elements, so $\Lambda(j\infty) = I$. This seems to suggest that the diagonal pairing should be used. However, at intermediate frequencies, the off-diagonal RGA elements are closest to 1*, see Figure 3.8(a). For example, at frequency $\omega = 0.01$ rad/s the RGA matrix becomes (see Table 3.1)*

$$\Lambda = \begin{bmatrix} 0.2469 + 0.0193i & 0.7531 - 0.0193i \\ 0.7531 - 0.0193i & 0.2469 + 0.0193i \end{bmatrix} \quad (3.66)$$

Thus, from pairing rule 1, the reverse pairings is probably best if we use decentralized control and the closed-loop bandwidth is around 0.01 rad/s. From a physical point of view the use of the reverse pairings is quite surprising, because it involves using the vapour flow (u_2) to control liquid level (y_1). and the liquid flow (u_1) to control pressure (y_2).

Remark. *Although it is possible to use decentralized control for this interactive process, see the following exercise, one may achieve much better performance with multivariable control. If one insists on using decentralized control, then it is recommended to add a liquid flow measurement and use an "inner" (lower layer) flow controller. The resulting u_1 is then the liquid flow rate rather than the valve position. Then u_2 (vapour flow) has no effect on y_1 (liquid volume), and the plant is triangular with $g_{12} = 0$. In this case the diagonal pairing is clearly best.*

Exercise 3.7 * *Design decentralized single-loop controllers for the plant (3.65) using (a) the diagonal pairings and (b) the off-diagonal pairings. Use the delay θ (which is nominally 5 seconds) as a*

Table 3.1: **Matlab program to calculate frequency-dependent RGA**

```
% Plant model (3.65)
s = tf('s');
G = (0.01/(s+1.72e-4)/(4.32*s + 1))*[-34.54*(s+0.0572),....
omega = logspace(-5,2,61);
% RGA
for i = 1:length(omega)
    Gf = freqresp(G,omega(i));                          % G(jω)
    RGAw(:,:,i) = Gf.*inv(Gf).';                        % RGA at frequency omega
    RGAno(i) = sum(sum(abs(RGAw(:,:,i) - eye(2))));     % RGA number
end
RGA = frd(RGAw,omega);
```

parameter. Use PI controllers independently tuned with the SIMC tuning rules (based on the paired elements).

Outline of solution: For tuning purposes the elements in $G(s)$ are approximated using the half rule to get

$$G(s) \approx \begin{bmatrix} -0.0823\frac{e^{-\theta s}}{s} & 0.01913\frac{e^{-(\theta+2.16)s}}{s} \\ -0.3022\frac{e^{-\theta s}}{4.32s+1} & -0.09188\frac{e^{-\theta s}}{4.32s+1} \end{bmatrix}$$

For the diagonal pairings this gives the PI settings

$$K_{c1} = -12.1/(\tau_{c1}+\theta), \tau_{I1} = 4(\tau_{c1}+\theta); K_{c2} = -47.0/(\tau_{c2}+\theta), \tau_{I2} = 4.32$$

and for the off-diagonal pairings (the index refers to the output)

$$K_{c1} = 52.3/(\tau_{c1}+\theta+2.16), \tau_{I1} = 4(\tau_{c1}+\theta+2.16); K_{c2} = -14.3/(\tau_{c2}+\theta), \tau_{I2} = 4.32$$

For improved robustness, the level controller (y_1) is tuned about 3 times slower than the pressure controller (y_2), i.e. use $\tau_{c1} = 3\theta$ and $\tau_{c2} = \theta$. This gives a crossover frequency of about $0.5/\theta$ in the fastest loop. With a delay of about 5 s or larger you should find, as expected from the RGA at crossover frequencies (pairing rule 1), that the off-diagonal pairing is best. However, if the delay is decreased from 5 s to 1 s, then the diagonal pairing is best, as expected since the RGA for the diagonal pairing approaches 1 at frequencies above 1 rad/s.

3.4.3 RGA number and iterative RGA

Note that in Figure 3.8(a) we plot only the magnitudes of λ_{ij}, but this may be misleading when selecting pairings. For example, a magnitude of 1 (seemingly a desirable pairing) may correspond to an RGA element of -1 (an undesirable pairing). The phase of the RGA elements should therefore also be considered. An alternative is to compute the RGA number, as defined next.

RGA number. A simple measure for selecting pairings according to rule 1 is to prefer pairings with a small *RGA number*. For a diagonal pairing,

$$\text{RGA number} \triangleq \|\Lambda(G) - I\|_{\text{sum}} \tag{3.67}$$

where we have (somewhat arbitrarily) chosen the sum norm, $\|A\|_{\text{sum}} = \sum_{i,j} |a_{ij}|$. The RGA number for other pairings is obtained by subtracting 1 for the selected pairings; for example, $\Lambda(G) - \begin{bmatrix} 0 & 1 \\ 1 & 0 \end{bmatrix}$ for the off-diagonal pairing for a 2×2 plant. The disadvantage with the RGA number, at least for larger systems, is that it needs to be recomputed for each alternative pairing. On the other hand, the RGA elements need to be computed only once.

Example 3.11 continued. *The RGA number for the plant $G(s)$ in (3.65) is plotted for the two alternative pairings in Figure 3.8(b). As expected, we see that the off-diagonal pairing is preferred at intermediate frequencies.*

Exercise 3.8 *Compute the RGA number for the six alternate pairings for the plant in (3.64). Which pairing would you prefer?*

Remark. Diagonal dominance. A more precise statement of pairing rule 1 (page 84) would be to prefer pairings that have "diagonal dominance" (see definition on page 10.6.4). There is a close relationship between a small RGA number and diagonal dominance, but unfortunately there are exceptions for plants of size 4×4 or larger, so a small RGA number does not always guarantee diagonal dominance; see Example 10.18 on page 440.

Iterative RGA. An iterative evaluation of the RGA, $\Lambda^2(G) = \Lambda(\Lambda(G))$ etc., is very useful for choosing pairings with diagonal dominance for large systems. Wolff (1994) found numerically that

$$\Lambda^\infty \triangleq \lim_{k\to\infty} \Lambda^k(G) \tag{3.68}$$

is a permuted identity matrix (except for "borderline" cases). More importantly, Johnson and Shapiro (1986, Theorem 2) have proven that Λ^∞ *always converges to the identity matrix if G is a generalized diagonally dominant matrix* (see definition in Remark 10.6.4 on page 439) . Since permuting the matrix G causes similar permutations of $\Lambda(G)$, Λ^∞ may then be used as a candidate pairing choice. Typically, Λ^k approaches Λ^∞ for k between 4 and 8. For example, for $G = \begin{bmatrix} 1 & 2 \\ -1 & 1 \end{bmatrix}$ we get $\Lambda = \begin{bmatrix} 0.33 & 0.67 \\ 0.67 & 0.33 \end{bmatrix}$, $\Lambda^2 = \begin{bmatrix} -0.33 & 1.33 \\ 1.33 & -0.33 \end{bmatrix}$, $\Lambda^3 = \begin{bmatrix} -0.07 & 1.07 \\ 1.07 & -0.07 \end{bmatrix}$ and $\Lambda^4 = \begin{bmatrix} 0.00 & 1.00 \\ 1.00 & 0.00 \end{bmatrix}$, which indicates that the off-diagonal pairing is diagonally dominant. Note that Λ^∞ may sometimes "recommend" a pairing on negative RGA elements, even if a positive pairing is possible.

Exercise 3.9 *Test the iterative RGA method on the plant (3.64) and confirm that it gives the diagonally dominant pairing (as it should according to the theory).*

3.4.4 Summary of algebraic properties of the RGA

The (complex) RGA matrix has a number of interesting *algebraic properties*, of which the most important are (see Appendix A.4, page 526, for more details):

A1. It is independent of input and output scaling.
A2. Its rows and columns sum to 1.
A3. The RGA is the identity matrix if G is upper or lower triangular.
A4. A relative change in an element of G equal to the negative inverse of its corresponding RGA element, $g'_{ij} = g_{ij}(1 - 1/\lambda_{ij})$, yields singularity.
A5. From (A.80), plants with large RGA elements are always ill-conditioned (with a large value of $\gamma(G)$), but the reverse may not hold (i.e. a plant with a large $\gamma(G)$ may have small RGA elements).

From property A3, it follows that the RGA (or more precisely $\Lambda - I$) provides a measure of *two-way interaction*.

Example 3.12 *Consider a diagonal plant for which we have*

$$G = \begin{bmatrix} 100 & 0 \\ 0 & 1 \end{bmatrix},\ \Lambda(G) = I,\ \gamma(G) = \frac{\bar{\sigma}(G)}{\underline{\sigma}(G)} = \frac{100}{1} = 100,\ \gamma^*(G) = 1 \tag{3.69}$$

Here the condition number is 100 *which means that the plant gain depends strongly on the input direction. However, since the plant is diagonal there are no interactions so* $\Lambda(G) = I$ *and the minimized condition number* $\gamma^*(G) = 1$.

Example 3.13 *Consider a triangular plant G for which we get*

$$G = \begin{bmatrix} 1 & 2 \\ 0 & 1 \end{bmatrix},\ G^{-1} = \begin{bmatrix} 1 & -2 \\ 0 & 1 \end{bmatrix},\ \Lambda(G) = I,\ \gamma(G) = \frac{2.41}{0.41} = 5.83,\ \gamma^*(G) = 1 \tag{3.70}$$

Note that for a triangular matrix, there is one-way interaction, but no two-way interaction, and the RGA is always the identity matrix.

Example 3.14 *Consider again the distillation process in (3.45) for which we have at steady-state*

$$G = \begin{bmatrix} 87.8 & -86.4 \\ 108.2 & -109.6 \end{bmatrix},\ G^{-1} = \begin{bmatrix} 0.399 & -0.315 \\ 0.394 & -0.320 \end{bmatrix},\ \Lambda(G) = \begin{bmatrix} 35.1 & -34.1 \\ -34.1 & 35.1 \end{bmatrix} \tag{3.71}$$

In this case $\gamma(G) = 197.2/1.391 = 141.7$ *is only slightly larger than* $\gamma^*(G) = 138.268$. *The magnitude sum of the elements in the RGA matrix is* $\|\Lambda\|_{\text{sum}} = 138.275$. *This confirms property A5 which states that, for* 2×2 *systems,* $\|\Lambda(G)\|_{\text{sum}} \approx \gamma^*(G)$ *when* $\gamma^*(G)$ *is large. The condition number is large, but since the minimum singular value* $\underline{\sigma}(G) = 1.391$ *is larger than* 1 *this does not by itself imply a control problem. However, the large RGA elements indicate problems, as discussed below (control property C1).*

Example 3.15 *Consider again the FCC process in (3.64) with* $\gamma = 69.6/1.63 = 42.6$ *and* $\gamma^* = 7.80$. *The magnitude sum of the elements in the RGA is* $\|\Lambda\|_{\text{sum}} = 8.86$ *which is close to* γ^* *as expected from property A5. Note that the rows and the columns of* Λ *in (3.64) sums to* 1. *Since* $\underline{\sigma}(G)$ *is larger than* 1 *and the RGA elements are relatively small, this steady-state analysis does not indicate any particular control problems for the plant.*

3.4.5 Summary of control properties of the RGA

In addition to the algebraic properties listed above, the RGA has a surprising number of useful *control properties*:

C1. *Large RGA elements (typically,* $5 - 10$ *or larger) at frequencies important for control indicate that the plant is fundamentally difficult to control due to strong interactions and sensitivity to uncertainty.*

   (a) *Uncertainty in the input channels (diagonal input uncertainty)*. Plants with large RGA elements (at crossover frequency) are fundamentally difficult to control because of sensitivity to input uncertainty, e.g. caused by uncertain or neglected actuator dynamics. In particular, decouplers or other inverse-based controllers should not be used for plants with large RGA elements (see page 251).

   (b) *Element uncertainty.* As implied by algebraic property A4 above, large RGA elements imply sensitivity to element-by-element uncertainty. However, this kind of uncertainty may not occur in practice due to physical couplings between the transfer function elements. Therefore, diagonal input uncertainty (which is always present) is usually of more concern for plants with large RGA elements.

C2. *RGA and RHP-zeros.* If the sign of an RGA element changes as we go from $s = 0$ to $s = \infty$, then there is a RHP-zero in G or in some subsystem of G (see Theorem 10.7, page 445).

C3. *Non-square plants*. The definition of the RGA may be generalized to non-square matrices by using the pseudo-inverse; see Appendix A.4.2. Extra inputs: If the sum of the elements in a column of RGA is small ($\ll 1$), then one may consider deleting the corresponding input. Extra outputs: If all elements in a row of RGA are small ($\ll 1$), then the corresponding output cannot be controlled.

C4. *RGA and decentralized control.* The usefulness of the RGA is summarized by the two pairing rules on page 84.

Example 3.14 continued. *For the steady-state distillation model in (3.71), the large RGA element of* 35.1 *indicates a control problem. More precisely, fundamental control problems are expected if analysis shows that* $G(j\omega)$ *has large RGA elements also in the crossover frequency range. Indeed, with the idealized dynamic model (3.93) used below, the RGA elements are large at all frequencies, and we will confirm in simulations that there is a strong sensitivity to input channel uncertainty with an inverse-based controller, see page 100. For decentralized control, we should, according to rule 2, avoid pairing on the negative RGA elements. Thus, the diagonal pairing is preferred.*

Example 3.16 *Consider the plant*

$$G(s) = \frac{1}{5s+1}\begin{pmatrix} s+1 & s+4 \\ 1 & 2 \end{pmatrix} \tag{3.72}$$

We find that $\lambda_{11}(\infty) = 2$ *and* $\lambda_{11}(0) = -1$ *have different signs. Since none of the diagonal elements have RHP-zeros we conclude from property C2 that* $G(s)$ *must have a RHP-zero. This is indeed true and* $G(s)$ *has a zero at* $s = 2$.

Let us elaborate a bit more on the use of RGA for decentralized control (control property C4). Assume we use decentralized control with integral action in each loop, and want to pair on one or more negative steady-state RGA elements. This may happen because this pairing is preferred for dynamic reasons or because there exists no pairing choice with only positive RGA elements, e.g. see the system in (10.80) on page 443. What will happen? Will the system be unstable? No, not necessarily. We may, for example, tune one loop at a time in a sequential manner (usually starting with the fastest loops), and we will end up with a stable overall system. However, due to the negative RGA element there will be some hidden problem, because the system is not *decentralized integral controllable* (DIC); see page 442. The stability of the overall system then depends on the individual loops being in service. This means that detuning one or more of the individual loops may result in instability for the overall system. Instability may also occur if an input saturates, because the corresponding loop is then effectively out of service. In summary, pairing on negative steady-state RGA elements should be avoided, and if it cannot be avoided then one should make sure that the loops remain in service.

For a detailed analysis of achievable performance of the plant (input–output controllability analysis), one must consider the singular values, as well as the RGA and condition number as functions of frequency. In particular, the crossover frequency range is important. In addition, disturbances and the presence of unstable (RHP) plant poles and zeros must be considered. All these issues are discussed in much more detail in Chapters 5 and 6 where we address achievable performance and input–output controllability analysis for SISO and MIMO plants, respectively.

3.5 Control of multivariable plants

3.5.1 Diagonal controller (decentralized control)

The simplest approach to multivariable controller design is to use a diagonal or block-diagonal controller $K(s)$. This is often referred to as decentralized control. Decentralized control works well if $G(s)$ is close to diagonal, because then the plant to be controlled is essentially a collection of independent sub-plants. However, if the off-diagonal elements in $G(s)$ are large, then the performance with decentralized diagonal control may be poor because no attempt is made to counteract the interactions. There are three basic approaches to the design of decentralized controllers:

- Fully coordinated design
- Independent design
- Sequential design

Decentralized control is discussed in more detail in Chapter 10 on page 428.

3.5.2 Two-step compensator design approach

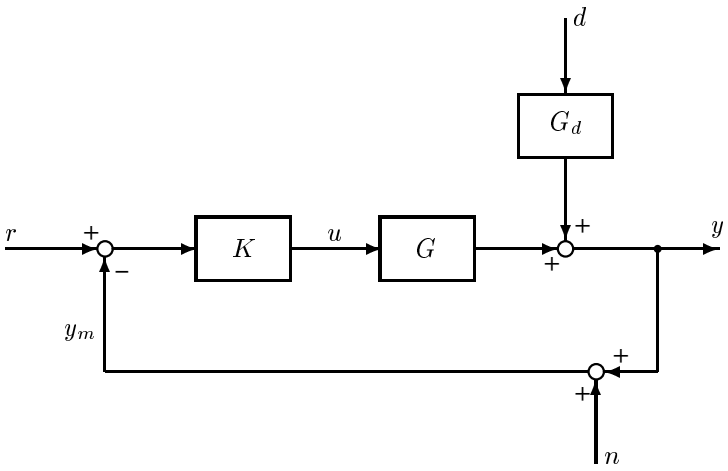

Figure 3.9: One degree-of-freedom feedback control configuration

Consider the simple feedback system in Figure 3.9. A conceptually simple approach to multivariable control is given by a two-step procedure in which we first design a "compensator" to deal with the interactions in G, and then design a *diagonal* controller using methods similar to those for SISO systems in Chapter 2. Several such approaches are discussed below.

The most common approach is to use a pre-compensator, $W_1(s)$, which counteracts the interactions in the plant and results in a "new" shaped plant:

$$G_s(s) = G(s)W_1(s) \tag{3.73}$$

which is more diagonal and easier to control than the original plant $G(s)$. After finding a suitable $W_1(s)$ we can design a *diagonal* controller $K_s(s)$ for the shaped plant $G_s(s)$. The

overall controller is then

$$K(s) = W_1(s)K_s(s) \tag{3.74}$$

In many cases effective compensators may be derived on physical grounds and may include nonlinear elements such as ratios.

Remark 1 Some design approaches in this spirit are the Nyquist array technique of Rosenbrock (1974) and the characteristic loci technique of MacFarlane and Kouvaritakis (1977).

Remark 2 The $\mathcal{H}_\infty$ loop-shaping design procedure, described in detail in Section 9.4, is similar in that a pre-compensator is first chosen to yield a shaped plant, $G_s = GW_1$, with desirable properties, and then a controller $K_s(s)$ is designed. The main difference is that in $\mathcal{H}_\infty$ loop shaping, $K_s(s)$ is a full multivariable controller, designed and based on optimization (to optimize $\mathcal{H}_\infty$ robust stability).

3.5.3 Decoupling

Decoupling control results when the compensator W_1 is chosen such that $G_s = GW_1$ in (3.73) is diagonal at a selected frequency. The following different cases are possible:

1. **Dynamic decoupling:** $G_s(s)$ is diagonal at all frequencies. For example, with $G_s(s) = I$ and a square plant, we get $W_1 = G^{-1}(s)$ (disregarding the possible problems involved in realizing $G^{-1}(s)$). If we then select $K_s(s) = l(s)I$ (e.g. with $l(s) = k/s$), the overall controller is
$$K(s) = K_{\text{inv}}(s) \triangleq l(s)G^{-1}(s) \tag{3.75}$$
We will later refer to (3.75) as an *inverse-based* controller. It results in a decoupled nominal system with identical loops, i.e. $L(s) = l(s)I$, $S(s) = \frac{1}{1+l(s)}I$ and $T(s) = \frac{l(s)}{1+l(s)}I$.

   Remark. In some cases we may want to keep the diagonal elements in the shaped plant unchanged by selecting $W_1 = G^{-1}G_{diag}$. In other cases we may want the diagonal elements in W_1 to be 1. This may be obtained by selecting $W_1 = G^{-1}((G^{-1})_{diag})^{-1}$, and the off-diagonal elements of W_1 are then called "decoupling elements".

2. **Steady-state decoupling:** $G_s(0)$ is diagonal. This may be obtained by selecting a constant pre-compensator $W_1 = G^{-1}(0)$ (and for a non-square plant we may use the pseudo-inverse provided $G(0)$ has full row (output) rank).
3. **Approximate decoupling at frequency w_o:** $G_s(j\omega_o)$ is as diagonal as possible. This is usually obtained by choosing a constant pre-compensator $W_1 = G_o^{-1}$ where G_o is a real approximation of $G(j\omega_o)$. G_o may be obtained, for example, using the align algorithm of Kouvaritakis (1974) (see file `align.m` available at the book's home page). The bandwidth frequency is a good selection for ω_o because the effect on performance of reducing interaction is normally greatest at this frequency.

The idea of decoupling control is appealing, but there are several difficulties:

1. As one might expect, decoupling may be very sensitive to modelling errors and uncertainties. This is illustrated below in Section 3.7.2 (page 100).
2. The requirement of decoupling and the use of an inverse-based controller may not be desirable for disturbance rejection. The reasons are similar to those given for SISO systems in Section 2.6.4, and are discussed further below; see (3.79).
3. If the plant has RHP-zeros then the requirement of decoupling generally introduces extra RHP-zeros into the closed-loop system (see Section 6.6.1, page 236).

Even though decoupling controllers may not always be desirable in practice, they are of interest from a theoretical point of view. They also yield insights into the limitations imposed by the multivariable interactions on achievable performance. One popular design method, which essentially yields a decoupling controller, is the internal model control (IMC) approach (Morari and Zafiriou, 1989).

Another common strategy, which avoids most of the problems just mentioned, is to use *partial (one-way) decoupling* where $G_s(s)$ in (3.73) is upper or lower triangular.

3.5.4 Pre- and post-compensators and the SVD controller

The above pre-compensator approach may be extended by introducing a post-compensator $W_2(s)$, as shown in Figure 3.10. One then designs a *diagonal* controller K_s for the shaped

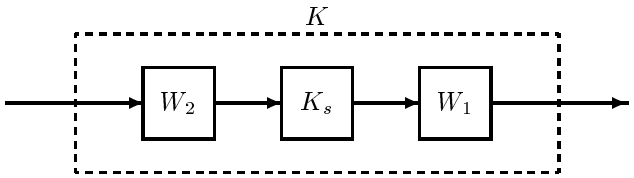

Figure 3.10: Pre- and post-compensators, W_1 and W_2. K_s is diagonal.

plant W_2GW_1. The overall controller is then

$$K(s) = W_1 K_s W_2 \tag{3.76}$$

The *SVD controller* is a special case of a pre- and post-compensator design. Here

$$W_1 = V_o \quad \text{and} \quad W_2 = U_o^T \tag{3.77}$$

where V_o and U_o are obtained from the SVD of $G_o = U_o \Sigma_o V_o^T$, where G_o is a real approximation of $G(j\omega_o)$ at a given frequency w_o (often around the bandwidth). SVD controllers are studied by Hung and MacFarlane (1982), and by Hovd et al. (1997) who found that the SVD-controller structure is optimal in some cases, e.g. for plants consisting of symmetrically interconnected subsystems.

In summary, the SVD controller provides a useful class of controllers. By selecting $K_s = l(s)\Sigma_o^{-1}$ a decoupling design is achieved, and selecting a diagonal K_s with a low condition number ($\gamma(K_s)$ small) generally results in a robust controller (see Section 6.10).

3.5.5 What is the shape of the "best" feedback controller?

Consider the problem of disturbance rejection. The closed-loop disturbance response is $y = SG_d d$. Suppose we have scaled the system (see Section 1.4) such that at each frequency the disturbances are of maximum magnitude 1, $\|d\|_2 \leq 1$, and our performance requirement is that $\|y\|_2 \leq 1$. This is equivalent to requiring $\bar{\sigma}(SG_d) \leq 1$. In many cases there is a trade-off between input usage and performance, such that the controller that minimizes the input magnitude is one that yields all singular values of SG_d equal to 1, i.e. $\sigma_i(SG_d) = 1, \forall\omega$. This corresponds to

$$S_{\min} G_d = U_1 \tag{3.78}$$

where $U_1(s)$ is some all-pass transfer function (which at each frequency has all its singular values equal to 1). The subscript min refers to the use of the smallest loop gain that satisfies the performance objective. For simplicity, we assume that G_d is square so $U_1(j\omega)$ is a unitary matrix. At frequencies where feedback is effective we have $S = (I + L)^{-1} \approx L^{-1}$, and (3.78) yields $L_{\min} = GK_{\min} \approx G_d U_1^{-1}$. In conclusion, the controller and loop shape with the minimum gain will often look like

$$K_{\min} \approx G^{-1} G_d U_2, \quad L_{\min} \approx G_d U_2 \tag{3.79}$$

where $U_2 = U_1^{-1}$ is some all-pass transfer function matrix. This provides a generalization of $|K_{\min}| \approx |G^{-1} G_d|$ which was derived in (2.66) for SISO systems, and the summary following (2.66) on page 48 therefore also applies to MIMO systems. For example, we see that for disturbances entering at the plant inputs, $G_d = G$, we get $K_{\min} = U_2$, so a simple constant unit gain controller yields a good trade-off between output performance and input usage. We also note with interest that it is generally not possible to select a unitary matrix U_2 such that $L_{\min} = G_d U_2$ is diagonal, so a decoupling design is generally not optimal for disturbance rejection. These insights can be used as a basis for a loop-shaping design; see more on $\mathcal{H}_\infty$ loop shaping in Chapter 9.

3.5.6 Multivariable controller synthesis

The above design methods are based on a two-step procedure in which we first design a pre-compensator (for decoupling control) or we make an input–output pairing selection (for decentralized control) and then we design a diagonal controller $K_s(s)$. Invariably this two-step procedure results in a suboptimal design.

The alternative is to synthesize directly a multivariable controller $K(s)$ based on minimizing some objective function (norm). Here we use the word *synthesize* rather than *design* to stress that this is a more formalized approach. Optimization in controller design became prominent in the 1960's with "optimal control theory" based on minimizing the expected value of the output variance in the face of stochastic disturbances. Later, other approaches and norms were introduced, such as $\mathcal{H}_\infty$ optimal control.

3.5.7 Summary of mixed-sensitivity $\mathcal{H}_\infty$ synthesis (S/KS)

We provide a brief summary here of one multivariable synthesis approach, namely the S/KS (mixed-sensitivity) $\mathcal{H}_\infty$ design method which is used in later examples in this chapter. In the S/KS problem, the objective is to minimize the $\mathcal{H}_\infty$ norm of

$$N = \begin{bmatrix} W_P S \\ W_u K S \end{bmatrix} \tag{3.80}$$

This problem was discussed earlier for SISO systems, and another look at Section 2.8.3 would be useful now. A sample Matlab file is provided in Example 2.17, page 64.

The following issues and guidelines are relevant when selecting the weights W_P and W_u:

1. S is the transfer function from r to $-e = r - y$. A common choice for the performance weight is $W_P = \mathrm{diag}\{w_{Pi}\}$ with

$$w_{Pi} = \frac{s/M_i + \omega^*_{Bi}}{s + \omega^*_{Bi} A_i}, \quad A_i \ll 1 \tag{3.81}$$

(see also Figure 2.29 on page 62). Selecting $A_i \ll 1$ ensures approximate integral action with $S(0) \approx 0$. Often we select M_i about 2 for all outputs, whereas the desired closed-loop bandwidth ω^*_{Bi} may be different for each output. A large value of ω^*_{Bi} yields a faster response for output i.

2. KS is the transfer function from references r to inputs u in Figure 3.9, so for a system which has been scaled as in Section 1.4, a reasonable initial choice for the input weight is $W_u = I$. However, if we require tight control at low frequencies (i.e. A_i small in (3.81)), then input usage is unavoidable at low frequencies, and it may be better to use a weight of the form $W_u = s/(s + \omega_1)$, where the adjustable frequency ω_1 is approximately the closed-loop bandwidth. One could also include additional high-frequency penalty in W_u, but often this is not necessary due to the low gain of G at high frequencies. If one wants to bound KS at high frequencies, it is often better instead to put a bound on T (see below).
3. To find a reasonable initial choice for the weight W_P, one can first obtain a controller with some other design method, plot the magnitude of the resulting diagonal elements of S as a function of frequency, and select $w_{Pi}(s)$ as a rational approximation of $1/|S_{ii}|$.
4. For disturbance rejection, we may in some cases want a steeper slope for $w_{Pi}(s)$ at low frequencies than that given in (3.81), e.g. see the weight in (2.106). However, it may be better to consider the disturbances explicitly by considering the $\mathcal{H}_\infty$ norm of

$$N = \begin{bmatrix} W_P S & W_P S G_d \\ W_u K S & W_u K S G_d \end{bmatrix} \tag{3.82}$$

or equivalently

$$N = \begin{bmatrix} W_P S W_d \\ W_u K S W_d \end{bmatrix} \text{ with } W_d = \begin{bmatrix} I & G_d \end{bmatrix} \tag{3.83}$$

where N represents the transfer function from $\begin{bmatrix} r \\ d \end{bmatrix}$ to the weighted e and u. In some situations we may want to adjust W_P or G_d in order to satisfy better our original objectives. The helicopter case study in Section 13.2 illustrates this by introducing a scalar parameter α to adjust the magnitude of G_d.

5. T is the transfer function from $-n$ to y. To reduce sensitivity to noise and uncertainty, we want T small at high frequencies, and so we may want additional roll-off in L. This can be achieved in several ways. One approach is to add $W_T T$ to the stack for N in (3.80), where $W_T = \mathrm{diag}\{w_{Ti}\}$ and $|w_{Ti}|$ is smaller than 1 at low frequencies and large at high frequencies. A more direct approach is to add high-frequency dynamics, $W_1(s)$, to the plant model to ensure that the resulting shaped plant, $G_s = GW_1$, rolls off with the desired slope. We then obtain an $\mathcal{H}_\infty$ optimal controller K_s for this shaped plant, and finally include $W_1(s)$ in the controller, $K = W_1 K_s$.

Numerically, the problem $\min_K \|N\|_\infty$ is often solved by γ-iteration, where one solves for the controllers that achieve $\|N\|_\infty < \gamma$, and then reduces γ iteratively to obtain the smallest value $\gamma_{\min}$ for which a solution exists. More details about $\mathcal{H}_\infty$ design are given in Chapter 9.

3.6 Introduction to multivariable RHP-zeros

By means of an example, we now give the reader an appreciation of the fact that MIMO systems have zeros even though their presence may not be obvious from the elements of $G(s)$. As for SISO systems, we find that RHP-zeros impose fundamental limitations on control.

The zeros z of MIMO systems are defined as the values $s = z$ where $G(s)$ loses rank, and we can find the *direction* of a zero by looking at the direction in which the matrix $G(z)$ has zero gain. For square systems we essentially have that the poles and zeros of $G(s)$ are the poles and zeros of $\det G(s)$. However, this crude method may fail in some cases, as it may incorrectly cancel poles and zeros with the same location but different directions (see Sections 4.5 and 4.5.3 for more details).

Example 3.17 *Consider the following plant:*

$$G(s) = \frac{1}{(0.2s+1)(s+1)} \begin{bmatrix} 1 & 1 \\ 1+2s & 2 \end{bmatrix} \tag{3.84}$$

The responses to a step in each individual input are shown in Figure 3.11(a) and (b). We see that the

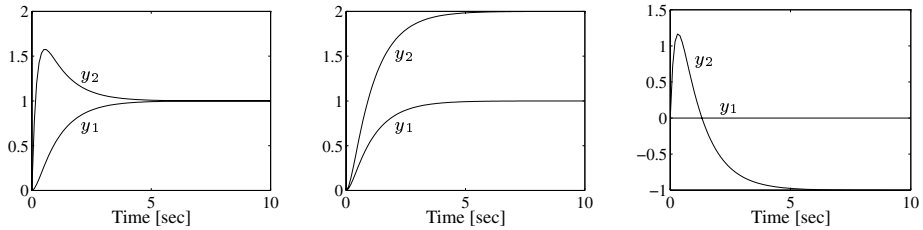

(a) Step in u_1, $u = [\,1 \quad 0\,]^T$

(b) Step in u_2, $u = [\,0 \quad 1\,]^T$

(c) Combined step in u_1 and u_2, $u = [\,1 \quad -1\,]^T$

Figure 3.11: Open-loop response for $G(s)$ in (3.84)

plant is interactive, but for these two inputs there is no inverse response to indicate the presence of a RHP-zero. Nevertheless, the plant does have a multivariable RHP-zero at $z = 0.5$; that is, $G(s)$ loses rank at $s = 0.5$, and $\det G(0.5) = 0$. The SVD of $G(0.5)$ is

$$G(0.5) = \frac{1}{1.65}\begin{bmatrix} 1 & 1 \\ 2 & 2 \end{bmatrix} = \underbrace{\begin{bmatrix} 0.45 & 0.89 \\ 0.89 & -0.45 \end{bmatrix}}_{U} \underbrace{\begin{bmatrix} 1.92 & 0 \\ 0 & 0 \end{bmatrix}}_{\Sigma} \underbrace{\begin{bmatrix} 0.71 & 0.71 \\ 0.71 & -0.71 \end{bmatrix}^H}_{V^H} \tag{3.85}$$

and we have as expected $\underline{\sigma}(G(0.5)) = 0$. The directions corresponding to the RHP-zero are $\underline{v} = \begin{bmatrix} 0.71 \\ -0.71 \end{bmatrix}$ (input direction) and $\underline{u} = \begin{bmatrix} 0.89 \\ -0.45 \end{bmatrix}$ (output direction). Thus, the RHP-zero is associated with both inputs and with both outputs. The presence of the multivariable RHP-zero is indeed observed from the time response in Figure 3.11(c), which is for a simultaneous input change in opposite directions, $u = \begin{bmatrix} 1 \\ -1 \end{bmatrix}$. We see that y_2 displays an inverse response whereas y_1 happens to remain at zero for this particular input change.

To see how the RHP-zero affects the closed-loop response, we design a controller which minimizes the $\mathcal{H}_\infty$ norm of the weighted S/KS matrix

$$N = \begin{bmatrix} W_P S \\ W_u K S \end{bmatrix} \tag{3.86}$$

with weights

$$W_u = I,\ W_P = \begin{bmatrix} w_{P1} & 0 \\ 0 & w_{P2} \end{bmatrix},\ w_{Pi} = \frac{s/M_i + \omega^*_{Bi}}{s + w^*_{Bi}A_i}, \quad A_i = 10^{-4} \tag{3.87}$$

The Matlab file for the design is the same as in Table 2.4 on page 64, except that we now have a 2×2 *system. Since there is a RHP-zero at* $z = 0.5$ *we expect that this will somehow limit the bandwidth of the closed-loop system.*

Design 1. *We weight the two outputs equally and select*

$$\text{Design 1}: \quad M_1 = M_2 = 1.5; \quad \omega^*_{B1} = \omega^*_{B2} = z/2 = 0.25$$

This yields an $\mathcal{H}_\infty$ *norm for* N *of* 2.80 *and the resulting singular values of* S *are shown by the solid lines in Figure 3.12(a). The closed-loop response to a reference change* $r = \begin{bmatrix} 1 & -1 \end{bmatrix}^T$ *is shown by the solid lines in Figure 3.12(b). We note that both outputs behave rather poorly and both display an inverse response.*

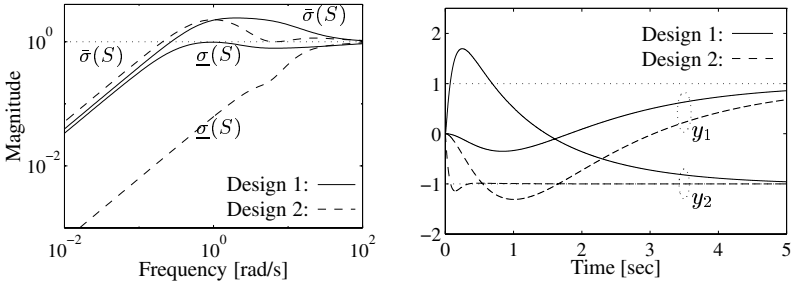

(a) Singular values of S

(b) Response to change in reference, $r = \begin{bmatrix} 1 & -1 \end{bmatrix}^T$

Figure 3.12: Alternative designs for 2×2 plant (3.84) with RHP-zero

Design 2. *For MIMO plants, one can often move most of the deteriorating effect (e.g. inverse response) of a RHP-zero to a particular output channel. To illustrate this, we change the weight* w_{P2} *so that more emphasis is placed on output* 2*. We do this by increasing the bandwidth requirement in output channel* 2 *by a factor of* 100*:*

$$\text{Design 2}: \quad M_1 = M_2 = 1.5; \quad \omega^*_{B1} = 0.25,\ \omega^*_{B2} = 25$$

This yields an $\mathcal{H}_\infty$ *norm for* N *of* 2.92*. In this case we see from the dashed line in Figure 3.12(b) that the response for output* 2 *(*y_2*) is excellent with no inverse response. However, this comes at the expense of output* 1 *(*y_1*) where the response is poorer than for Design* 1*.*

Design 3. *We can also interchange the weights* w_{P1} *and* w_{P2} *to stress output* 1 *rather than output* 2*. In this case (not shown) we get an excellent response in output* 1 *with no inverse response, but output* 2 *responds very poorly (much poorer than output* 1 *for Design* 2*). Furthermore, the* $\mathcal{H}_\infty$ *norm for* N *is* 6.73*, whereas it was only* 2.92 *for Design* 2*.*

Thus, we see that it is easier, for this example, to get tight control of output 2 *than of output* 1*. This may be expected from the output direction of the RHP-zero,* $\underline{u} = \begin{bmatrix} 0.89 \\ -0.45 \end{bmatrix}$*, which is mostly in the direction of output* 1*. We will discuss this in more detail in Section 6.6.1.*

Remark 1 We find from this example that we can direct the effect of the RHP-zero to either of the two outputs. This is typical of multivariable RHP-zeros, but in other cases the RHP-zero is associated with a particular output channel and it is *not* possible to move its effect to another channel. The zero is then called a "pinned zero" (see Section 4.6).

Remark 2 It is observed from the plot of the singular values in Figure 3.12(a) that we were able to obtain by Design 2 a very large improvement in the "good" direction (corresponding to $\underline{\sigma}(S)$) at the

expense of only a minor deterioration in the "bad" direction (corresponding to $\bar{\sigma}(S)$). Thus Design 1 demonstrates a shortcoming of the $\mathcal{H}_\infty$ norm: only the worst direction (maximum singular value) contributes to the $\mathcal{H}_\infty$ norm and it may not always be easy to get a good trade-off between the various directions.

3.7 Introduction to MIMO robustness

To motivate the need for a deeper understanding of robustness, we present two examples which illustrate that MIMO systems can display a sensitivity to uncertainty not found in SISO systems. We focus our attention on diagonal input uncertainty, which is present in any real system and often limits achievable performance because it enters between the controller and the plant.

3.7.1 Motivating robustness example no. 1: spinning satellite

Consider the following plant (Doyle, 1986; Packard et al., 1993) which can itself be motivated by considering the angular velocity control of a satellite spinning about one of its principal axes:

$$G(s) = \frac{1}{s^2 + a^2} \begin{bmatrix} s - a^2 & a(s+1) \\ -a(s+1) & s - a^2 \end{bmatrix}; \quad a = 10 \tag{3.88}$$

A minimal state-space realization, $G = C(sI - A)^{-1}B + D$, is

$$\left[\begin{array}{c|c} A & B \\ \hline C & D \end{array}\right] = \left[\begin{array}{cc|cc} 0 & a & 1 & 0 \\ -a & 0 & 0 & 1 \\ \hline 1 & a & 0 & 0 \\ -a & 1 & 0 & 0 \end{array}\right] \tag{3.89}$$

The plant has a pair of $j\omega$-axis poles at $s = \pm ja$ so it needs to be stabilized. Let us apply negative feedback and try the simple diagonal constant controller

$$K = I$$

The complementary sensitivity function is

$$T(s) = GK(I + GK)^{-1} = \frac{1}{s+1} \begin{bmatrix} 1 & a \\ -a & 1 \end{bmatrix} \tag{3.90}$$

Nominal stability (NS). The closed-loop system has two poles at $s = -1$ and so it is stable. This can be verified by evaluating the closed-loop state matrix

$$A_{cl} = A - BKC = \begin{bmatrix} 0 & a \\ -a & 0 \end{bmatrix} - \begin{bmatrix} 1 & a \\ -a & 1 \end{bmatrix} = \begin{bmatrix} -1 & 0 \\ 0 & -1 \end{bmatrix}$$

(To derive A_{cl} use $\dot{x} = Ax + Bu$, $y = Cx$ and $u = -Ky$.)

Nominal performance (NP). The singular values of $L = GK = G$ are shown in Figure 3.7(a), page 80. We see that $\underline{\sigma}(L) = 1$ at low frequencies and starts dropping off at about $\omega = 10$. Since $\underline{\sigma}(L)$ never exceeds 1, we do not have tight control in the low-gain

direction for this plant (recall the discussion following (3.51)), so we expect poor closed-loop performance. This is confirmed by considering S and T. For example, at steady-state $\bar{\sigma}(T) = 10.05$ and $\bar{\sigma}(S) = 10$. Furthermore, the large off-diagonal elements in $T(s)$ in (3.90) show that we have strong interactions in the closed-loop system. (For reference tracking, however, this may be counteracted by use of a two degrees-of-freedom controller.)

Robust stability (RS). Now let us consider stability robustness. In order to determine stability margins with respect to perturbations in each input channel, one may consider Figure 3.13 where we have broken the loop at the first input. The loop transfer function at this point (the transfer function from w_1 to z_1) is $L_1(s) = 1/s$ (which can be derived from $t_{11}(s) = \frac{1}{1+s} = \frac{L_1(s)}{1+L_1(s)}$). This corresponds to an infinite gain margin and a phase margin of 90°. On breaking the loop at the second input we get the same result. This suggests good robustness properties irrespective of the value of a. However, the design is far from robust as a further analysis shows. Consider input gain uncertainty, and let ϵ_1 and ϵ_2 denote the relative

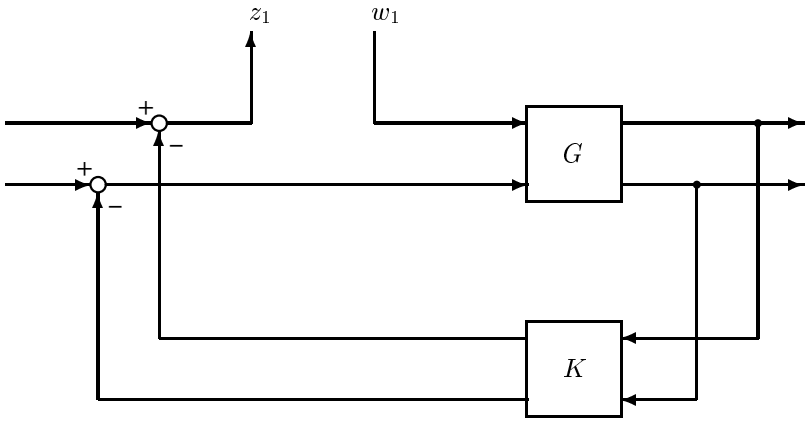

Figure 3.13: Checking stability margins "one-loop-at-a-time"

error in the gain in each input channel. Then

$$u_1' = (1+\epsilon_1)u_1, \quad u_2' = (1+\epsilon_2)u_2 \tag{3.91}$$

where u_1' and u_2' are the actual changes in the manipulated inputs, while u_1 and u_2 are the desired changes as computed by the controller. It is important to stress that this diagonal input uncertainty, which stems from our inability to know the exact values of the manipulated inputs, is *always* present. In terms of a state-space description, (3.91) may be represented by replacing B by

$$B' = \begin{bmatrix} 1+\epsilon_1 & 0 \\ 0 & 1+\epsilon_2 \end{bmatrix}$$

The corresponding closed-loop state matrix is

$$A_{cl}' = A - B'KC = \begin{bmatrix} 0 & a \\ -a & 0 \end{bmatrix} - \begin{bmatrix} 1+\epsilon_1 & 0 \\ 0 & 1+\epsilon_2 \end{bmatrix} \begin{bmatrix} 1 & a \\ -a & 1 \end{bmatrix}$$

which has a characteristic polynomial given by

$$\det(sI - A_{cl}') = s^2 + \underbrace{(2+\epsilon_1+\epsilon_2)}_{a_1} s + \underbrace{1+\epsilon_1+\epsilon_2+(a^2+1)\epsilon_1\epsilon_2}_{a_0} \tag{3.92}$$

The perturbed system is stable if and only if both the coefficients a_0 and a_1 are positive. We therefore see that *the system is always stable if we consider uncertainty in only one channel at a time* (at least as long as the channel gain is positive). More precisely, we have stability for $(-1 < \epsilon_1 < \infty, \epsilon_2 = 0)$ and $(\epsilon_1 = 0, -1 < \epsilon_2 < \infty)$. This confirms the infinite gain margin seen earlier. However, the system can only tolerate *small simultaneous changes* in the two channels. For example, let $\epsilon_1 = -\epsilon_2$, then the system is unstable ($a_0 < 0$) for

$$|\epsilon_1| > \frac{1}{\sqrt{a^2+1}} \approx 0.1$$

In summary, we have found that checking single-loop margins is inadequate for MIMO problems. We have also observed that large values of $\bar{\sigma}(T)$ or $\bar{\sigma}(S)$ indicate robustness problems. We will return to this in Chapter 8, where we show that with input uncertainty of magnitude $|\epsilon_i| < 1/\bar{\sigma}(T)$, we are guaranteed robust stability (even for "full-block complex perturbations").

In the next example we find that there can be sensitivity to diagonal input uncertainty even in cases where $\bar{\sigma}(T)$ and $\bar{\sigma}(S)$ have no large peaks. This cannot happen for a diagonal controller, see (6.92), but it will happen if we use an inverse-based controller for a plant with large RGA elements, see (6.93).

3.7.2 Motivating robustness example no. 2: distillation process

The following is an idealized dynamic model of a distillation column:

$$G(s) = \frac{1}{75s+1}\begin{bmatrix} 87.8 & -86.4 \\ 108.2 & -109.6 \end{bmatrix} \tag{3.93}$$

(time is in minutes). The physics of this example was discussed in Example 3.6. The plant is ill-conditioned with condition number $\gamma(G) = 141.7$ at all frequencies. The plant is also strongly two-way interactive and the RGA matrix at all frequencies is

$$\Lambda(G) = \begin{bmatrix} 35.1 & -34.1 \\ -34.1 & 35.1 \end{bmatrix} \tag{3.94}$$

The large elements in this matrix indicate that this process is fundamentally difficult to control.

Remark. Equation (3.93) is admittedly a very crude model of a real distillation column; there should be a high-order lag in the transfer function from input 1 to output 2 to represent the liquid flow down to the column, and higher-order composition dynamics should also be included. Nevertheless, the model is simple and displays important features of distillation column behaviour. It should be noted that with a more detailed model, the RGA elements would approach 1 at frequencies around 1 rad/min, indicating less of a control problem.

We consider the following inverse-based controller, which may also be looked upon as a steady-state decoupler with a PI controller:

$$K_{\text{inv}}(s) = \frac{k_1}{s}G^{-1}(s) = \frac{k_1(1+75s)}{s}\begin{bmatrix} 0.3994 & -0.3149 \\ 0.3943 & -0.3200 \end{bmatrix}, \quad k_1 = 0.7 \tag{3.95}$$

Nominal performance (NP). We have $GK_{\text{inv}} = K_{\text{inv}}G = \frac{0.7}{s}I$. With no model error this controller should counteract all the interactions in the plant and give rise to two decoupled

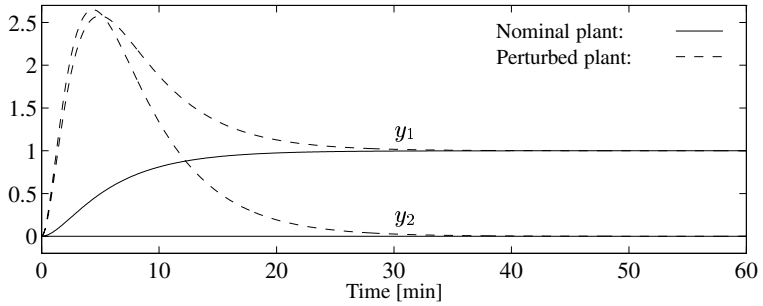

Figure 3.14: Response with decoupling controller to filtered reference input $r_1 = 1/(5s+1)$. The perturbed plant has 20% gain uncertainty as given by (3.97).

first-order responses each with a time constant of $1/0.7 = 1.43$ min. This is confirmed by the solid line in Figure 3.14 which shows the simulated response to a reference change in y_1. The responses are clearly acceptable, and we conclude that *nominal performance (NP) is achieved with the decoupling controller*.

Robust stability (RS). The resulting sensitivity and complementary sensitivity functions with this controller are

$$S = S_I = \frac{s}{s+0.7}I; \quad T = T_I = \frac{1}{1.43s+1}I \tag{3.96}$$

Thus, $\bar{\sigma}(S)$ and $\bar{\sigma}(T)$ are both less than 1 at all frequencies, so there are no peaks which would indicate robustness problems. We also find that this controller gives an infinite gain margin (GM) and a phase margin (PM) of 90° in each channel. Thus, use of the traditional margins and the peak values of S and T indicate no robustness problems. However, from the large RGA elements there is cause for concern, and this is confirmed in the following.

We consider again the input gain uncertainty (3.91) as in the previous example, and we select $\epsilon_1 = 0.2$ and $\epsilon_2 = -0.2$. We then have

$$u_1' = 1.2u_1, \quad u_2' = 0.8u_2 \tag{3.97}$$

Note that the uncertainty is on the *change* in the inputs (flow rates), and not on their absolute values. A 20% error is typical for process control applications (see Remark 2 on page 297). The uncertainty in (3.97) does not by itself yield instability. This is verified by computing the closed-loop poles, which, assuming no cancellations, are solutions to $\det(I + L(s)) = \det(I + L_I(s)) = 0$ (see (4.105) and (A.12)). In our case

$$L_I'(s) = K_{\text{inv}}G' = K_{\text{inv}}G\begin{bmatrix} 1+\epsilon_1 & 0 \\ 0 & 1+\epsilon_2 \end{bmatrix} = \frac{0.7}{s}\begin{bmatrix} 1+\epsilon_1 & 0 \\ 0 & 1+\epsilon_2 \end{bmatrix}$$

so the perturbed closed-loop poles are

$$s_1 = -0.7(1+\epsilon_1), \quad s_2 = -0.7(1+\epsilon_2) \tag{3.98}$$

and we have closed-loop stability as long as the input gains $1+\epsilon_1$ and $1+\epsilon_2$ remain positive, so we can have up to 100% error in each input channel. We thus conclude that *we have robust stability (RS) with respect to input gain errors for the decoupling controller.*

Robust performance (RP). For SISO systems we generally have that nominal performance (NP) and robust stability (RS) imply robust performance (RP), but this is not the case for MIMO systems. This is clearly seen from the dashed lines in Figure 3.14 which show the closed-loop response of the perturbed system. It differs drastically from the nominal response represented by the solid line, and even though it is stable, the response is clearly not acceptable; it is no longer decoupled, and $y_1(t)$ and $y_2(t)$ reach a value of about 2.5 before settling at their desired values of 1 and 0. *Thus RP is not achieved by the decoupling controller.*

Remark 1 There is a simple reason for the observed poor response to the reference change in y_1. To accomplish this change, which occurs mostly in the direction corresponding to the low plant gain, the inverse-based controller generates relatively *large* inputs u_1 and u_2, while trying to keep $u_1 - u_2$ very *small*. However, the input uncertainty makes this impossible – the result is an undesired *large* change in the actual value of $u_1' - u_2'$, which subsequently results in large changes in y_1 and y_2 because of the large plant gain ($\bar{\sigma}(G) = 197.2$) in this direction, as seen from (3.46).

Remark 2 The system remains stable for gain uncertainty up to 100% because the uncertainty occurs only at one side of the plant (at the input). If we also consider uncertainty at the output then we find that the decoupling controller yields instability for relatively small errors in the input and output gains. This is illustrated in Exercise 3.11 below.

Remark 3 It is also difficult to get a robust controller with other standard design techniques for this model. For example, an S/KS design as in (3.80) with $W_P = w_P I$ (using $M = 2$ and $\omega_B = 0.05$ in the performance weight (3.81)) and $W_u = I$ yields a good nominal response (although not decoupled), but the system is very sensitive to input uncertainty, and the outputs go up to about 3.4 and settle very slowly when there is 20% input gain error.

Remark 4 Attempts to make the inverse-based controller robust using the second step of the Glover–McFarlane $\mathcal{H}_\infty$ loop-shaping procedure are also unhelpful; see Exercise 3.12. This shows that robustness with respect to general coprime factor uncertainty does not necessarily imply robustness with respect to input uncertainty. In any case, the solution is to avoid inverse-based controllers for a plant with large RGA elements.

Exercise 3.10* *Design an SVD controller $K = W_1 K_s W_2$ for the distillation process in (3.93), i.e. select $W_1 = V$ and $W_2 = U^T$ where U and V are given in (3.46). Select K_s in the form*

$$K_s = \begin{bmatrix} c_1 \frac{75s+1}{s} & 0 \\ 0 & c_2 \frac{75s+1}{s} \end{bmatrix}$$

and try the following values:

(a) $c_1 = c_2 = 0.005$*;*

(b) $c_1 = 0.005$, $c_2 = 0.05$*;*

(c) $c_1 = 0.7/197 = 0.0036$, $c_2 = 0.7/1.39 = 0.504$.

Simulate the closed-loop reference response with and without uncertainty. Designs (a) and (b) should be robust. Which has the best performance? Design (c) should give the response in Figure 3.14. In the simulations, include high-order plant dynamics by replacing $G(s)$ by $\frac{1}{(0.02s+1)^5} G(s)$. What is the condition number of the controller in the three cases? Discuss the results. (See also the conclusion on page 251.)

Exercise 3.11 *Consider again the distillation process (3.93) with the decoupling controller, but also include output gain uncertainty $\widehat{\epsilon}_i$. That is, let the perturbed loop transfer function be*

$$L'(s) = G'K_{\text{inv}} = \frac{0.7}{s}\underbrace{\begin{bmatrix} 1+\widehat{\epsilon}_1 & 0 \\ 0 & 1+\widehat{\epsilon}_2 \end{bmatrix} G \begin{bmatrix} 1+\epsilon_1 & 0 \\ 0 & 1+\epsilon_2 \end{bmatrix} G^{-1}}_{L_0} \tag{3.99}$$

where L_0 is a constant matrix for the distillation model (3.93), since all elements in G share the same dynamics, $G(s) = g(s)G_0$. The closed-loop poles of the perturbed system are solutions to $\det(I + L'(s)) = \det(I + (k_1/s)L_0) = 0$, or equivalently

$$\det\left(\frac{s}{k_1}I + L_0\right) = (s/k_1)^2 + \text{tr}(L_0)(s/k_1) + \det(L_0) = 0 \tag{3.100}$$

For $k_1 > 0$ we have from the Routh–Hurwitz stability condition that instability occurs if and only if the trace and/or the determinant of L_0 are negative. Since $\det(L_0) > 0$ for any gain error less than 100%, instability can only occur if $\text{tr}(L_0) < 0$. Evaluate $\text{tr}(L_0)$ and show that with gain errors of equal magnitude the combination of errors which most easily yields instability is with $\widehat{\epsilon}_1 = -\widehat{\epsilon}_2 = -\epsilon_1 = \epsilon_2 = \epsilon$. Use this to show that the perturbed system is unstable if

$$|\epsilon| > \sqrt{\frac{1}{2\lambda_{11} - 1}} \tag{3.101}$$

where $\lambda_{11} = g_{11}g_{22}/\det G$ is the $1,1$ element of the RGA of G. In our case $\lambda_{11} = 35.1$ and we get instability for $|\epsilon| > 0.120$. Check this numerically, e.g. using Matlab.

Remark. The instability condition in (3.101) for simultaneous input and output gain uncertainty applies to the very special case of a 2×2 plant, in which all elements share the same dynamics, $G(s) = g(s)G_0$, and an inverse-based controller, $K(s) = (k_1/s)G^{-1}(s)$.

Exercise 3.12* *Consider again the distillation process $G(s)$ in (3.93). The response using the inverse-based controller K_{inv} in (3.95) was found to be sensitive to input gain errors. We want to see if the controller can be modified to yield a more robust system by using the Glover–McFarlane $\mathcal{H}_\infty$ loop-shaping procedure. To this effect, let the shaped plant be $G_s = GK_{\text{inv}}$, i.e. $W_1 = K_{\text{inv}}$, and design an $\mathcal{H}_\infty$ controller K_s for the shaped plant (see page 370 and Chapter 9), such that the overall controller becomes $K = K_{\text{inv}}K_s$. (You will find that $\gamma_{\min} = 1.414$ which indicates good robustness with respect to coprime factor uncertainty, but the loop shape is almost unchanged and the system remains sensitive to input uncertainty.)*

3.7.3 Robustness conclusions

From the two motivating examples above we found that multivariable plants can display a sensitivity to uncertainty (in this case input uncertainty) which is fundamentally different from what is possible in SISO systems.

In the first example (spinning satellite), we had excellent stability margins (PM and GM) when considering one loop at a time, but small simultaneous input gain errors gave instability. This might have been expected from the peak values ($\mathcal{H}_\infty$ norms) of S and T, defined as

$$\|T\|_\infty = \max_\omega \bar{\sigma}(T(j\omega)), \quad \|S\|_\infty = \max_\omega \bar{\sigma}(S(j\omega)) \tag{3.102}$$

which were both large (about 10) for this example.

In the second example (distillation process), we again had excellent stability margins (PM and GM), and the system was also robustly stable to errors (even simultaneous) of up to

100% in the input gains. However, in this case small input gain errors gave very poor output performance, so robust performance was not satisfied, and adding simultaneous output gain uncertainty resulted in instability (see Exercise 3.11). These problems with the decoupling controller might have been expected because the plant has large RGA elements. For this second example the $\mathcal{H}_\infty$ norms of S and T were both about 1, so the absence of peaks in S and T does not guarantee robustness.

Although sensitivity peaks, RGA elements, etc., are useful indicators of robustness problems, they provide no exact answer to whether a given source of uncertainty will yield instability or poor performance. This motivates the need for better tools for analyzing the effects of model uncertainty. We want to avoid a trial-and-error procedure based on checking stability and performance for a large number of candidate plants. This is very time consuming, and in the end one does not know whether those plants are the limiting ones. What is desired, is a simple tool which is able to identify the worst-case plant. This will be the focus of Chapters 7 and 8 where we show how to represent model uncertainty in the $\mathcal{H}_\infty$ framework, and introduce the structured singular value μ as our tool. The two motivating examples are studied in more detail in Example 8.10 and Section 8.11.3 where a μ-analysis predicts the robustness problems found above.

3.8 General control problem formulation

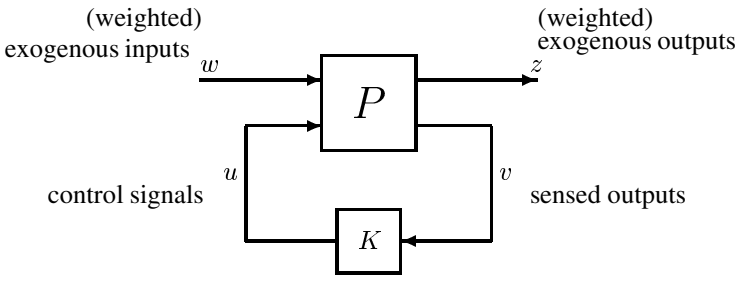

Figure 3.15: General control configuration for the case with no model uncertainty

In this section we consider a general method of formulating control problems introduced by Doyle (1983; 1984). The formulation makes use of the general control configuration in Figure 3.15, where P is the generalized plant and K is the generalized controller as explained in Table 1.1 on page 13. Note that positive feedback is used.

The overall control objective is to minimize some norm of the transfer function from w to z, e.g. the $\mathcal{H}_\infty$ norm. The controller design problem is then:

- Find a controller K, which, based on the information in v, generates a control signal u, which counteracts the influence of w on z, thereby minimizing the closed-loop norm from w to z.

The most important point of this section is to appreciate that almost any linear control problem can be formulated using the block diagram in Figure 3.15 (for the nominal case) or in Figure 3.23 (with model uncertainty).

Remark 1 The configuration in Figure 3.15 may at first glance seem restrictive. However, this is not the case, and we will demonstrate the generality of the setup with a few examples, including the design of observers (the estimation problem) and feedforward controllers.

Remark 2 We may generalize the control configuration still further by including diagnostics as additional outputs from the controller giving the *4-parameter controller* introduced by Nett (1986), but this is not considered in this book.

3.8.1 Obtaining the generalized plant P

The routines in Matlab for synthesizing $\mathcal{H}_\infty$ and $\mathcal{H}_2$ optimal controllers assume that the problem is in the general form of Figure 3.15; that is, they assume that P is given. To derive P (and K) for a specific case we must first find a block diagram representation and identify the signals w, z, u and v. To construct P one should note that it is an *open-loop* system and remember to break all "loops" entering and exiting the controller K. Some examples are given below and further examples are given in Section 9.3 (Figures 9.9, 9.10, 9.11 and 9.12).

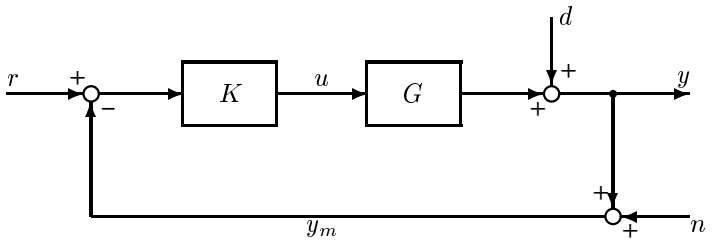

Figure 3.16: One degree-of-freedom control configuration

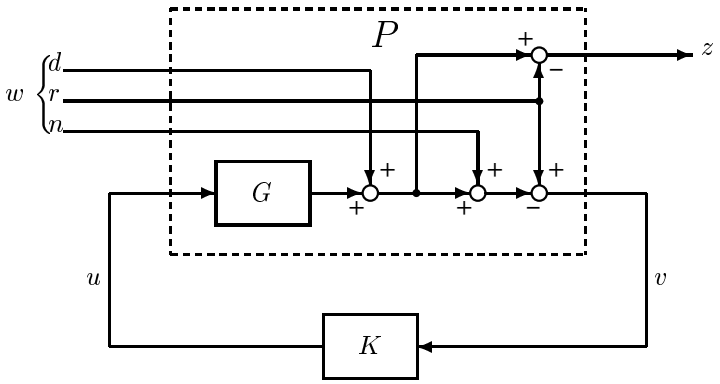

Figure 3.17: Equivalent representation of Figure 3.16 where the error signal to be minimized is $z = y - r$ and the input to the controller is $v = r - y_m$

Example 3.18 One degree-of-freedom feedback control configuration. *We want to find P for the conventional one degree-of-freedom control configuration in Figure 3.16. The first step is to identify the signals for the generalized plant:*

$$w = \begin{bmatrix} w_1 \\ w_2 \\ w_3 \end{bmatrix} = \begin{bmatrix} d \\ r \\ n \end{bmatrix}; \quad z = e = y - r; \quad v = r - y_m = r - y - n \tag{3.103}$$

With this choice of v, the controller only has information about the deviation $r - y_m$. Also note that $z = y - r$, which means that performance is specified in terms of the actual output y and not *in terms of the measured output y_m. The block diagram in Figure 3.16 then yields*

$$\begin{aligned} z &= y - r = Gu + d - r = Iw_1 - Iw_2 + 0w_3 + Gu \\ v &= r - y_m = r - Gu - d - n = -Iw_1 + Iw_2 - Iw_3 - Gu \end{aligned}$$

and P which represents the transfer function matrix from $\begin{bmatrix} w & u \end{bmatrix}^T$ to $\begin{bmatrix} z & v \end{bmatrix}^T$ is

$$P = \begin{bmatrix} I & -I & 0 & G \\ -I & I & -I & -G \end{bmatrix} \tag{3.104}$$

Note that P does not *contain the controller. Alternatively, P can be obtained by inspection from the representation in Figure 3.17.*

Remark. Obtaining the generalized plant P may seem tedious. However, when performing numerical calculations P can be generated using software. For example, in Matlab we may use the `simulink` program, or we may use the `sysic` program in the Robust Control toolbox. The code in Table 3.2 generates the generalized plant P in (3.104) for Figure 3.16.

Table 3.2: **Matlab program to generate P in (3.104)**

```
% Uses the Robust Control toolbox
systemnames = 'G';                          % G is the SISO plant.
inputvar = '[d(1);r(1);n(1);u(1)]';         % Consists of vectors w and u.
input_to_G = '[u]';
outputvar = '[G+d-r; r-G-d-n]';             % Consists of vectors z and v.
sysoutname = 'P';
sysic;
```

3.8.2 Controller design: including weights in P

To get a meaningful controller synthesis problem, e.g. in terms of the $\mathcal{H}_\infty$ or $\mathcal{H}_2$ norms, we generally have to include weights W_z and W_w in the generalized plant P, see Figure 3.18. That is, we consider the weighted or normalized exogenous inputs w (where $\widetilde{w} = W_w w$ consists of the "physical" signals entering the system; disturbances, references and noise), and the weighted or normalized controlled outputs $z = W_z \widetilde{z}$ (where $\widetilde{z}$ often consists of the control error $y-r$ and the manipulated input u). The weighting matrices are usually frequency dependent and typically selected such that weighted signals w and z are of magnitude 1; that is, the norm from w to z should be less than 1. Thus, in most cases only the magnitude of the weights matter, and we may without loss of generality assume that $W_w(s)$ and $W_z(s)$ are stable and minimum-phase (they need not even be rational transfer functions but if not they will be unsuitable for controller synthesis using current software).

Example 3.19 Stacked $S/T/KS$ problem. *Consider an $\mathcal{H}_\infty$ problem where we want to bound $\bar{\sigma}(S)$ (for performance), $\bar{\sigma}(T)$ (for robustness and to avoid sensitivity to noise) and $\bar{\sigma}(KS)$ (to penalize large*

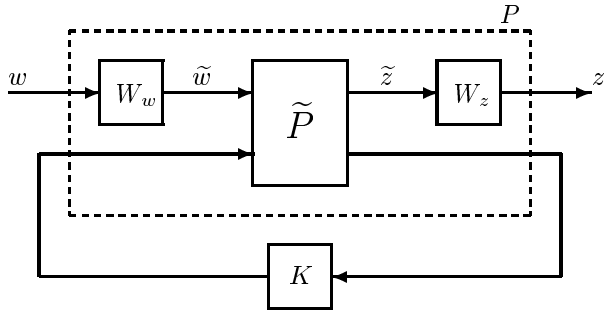

Figure 3.18: General control configuration for the case with no model uncertainty

inputs). These requirements may be combined into a stacked $\mathcal{H}_\infty$ problem

$$\min_K \|N(K)\|_\infty, \quad N = \begin{bmatrix} W_u KS \\ W_T T \\ W_P S \end{bmatrix} \tag{3.105}$$

where K is a stabilizing controller. In other words, we have $z = Nw$ and the objective is to minimize the $\mathcal{H}_\infty$ norm from w to z. Except for some negative signs which have no effect when evaluating $\|N\|_\infty$, the N in (3.105) may be represented by the block diagram in Figure 3.19 (convince yourself that this is true). Here w represents a reference command ($w = -r$, where the negative sign does not really matter) or a disturbance entering at the output ($w = d_y$), and z consists of the weighted input $z_1 = W_u u$, the weighted output $z_2 = W_T y$, and the weighted control error $z_3 = W_P(y - r)$. We get from Figure 3.19 the following set of equations:

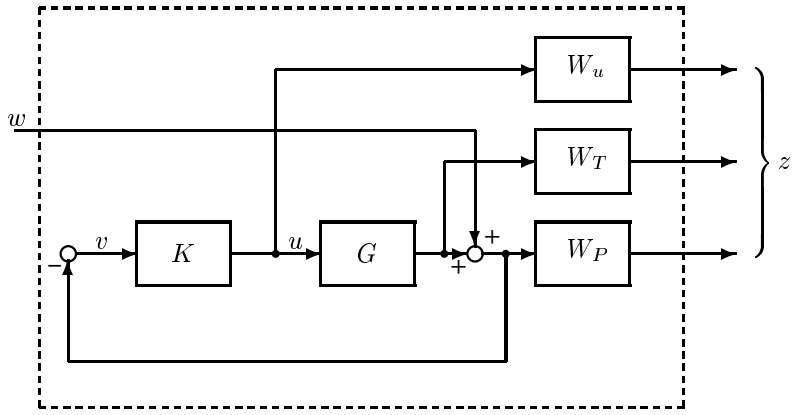

Figure 3.19: Block diagram corresponding to $z = Nw$ in (3.105)

$$\begin{aligned} z_1 &= W_u u \\ z_2 &= W_T G u \\ z_3 &= W_P w + W_P G u \\ v &= -w - Gu \end{aligned}$$

so the generalized plant P from $[\ w \quad u\ ]^T$ to $[\ z \quad v\ ]^T$ is

$$P = \begin{bmatrix} 0 & W_u I \\ 0 & W_T G \\ W_P I & W_P G \\ -I & -G \end{bmatrix} \tag{3.106}$$

3.8.3 Partitioning the generalized plant P

We often partition P as

$$P = \begin{bmatrix} P_{11} & P_{12} \\ P_{21} & P_{22} \end{bmatrix} \tag{3.107}$$

such that its parts are compatible with the signals w, z, u and v in the generalized control configuration,

$$z = P_{11}w + P_{12}u \tag{3.108}$$
$$v = P_{21}w + P_{22}u \tag{3.109}$$

The reader should become familiar with this notation. In Example 3.19 we get

$$P_{11} = \begin{bmatrix} 0 \\ 0 \\ W_P I \end{bmatrix}, \quad P_{12} = \begin{bmatrix} W_u I \\ W_T G \\ W_P G \end{bmatrix} \tag{3.110}$$

$$P_{21} = -I, \quad P_{22} = -G \tag{3.111}$$

Note that P_{22} has dimensions compatible with the controller, i.e. if K is an $n_u \times n_v$ matrix, then P_{22} is an $n_v \times n_u$ matrix. For cases with one degree-of-freedom negative feedback control we have $P_{22} = -G$.

3.8.4 Analysis: closing the loop to get N

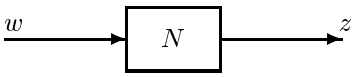

Figure 3.20: General block diagram for analysis with no uncertainty

The general feedback configurations in Figures 3.15 and 3.18 have the controller K as a separate block. This is useful when synthesizing the controller. However, for *analysis* of closed-loop performance the controller is given, and we may absorb K into the interconnection structure and obtain the system N as shown in Figure 3.20 where

$$z = Nw \tag{3.112}$$

where N is a function of K. To find N, we first partition the generalized plant P as given in (3.107)–(3.109), combine this with the controller equation

$$u = Kv \tag{3.113}$$

and eliminate u and v from (3.108), (3.109) and (3.113) to yield $z = Nw$ where N is given by

$$N = P_{11} + P_{12}K(I - P_{22}K)^{-1}P_{21} \triangleq F_l(P, K) \tag{3.114}$$

Here $F_l(P, K)$ denotes a lower *linear fractional transformation (LFT)* of P with K as the parameter. Some properties of LFTs are given in Appendix A.8. In words, N is obtained from Figure 3.15 by using K to close a lower feedback loop around P. Since positive feedback is used in the general configuration in Figure 3.15 the term $(I - P_{22}K)^{-1}$ has a negative sign.

Remark. To assist in remembering the sequence of P_{12} and P_{21} in (3.114), notice that the first (last) index in P_{11} is the same as the first (last) index in $P_{12}K(I - P_{22}K)^{-1}P_{21}$. The lower LFT in (3.114) is also represented by the block diagram in Figure 3.2.

The reader is advised to become comfortable with the above manipulations before progressing further.

Example 3.20 *We want to derive N for the partitioned P in (3.110) and (3.111) using the LFT formula in (3.114). We get*

$$N = \begin{bmatrix} 0 \\ 0 \\ W_P I \end{bmatrix} + \begin{bmatrix} W_u I \\ W_T G \\ W_P G \end{bmatrix} K(I + GK)^{-1}(-I) = \begin{bmatrix} -W_u KS \\ -W_T T \\ W_P S \end{bmatrix}$$

where we have made use of the identities $S = (I + GK)^{-1}$, $T = GKS$ and $I - T = S$. With the exception of the two negative signs, this is identical to N given in (3.105). Of course, the negative signs have no effect on the norm of N.

Again, it should be noted that deriving N from P is much simpler using available software. For example, in the Matlab Robust Control toolbox we can evaluate $N = F_l(P, K)$ using the command `N=lft(P,K)`.

Exercise 3.13 *Consider the two degrees-of-freedom feedback configuration in Figure 1.3(b). (i) Find P when*

$$w = \begin{bmatrix} d \\ r \\ n \end{bmatrix}; \quad z = \begin{bmatrix} y - r \\ u \end{bmatrix}; \quad v = \begin{bmatrix} r \\ y_m \end{bmatrix} \tag{3.115}$$

(ii) Let $z = Nw$ and derive N in two different ways: directly from the block diagram and using $N = F_l(P, K)$.

3.8.5 Generalized plant P: further examples

To illustrate the generality of the configuration in Figure 3.15, we now present two further examples: one in which we derive P for a problem involving feedforward control, and one for a problem involving estimation.

Example 3.21 *Consider the control system in Figure 3.21, where y_1 is the output we want to control, y_2 is a secondary output (extra measurement), and we also measure the disturbance d. By secondary we mean that y_2 is of secondary importance for control; that is, there is no control objective associated with it. The control configuration includes a two degrees-of-freedom controller, a feedforward controller*

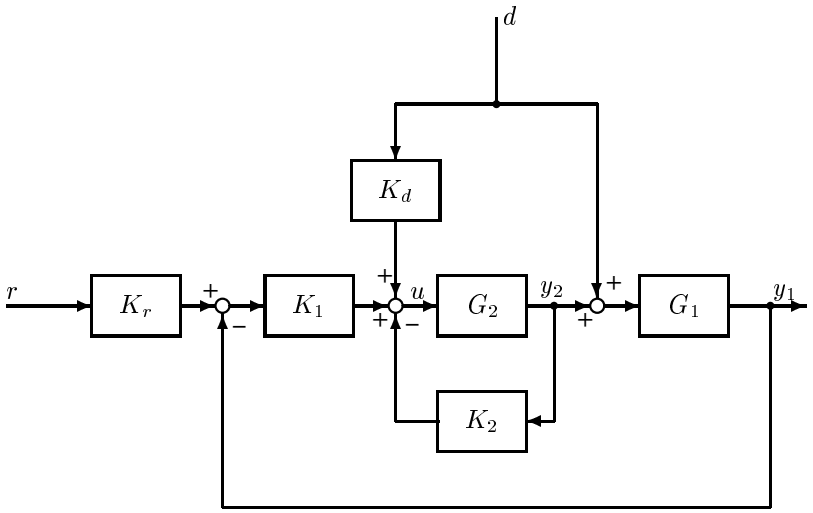

Figure 3.21: System with feedforward, local feedback and two degrees-of-freedom control

and a local feedback controller based on the extra measurement y_2. To recast this into our standard configuration of Figure 3.15 we define

$$w = \begin{bmatrix} d \\ r \end{bmatrix}; \quad z = y_1 - r; \quad v = \begin{bmatrix} r \\ y_1 \\ y_2 \\ d \end{bmatrix} \tag{3.116}$$

Note that d and r are both inputs and outputs to P and we have assumed a perfect measurement of the disturbance d. Since the controller has explicit information about r we have a two degrees-of-freedom controller. The generalized controller K may be written in terms of the individual controller blocks in Figure 3.21 as follows:

$$K = [\, K_1 K_r \quad -K_1 \quad -K_2 \quad K_d \,] \tag{3.117}$$

By writing down the equations or by inspection from Figure 3.21 we get

$$P = \begin{bmatrix} G_1 & -I & G_1 G_2 \\ 0 & I & 0 \\ G_1 & 0 & G_1 G_2 \\ 0 & 0 & G_2 \\ I & 0 & 0 \end{bmatrix} \tag{3.118}$$

Then partitioning P as in (3.108) and (3.109) yields $P_{22} = [\, 0^T \quad (G_1 G_2)^T \quad G_2^T \quad 0^T \,]^T$.

Exercise 3.14* **Cascade implementation.** *Consider Example 3.21 further. The local feedback based on y_2 is often implemented in a cascade manner; see also Figure 10.11. In this case the output from K_1 enters into K_2 and it may be viewed as a reference signal for y_2. Derive the generalized controller K and the generalized plant P in this case.*

Remark. From Example 3.21 and Exercise 3.14, we see that a cascade *implementation* does not usually limit the achievable performance since, unless the optimal K_2 or K_1 have RHP-zeros, we can obtain from the optimal overall K the subcontrollers K_2 and K_1 (although we may have to add a small D-term

to K to make the controllers proper). However, if we impose restrictions on the *design* such that, for example, K_2 or K_1 are designed "locally" (without considering the whole problem), then this will limit the achievable performance. For example, for a *two degrees-of-freedom controller* a common approach is first to design the feedback controller K_y for disturbance rejection (without considering reference tracking) and then design K_r for reference tracking. This will generally give some performance loss compared to a simultaneous design of K_y and K_r.

Example 3.22 Output estimator. *Consider a situation where we have no measurement of the output y which we want to control. However, we do have a measurement of another output variable y_2. Let d denote the unknown external inputs (including noise and disturbances) and u_G the known plant inputs (a subscript $_G$ is used because in this case the output u from K is not the plant input). Let the model be*

$$y = Gu_G + G_d d; \quad y_2 = Fu_G + F_d d$$

The objective is to design an estimator, K_{est}, such that the estimated output $\widehat{y} = K_{\text{est}} \begin{bmatrix} y_2 \\ u_G \end{bmatrix}$ is as close as possible in some sense to the true output y; see Figure 3.22. This problem may be written in the general framework of Figure 3.15 with

$$w = \begin{bmatrix} d \\ u_G \end{bmatrix},\ u = \widehat{y},\ z = y - \widehat{y},\ v = \begin{bmatrix} y_2 \\ u_G \end{bmatrix}$$

Note that $u = \widehat{y}$; that is, the output u from the generalized controller is the estimate of the plant output. Furthermore, $K = K_{\text{est}}$ and

$$P = \begin{bmatrix} G_d & G & -I \\ F_d & F & 0 \\ 0 & I & 0 \end{bmatrix} \tag{3.119}$$

We see that $P_{22} = \begin{bmatrix} 0 \\ 0 \end{bmatrix}$ since the estimator problem does not involve feedback.

Exercise 3.15 State estimator (observer). *In the Kalman filter problem studied in Section 9.2 the objective is to minimize $x - \widehat{x}$ (whereas in Example 3.22 the objective was to minimize $y - \widehat{y}$). Show how the Kalman filter problem can be represented in the general configuration of Figure 3.15 and find P.*

3.8.6 Deriving P from N

For cases where N is given and we wish to find a P such that

$$N = F_l(P, K) = P_{11} + P_{12}K(I - P_{22}K)^{-1}P_{21}$$

it is usually best to work from a block diagram representation. This was illustrated above for the stacked N in (3.105). Alternatively, the following procedure may be useful:

1. Set $K = 0$ in N to obtain P_{11}.
2. Define $Q = N - P_{11}$ and rewrite Q such that each term has a common factor $R = K(I - P_{22}K)^{-1}$ (this gives P_{22}).
3. Since $Q = P_{12}RP_{21}$, we can now usually obtain P_{12} and P_{21} by inspection.

Example 3.23 Weighted sensitivity. *We will use the above procedure to derive P when $N = w_P S = w_P(I + GK)^{-1}$, where w_P is a scalar weight.*

1. $P_{11} = N(K = 0) = w_P I$.

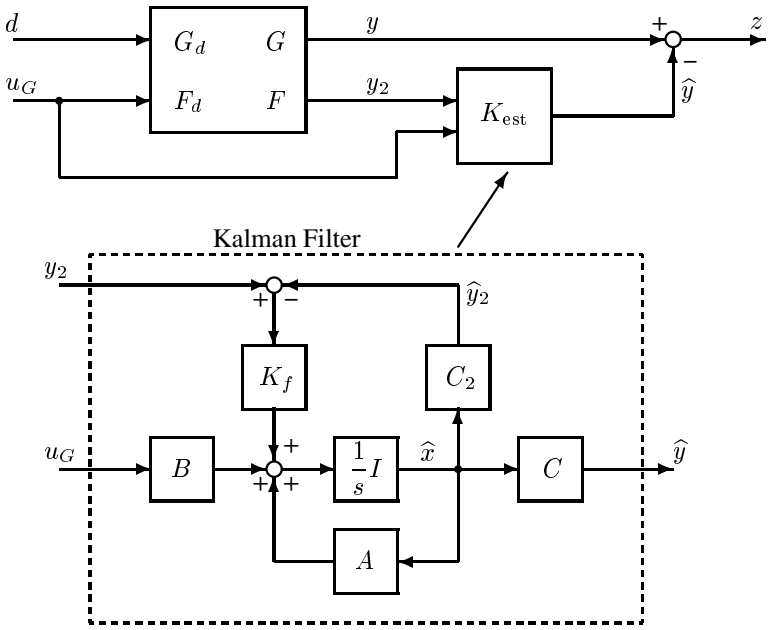

Figure 3.22: Output estimation problem. One particular estimator K_{est} is a Kalman filter

2. $Q = N - w_P I = w_P(S-I) = -w_P T = -w_P GK(I+GK)^{-1}$, *and we have* $R = K(I+GK)^{-1}$ *so* $P_{22} = -G$.
3. $Q = -w_P GR$ *so we have* $P_{12} = -w_P G$ *and* $P_{21} = I$, *and we get*

$$P = \begin{bmatrix} w_P I & -w_P G \\ I & -G \end{bmatrix} \tag{3.120}$$

Remark. When obtaining P from a given N, we have that P_{11} and P_{22} are unique, whereas from step 3 in the above procedure we see that P_{12} and P_{21} are not unique. For instance, let α be a real scalar, then we may instead choose $\widetilde{P}_{12} = \alpha P_{12}$ and $\widetilde{P}_{21} = (1/\alpha)P_{21}$. For P in (3.120) this means that we may move the negative sign of the scalar w_P from P_{12} to P_{21}.

Exercise 3.16 * **Mixed sensitivity.** *Use the above procedure to derive the generalized plant P for the stacked N in (3.105).*

3.8.7 Problems not covered by the general formulation

The above examples have demonstrated the generality of the control configuration in Figure 3.15. Nevertheless, there are some controller design problems which are not covered. Let N be some closed-loop transfer function whose norm we want to minimize. To use the general form we must first obtain a P such that $N = F_l(P, K)$. However, this is not always possible, since there may not exist a block diagram representation for N. As a simple example, consider the stacked transfer function

$$N = \begin{bmatrix} (I+GK)^{-1} \\ (I+KG)^{-1} \end{bmatrix} \tag{3.121}$$

The transfer function $(I + GK)^{-1}$ may be represented on a block diagram with the input and output signals *after* the plant, whereas $(I + KG)^{-1}$ may be represented by another block diagram with input and output signals *before* the plant. However, in N there are no cross coupling terms between an input before the plant and an output after the plant (corresponding to $G(I + KG)^{-1}$), or between an input after the plant and an output before the plant (corresponding to $-K(I + GK)^{-1}$) so N cannot be represented in block diagram form. Equivalently, if we apply the procedure in Section 3.8.6 to N in (3.121), we are not able to find solutions to P_{12} and P_{21} in step 3.

Another stacked transfer function which *cannot* in general be represented in block diagram form is

$$N = \begin{bmatrix} W_P S \\ S G_d \end{bmatrix} \tag{3.122}$$

Remark. The case where N cannot be written as an LFT of K is a special case of the Hadamard-weighted $\mathcal{H}_\infty$ problem studied by van Diggelen and Glover (1994a). Although the solution to this $\mathcal{H}_\infty$ problem remains intractable, van Diggelen and Glover (1994b) present a solution for a similar problem where the Frobenius norm is used instead of the singular value to "sum up the channels".

Exercise 3.17 *Show that N in (3.122) can be represented in block diagram form if $W_P = w_P I$ where w_P is a scalar.*

3.8.8 A general control configuration including model uncertainty

The general control configuration in Figure 3.15 may be extended to include model uncertainty as shown by the block diagram in Figure 3.23. Here the matrix Δ is a *block-diagonal* matrix that includes all possible perturbations (representing uncertainty) to the system. It is usually normalized in such a way that $\|\Delta\|_\infty \leq 1$.

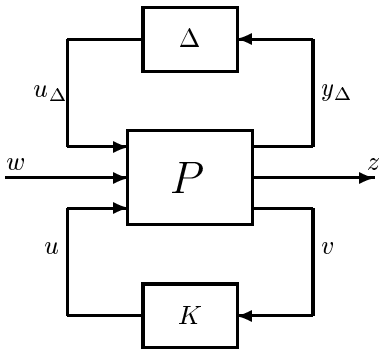

Figure 3.23: General control configuration for the case with model uncertainty

The block diagram in Figure 3.23 in terms of P (for synthesis) may be transformed into the block diagram in Figure 3.24 in terms of N (for analysis) by using K to close a lower loop around P. If we partition P to be compatible with the controller K, then the same *lower LFT* as found in (3.114) applies, and

$$N = F_l(P, K) = P_{11} + P_{12}K(I - P_{22}K)^{-1}P_{21} \tag{3.123}$$

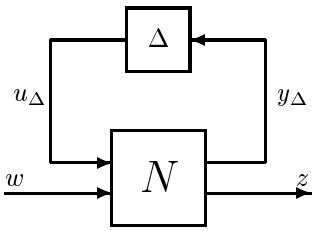

Figure 3.24: General block diagram for analysis with uncertainty included

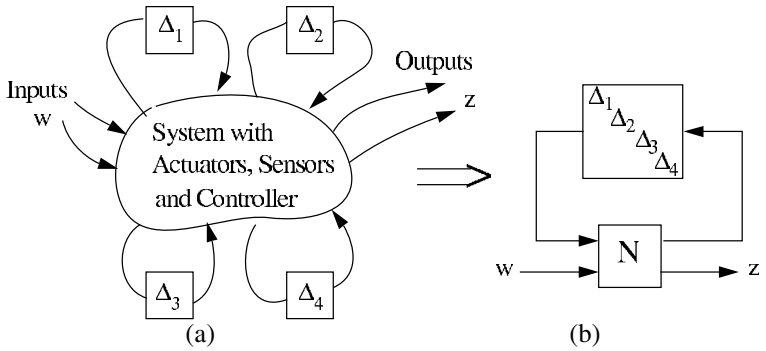

Figure 3.25: Rearranging a system with multiple perturbations into the $N\Delta$-structure

To evaluate the perturbed (uncertain) transfer function from external inputs w to external outputs z, we use Δ to close the upper loop around N (see Figure 3.24), resulting in an *upper LFT* (see Appendix A.8):

$$z = F_u(N, \Delta)w; \quad F_u(N, \Delta) \triangleq N_{22} + N_{21}\Delta(I - N_{11}\Delta)^{-1}N_{12} \tag{3.124}$$

Remark 1 Controller synthesis based on Figure 3.23 is still an unsolved problem, although good practical approaches like DK-iteration to find the "μ-optimal" controller are in use (see Section 8.12). For analysis (with a given controller), the situation is better and with the $\mathcal{H}_\infty$ norm an assessment of robust performance involves computing the structured singular value, μ. This is discussed in more detail in Chapter 8.

Remark 2 In (3.124) N has been partitioned to be compatible with Δ; that is, N_{11} has dimensions compatible with Δ. Usually, Δ is square, in which case N_{11} is a square matrix of the same dimension as Δ. For the nominal case with no uncertainty we have $F_u(N, \Delta) = F_u(N, 0) = N_{22}$, so N_{22} is the nominal transfer function from w to z.

Remark 3 Note that P and N here also include information about how the uncertainty affects the system, so they are *not* the same P and N as used earlier, e.g. in (3.114). Actually, the parts P_{22} and N_{22} of P and N in (3.123) (with uncertainty) are equal to the P and N in (3.114) (without uncertainty). Strictly speaking, we should have used another symbol for N and P in (3.123), but for notational simplicity we did not.

Remark 4 The fact that almost any control problem with uncertainty can be represented by Figure 3.23 may seem surprising, so some explanation is in order. First, represent each source of uncertainty by a perturbation block, Δ_i, which is normalized such that $\|\Delta_i\| \leq 1$. These perturbations may result from

parametric uncertainty, neglected dynamics, etc., as will be discussed in more detail in Chapters 7 and 8. Then "pull out" each of these blocks from the system so that an input and an output can be associated with each Δ_i as shown in Figure 3.25(a). Finally, collect these perturbation blocks into a large block-diagonal matrix having perturbation inputs and outputs as shown in Figure 3.25(b). In Chapter 8 we discuss in detail how to obtain N and Δ. Generally, it is difficult to perform these tasks manually, but this can be easily done using software; see examples in Chapters 7.

3.9 Additional exercises

Most of these exercises are based on material presented in Appendix A. The exercises illustrate material which the reader should know before reading the subsequent chapters.

Exercise 3.18* *Consider the performance specification $\|w_P S\|_\infty < 1$. Suggest a rational transfer function weight $w_P(s)$ and sketch it as a function of frequency for the following two cases:*

1. *We desire no steady-state offset, a bandwidth better than 1 rad/s and a resonance peak (worst amplification caused by feedback) lower than 1.5.*
2. *We desire less than 1% steady-state offset, less than 10% error up to frequency 3 rad/s, a bandwidth better than 10 rad/s, and a resonance peak lower than 2. (Hint: See (2.105) and (2.106).)*

Exercise 3.19 *By $\|M\|_\infty$ one can mean either a spatial or temporal norm. Explain the difference between the two and illustrate by computing the appropriate infinity norm for*

$$M_1 = \begin{bmatrix} 3 & 4 \\ -2 & 6 \end{bmatrix}, \quad M_2(s) = \frac{s-1}{s+1}\frac{3}{s+2}$$

Exercise 3.20* *What is the relationship between the RGA matrix and uncertainty in the individual elements? Illustrate this for perturbations in the $1,1$ element of the matrix*

$$A = \begin{bmatrix} 10 & 9 \\ 9 & 8 \end{bmatrix} \tag{3.125}$$

Exercise 3.21 *Assume that A is non-singular. (i) Formulate a condition in terms of the maximum singular value of E for the matrix $A + E$ to remain non-singular. Apply this to A in (3.125) and (ii) find an E of minimum magnitude which makes $A + E$ singular.*

Exercise 3.22* *Compute $\|A\|_{i1}$, $\bar{\sigma}(A) = \|A\|_{i2}$, $\|A\|_{i\infty}$, $\|A\|_F$, $\|A\|_{\max}$ and $\|A\|_{\text{sum}}$ for the following matrices and tabulate your results:*

$$A_1 = I; \quad A_2 = \begin{bmatrix} 1 & 0 \\ 0 & 0 \end{bmatrix}; A_3 = \begin{bmatrix} 1 & 1 \\ 1 & 1 \end{bmatrix}; A_4 = \begin{bmatrix} 1 & 1 \\ 0 & 0 \end{bmatrix}; A_5 = \begin{bmatrix} 1 & 0 \\ 1 & 0 \end{bmatrix}$$

Show using the above matrices that the following bounds are tight (i.e. we may have equality) for 2×2 matrices ($m = 2$):

$$\bar{\sigma}(A) \le \|A\|_F \le \sqrt{m}\,\bar{\sigma}(A)$$
$$\|A\|_{\max} \le \bar{\sigma}(A) \le m\|A\|_{\max}$$
$$\|A\|_{i1}/\sqrt{m} \le \bar{\sigma}(A) \le \sqrt{m}\|A\|_{i1}$$
$$\|A\|_{i\infty}/\sqrt{m} \le \bar{\sigma}(A) \le \sqrt{m}\|A\|_{i\infty}$$
$$\|A\|_F \le \|A\|_{\text{sum}}$$

Exercise 3.23 *Find example matrices to illustrate that the above bounds are also tight when A is a square $m \times m$ matrix with $m > 2$.*

Exercise 3.24* *Do the extreme singular values bound the magnitudes of the elements of a matrix? That is, is $\bar{\sigma}(A)$ greater than the largest element (in magnitude), and is $\underline{\sigma}(A)$ smaller than the smallest element? For a non-singular matrix, how is $\underline{\sigma}(A)$ related to the largest element in A^{-1}?*

Exercise 3.25 *Consider a lower triangular $m \times m$ matrix A with $a_{ii} = -1$, $a_{ij} = 1$ for all $i > j$, and $a_{ij} = 0$ for all $i < j$.*

(a) *What is* $\det A$*?*

(b) *What are the eigenvalues of A?*

(c) *What is the RGA of A?*

(d) *Let $m = 4$ and find an E with the smallest value of $\bar{\sigma}(E)$ such that $A + E$ is singular.*

Exercise 3.26* *Find two matrices A and B such that $\rho(A + B) > \rho(A) + \rho(B)$ which proves that the spectral radius does not satisfy the triangle inequality and is thus not a norm.*

Exercise 3.27 *Write $T = GK(I + GK)^{-1}$ as an LFT of K, i.e. find P such that $T = F_l(P, K)$.*

Exercise 3.28* *Write K as an LFT of $T = GK(I + GK)^{-1}$, i.e. find J such that $K = F_l(J, T)$.*

Exercise 3.29 *State-space descriptions may be represented as LFTs. To demonstrate this find H for*

$$F_l(H, 1/s) = C(sI - A)^{-1}B + D$$

Exercise 3.30* *Show that the set of all stabilizing controllers in (4.94) can be written as $K = F_l(J, Q)$ and find J.*

Exercise 3.31 *In (3.11) we stated that the sensitivity of a perturbed plant, $S' = (I + G'K)^{-1}$, is related to that of the nominal plant, $S = (I + GK)^{-1}$, by*

$$S' = S(I + E_O T)^{-1}$$

where $E_O = (G' - G)G^{-1}$. This exercise deals with how the above result may be derived in a systematic (though cumbersome) manner using LFTs (see also Skogestad and Morari, 1988a).

(a) First find F such that $S' = (I + G'K)^{-1} = F_l(F, K)$, and find J such that $K = F_l(J, T)$ (see Exercise 3.28).

(b) Combine these LFTs to find $S' = F_l(N, T)$. What is N in terms of G and G'? Note that since $J_{11} = 0$ we have from (A.164)

$$N = \begin{bmatrix} F_{11} & F_{12}J_{12} \\ J_{21}F_{21} & J_{22} + J_{21}F_{22}J_{12} \end{bmatrix}$$

(c) Evaluate $S' = F_l(N, T)$ and show that

$$S' = I - G'G^{-1}T(I - (I - G'G^{-1})T)^{-1}$$

(d) Finally, show that this may be rewritten as $S' = S(I + E_O T)^{-1}$.

3.10 Conclusion

The main purpose of this chapter has been to give an overview of methods for analysis and design of multivariable control systems.

In terms of analysis, we have shown how to evaluate MIMO transfer functions and how to use the singular value decomposition of the frequency-dependent plant transfer function matrix to provide insight into multivariable directionality. Other useful tools for analyzing directionality and interactions are the condition number and the RGA. Closed-loop performance may be analyzed in the frequency domain by evaluating the maximum singular value of the sensitivity function as a function of frequency. Multivariable RHP-zeros impose fundamental limitations on closed-loop performance, but for MIMO systems we can often direct the undesired effect of a RHP-zero to a subset of the outputs. MIMO systems are often more sensitive to uncertainty than SISO systems, and we demonstrated in two examples the possible sensitivity to input gain uncertainty.

In terms of controller design, we discussed some simple approaches such as decoupling and decentralized control. We also introduced a general control configuration in terms of the generalized plant P, which can be used as a basis for synthesizing multivariable controllers using a number of methods, including LQG, $\mathcal{H}_2$, $\mathcal{H}_\infty$ and μ-optimal control. These methods are discussed in much more detail in Chapters 8 and 9. In this chapter we have only discussed the $\mathcal{H}_\infty$ weighted sensitivity method.

INDEX

[1] Page numbers in *italic* refer to definitions.

The End Has No End

The Strokes
From the album “Room on Fire”
October 2003